

WAX-BASED EMULSIFIERS

**WAX-BASED EMULSIFIERS FOR USE IN EMULSIONS TO IMPART
WATER REPELLENCY TO GYPSUM WALLBOARDS**

By MARK T. RATTLE, B.Sc.(Eng.)

A Thesis Submitted to the School of Graduate Studies in Partial Fulfillment of the Requirements
for the Degree of Master of Applied Science

McMaster University © Copyright by Mark T. Rattle, July 2012

McMaster University MASTER OF APPLIED SCIENCE (2012) Hamilton, Ontario (Chemical Engineering)

TITLE: Wax Based Emulsifiers for use in Emulsions to Impart Water Repellency to Gypsum Wallboards AUTHOR: Mark T. Rattle, B.Sc.(Eng.) (Queen's University) SUPERVISOR: Professor Shiping Zhu NUMBER OF PAGES: xv, 97

Abstract

Maleation is a common means of modification for many commodity polymers and is used to several ends. In this study, various waxes were functionalized with maleic anhydride through several maleation processes, with the end goal of obtaining a cost effective processes to make emulsifiers to be used in emulsions that impart water-resistance to building products, such as gypsum wallboards. Research was done in collaboration with an industrial partner, in order to replace commercially available emulsifiers currently being used in their processes with a less costly product that could easily be made on-site based on their consumption requirements, through a solvent-free approach. Reactions involving both the free-radical initiated maleation of paraffin waxes and thermal addition of maleic anhydride to alpha-olefins were examined extensively. It was found that emulsions with properties matching or exceeding those of control emulsion formulations were obtainable using experimental emulsifiers made through both maleation methods. When used in gypsum wallboards, emulsifiers made through thermal maleation showed levels of water-repellency that matched or exceeded those of control formulations at lower loading levels, while emulsifiers made through free-radical maleation were subject to performance issues.

Acknowledgments

I would like to thank Dr. Shiping Zhu for his help and thoughtful supervision throughout the course of my research, and the rest of the PolyMac Zhu research group for being there to bounce ideas off of and for being an all-around outstanding group of people. I would like to thank Nels Grauman Neander for being a great colleague and friend during our time spent working on this project. I would also like to thank everyone who I've had the privilege to learn from through my time spent at both McMaster University and Queen's University. Finally, I would like to thank Larry Sinnige, Maria Racota and Jason Bertrim of Norjohn Limited for their guidance and technical assistance in the making of emulsions and board test samples.

To all of my amazing friends and family: thank you for standing behind me every step of the way. I couldn't have gotten here without you.

Table of Contents

Chapter 1: Introduction, Background and Objectives.....	1
1.1 Surfactants and emulsifiers	1
1.2 Waxes – properties and production.....	4
1.3 Emulsions.....	7
1.4 Gypsum wallboards.....	18
1.5 Research objectives and outlines.....	24
Chapter 2: Wax Maleation	26
2.1 Introduction	26
2.2 Wax maleation methods.....	27
2.3 Materials used in experiments.....	31
2.4 Experimental procedures.....	34
2.5 Results and discussion of wax maleation methods	44
Chapter 3: Emulsion Formulations for use in Gypsum Wallboards.....	69
3.1 Experimental procedures.....	69
3.2 Results and discussion of emulsion production	70
3.3 Gypsum wallboard results.....	74
3.4 Additional applications of experimentally obtained maleated waxes.....	75
3.5 Cost analysis for application with an industrial partner.....	76
Chapter 4: Conclusions and Recommendations	78

4.1	Conclusions	78
	References (Bibliography)	79
	Appendix A: Raw Data for Wax, Emulsion and Board Samples	82
	Appendix B: FTIR Reference Spectra	91
	Appendix C: Cost Estimation	95

List of Figures

Figure 1 – A typical schematic representation of an ionic surfactant.....	1
Figure 2 - Chemical formulae of some common anionic surfactants	2
Figure 3 – Mechanism by which an amidinium-based switchable surfactant operates	3
Figure 4 – Forms of hydrocarbons present in paraffin wax.....	5
Figure 5 - Example of an oil-in-water emulsion.....	9
Figure 6 – Micelle structure showing organization of surfactant molecules (Barnes, 2005)	11
Figure 7 – Example of property changes at a critical micellar concentration for sodium dodecyl sulfate (Preston, 1948)	11
Figure 8 - Diagram showing surface charges and the presence of each part of the electrical double layer.....	13
Figure 9 – Potential energy present between two emulsion droplets (Barnes, 2005).....	15
Figure 10 - Distribution of polymeric surfactant in liquid/liquid and liquid/solid colloids (Barnes, 2005).....	16
Figure 11 – Example industrial apparatus for continuous gypsum wallboard production (Burke, 2000).....	20
Figure 12 – Example comparing water absorbed by a sample of gypsum wallboard using an emulsion including only wax to a sample using an optimized mixture of wax and asphalt (Camp, 1947).....	21
Figure 13 – Example comparing water absorption values obtained using a range of emulsions with compositions containing from 2.9 parts asphalt:1 part wax to 58 parts asphalt:18 parts wax (Camp, 1947)	22
Figure 14 - Mechanism for grafting MAH to a polyethylene backbone.....	28

Figure 15 – Bridged side product formed through termination by coupling and homopolymerized MAH	29
Figure 16 - Reaction mechanism of the ene reaction occurring between MAH and a-olefin	31
Figure 17 - Apparatus used in bulk addition method.....	37
Figure 18 - Apparatus used in continuous peroxide addition method	38
Figure 19 - Apparatus used in an 'open' thermal maleation system.....	41
Figure 20 - Apparatus used in a 'closed' thermal maleation system	42
Figure 21 - Collected results of wax grafting experiments with region I representing the continuous peroxide addition experiments, region II representing the pulse peroxide addition and region III representing the bulk addition of peroxide and MAH addition reaction methods	44
Figure 22 - Time lapse showing reaction progression of a continuous peroxide pumping experiment.....	46
Figure 23 – Acid number vs. molar ratio of initiator TBP to MAH in the product formulation at 160 °C, bulk addition of peroxide reaction method.....	47
Figure 24 – Grafting efficiency vs. molar ratio of initiator TBP to MAH in the product formulation at 160 °C, bulk addition of peroxide reaction method	48
Figure 25 - Acid number vs. molar ratio of initiator TBPB to MAH in the product formulation at 130 °C, bulk addition of peroxide reaction method.....	49
Figure 26 - Grafting efficiency vs. molar ratio of initiator TBPB to MAH in the product formulation at 130 °C, bulk addition of peroxide reaction method	49
Figure 27 – Acid number vs. molar ratio of initiator TBP to MAH in the product formulation at 160 °C, MAH addition reaction method.....	50

Figure 28 – Efficiency vs. molar ratio of initiator TBP to MAH in the product formulation at 160 °C, MAH addition reaction method	51
Figure 29 - <i>t</i> -Butyl and peroxybenzoyl radicals formed in grafting reactions.....	52
Figure 30 – Grafting over time experiment – 10% MAH by weight of wax, 1:1 mol ratio TBP:MAH, 160 °C	53
Figure 31 – Thermal stability experiment - 10% MAH by weight of wax, 1:1 mol ratio TBP:MAH, 160 °C	54
Figure 32 – Possible products of radical termination reactions	55
Figure 33 - Six-membered ring transition state formed between MAH and backbone polymer, R= H or alkyl group	56
Figure 34 - FTIR spectrum of 10% MAH loading / 1:1 TBP / 60 AN.....	59
Figure 35 - Resonance structure and interactions of maleic anhydride	60
Figure 36 - Reaction progression for thermal addition of MAH, sample #17.....	63
Figure 37 - Titration reaction to determine acid number of emulsifier	64
Figure 38 - FTIR spectra taken from unmodified C30+HA wax (a), sample #1 (table 8) - 72 AN (b), sample #18 washed with acetone – 119.5 AN (c) and sample #18 unwashed – 123 AN (d)	66
Figure 39 - Reference FTIR spectrum of maleic anhydride	91
Figure 40 - FTIR Spectrum of maleic anhydride recaptured from thermal grafting experiments	91
Figure 41 - Reference FTIR spectrum of paraffin wax.....	92
Figure 42 - Reference FTIR spectrum of 1-octadecene.....	93
Figure 43 - Reference FTIR spectrum of n-octadecylsuccinic anhydride	94

List of Tables

Table 1 - Classification of different colloid types	8
Table 2 - Properties of paraffin waxes used in grafting experiments	32
Table 3 - Properties of synthetic waxes used in thermal addition experiments.....	33
Table 4- Properties of peroxides used in grafting experiments	33
Table 5 - Comparison of average values for 20% MAH loading for each reaction method, across varying reaction conditions.....	45
Table 6 - FTIR peak assignments of model compounds used to evaluate MAH grafting types ..	58
Table 7 - Peak assignment for MAH loading spectrum.....	59
Table 8 - Results of thermal addition experiments conducted at a reaction temperature of 200°C for 8 hours. 18.7 wt% MAH loading	61
Table 9 - Comparison of the effects of each experimental variable on the AN of products with experiments conducted at a reaction temperature of 200°C for 8 hours, with 18.7 wt% MAH loading.....	62
Table 10 - Important properties of CP 30+HA wax	64
Table 11 - Peak assignments for FTIR taken from products of thermal addition reactions	67
Table 12 - Selected formulations of experimental emulsion formulations.....	71
Table 13- Selected results of emulsion performance testing	72
Table 14 - Results of gypsum wall board samples created with experimental emulsifiers	74
Table 15 - Yearly requirements for each ingredient in an industrial process	76
Table 16 - Cost of ingredients used in emulsion production	76
Table 17 - Sample dimensions of reactor required to produce emulsifier	77
Table 18 - Raw data from experiments using bulk addition of peroxide.....	82

Table 19 - Raw data of experiments using pulse addition of peroxide.....	82
Table 20 - Raw data of experiments using continuous addition of peroxide.....	83
Table 21 - Raw data of experiments using MAH addition	84
Table 22 - Raw data of experiments using ball milling approach	85
Table 23 - Raw data for experiments using thermal addition of MAH to alpha-olefins at 200 °C for 8 hours,	85
Table 24 - Raw data for formulations of emulsions to be used in gypsum wallboards.....	87
Table 25 - Raw data for emulsion performance.....	89

List of Abbreviations

O/W – Oil-in-water

W/O – Water-in-oil

SDS – Sodium dodecyl sulfate

CMC – Critical micellar concentration

MAH – Maleic anhydride

SA – Succinic anhydride

AN – Acid number

TBP – *tert*-Butyl peroxide

TBPB – *tert*-Butyl peroxybenzoate

DG – Degree of grafting

GE – Grafting efficiency

PVA – Polyvinyl alcohol

RT – Room temperature

List of Symbols

ψ_s – Electrical potential at the border of Stern layer

ψ_d – Electrical potential at the border of the diffuse layer

ξ – Zeta potential at the slipping plane

κ^{-1} – Debye length

n – Concentration of ions at a distance from the double layer

z – Valence of ions opposite in charge to the surface charge

e – Elementary charge

ε – Dielectric constant

k – Boltzmann constant

T – Absolute temperature

v – Settling velocity of particles

g – Acceleration due to gravity

r – Radius

ρ_o – Density of oil phase

ρ_w – Density of aqueous phase

η_w – Viscosity of aqueous phase

V_B – Volume of base used in titration

C_B – Concentration of base solution used in titration

MW_{KOH} – Molecular weight of potassium hydroxide

M_{wax} – Mass of wax used in acid number test

$[P]_t$ – Peroxide concentration at time 't'

$[P]_0$ – Initial peroxide concentration

f – Initiator decomposition efficiency factor

t – Current time

$t_{1/2}$ – Half-life time

Declaration of Academic Achievement

The work in this thesis was completed in part with Nels Grauman Neander, my colleague from McMaster University. Together we are responsible for the results of the wax maleation experiments. I am responsible for the results of the application of the modified waxes to emulsion formulations used in gypsum wallboards while he is responsible for those used in engineered wood products. I am responsible for the cost analysis to determine the financial feasibility of the project. Technical assistance in creating board samples was provided by Maria Racota and Jason Bertrim at Norjohn Limited.

Chapter 1: Introduction, Background and Objectives

1.1 Surfactants and emulsifiers

Surfactants, or surface active agents, are amphiphilic molecules that typically have a hydrophobic tail composed of a linear or branched polymeric chain and a hydrophilic head group that can be ionic or non-ionic in nature, as shown in Figure 1. Surfactants are classified under the following categories: anionic, cationic, nonionic or zwitterionic (amphoteric). They may be naturally occurring or synthetic in nature.

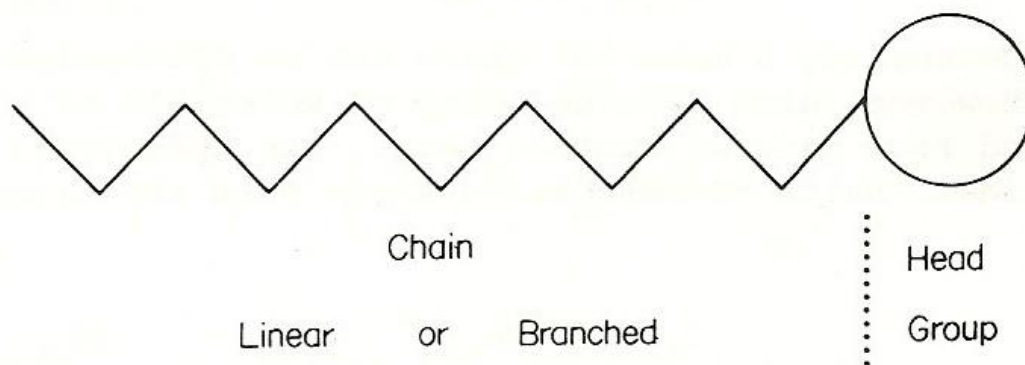


Figure 1 – A typical schematic representation of an ionic surfactant

Anionic surfactants have a hydrophobic tail with an anionic head, usually composed of a metal salt. In solution, they yield a large molecule with negative charge and a small positive ion. Typical functional groups associated with anionic surfactants are sulfates, alkyl sulfonic acids, carboxylic acids and alkylaryl sulfonic acids, along with their corresponding salts (Bennett et al., 1968). Examples of commonly used anionic surfactants are sodium dodecyl sulfate (SDS) and sodium dodecanoate, shown in Figure 2. Soaps are anionic surfactants that are salts of carboxylic acids, formed through the hydrolysis of triglycerides (Tadrous, 1984). Sulfated alcohols are often derived from natural fats such as coconut oil (Oh et al., 1985), usually being a

sodium or calcium salt. Calcium salts of these compounds give the added benefit of being highly soluble in hard water and do not precipitate out of solution. Soaps of carboxylic acids, on the other hand, are calcium sensitive and form insoluble calcium salts in hard water, which may commonly be found in many applications (Bennett et al., 1968).

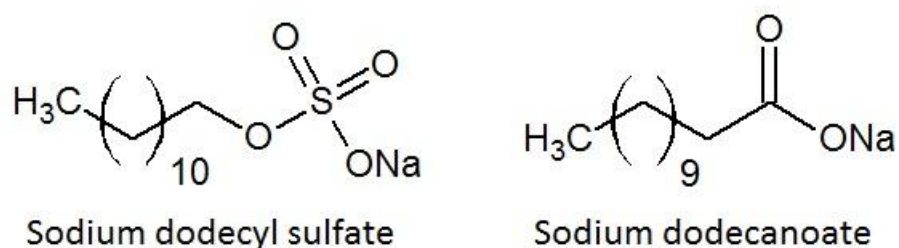


Figure 2 - Chemical formulae of some common anionic surfactants

Conversely, cationic surfactants are those that have a hydrophobic tail with a cationic head, forming a large positively charged molecule and a small anion in solution. Cationic surfactants are usually comprised of a primary, secondary or tertiary amine salt, a quaternary ammonium or another nitrogenous or non-nitrogenous component, such as a phosphonium or sulfonium compound (Bennett et al., 1968). They are generally attracted to surfaces with a negative charge, e.g. cellulose; they give a soft feel to textiles, hair and skin and have excellent antimicrobial properties. Amine based surfactants are generally soluble only in acidic solutions, while those based on quaternary ammonium are more soluble in both acidic and basic media.

Nonionic surfactants do not ionize in solution and as such, their solubility is generally independent of solution pH or water hardness. Nonionic surfactants are synthesized by several means, most notably through ether, ester and amide linkage chemistry. A large number of nonionic surfactants use ether linkages formed from reacting polyethylene oxide or low weight polypropylene oxide with a hydrophobic alcohol or mercaptan to form a block copolymer

structure (Bennett et al.). These surfactants can have their surface activities tailored by modifying the length of the polar oxide chain or the size of the nonpolar head.

Amphoteric surfactants have been known of for some time but have recently become a more prominent subject of interest. These compounds are also known as switchable surfactants as their ionic character can be changed by modifying characteristics of the system they are used in. These surfactants are of particular interest in processes where an emulsion is desired during one of several steps and offer convenient mechanisms for forming or breaking emulsions when required. Areas where switchable surfactants are of special importance include emulsion polymerization, oil transportation and oil separation (Liu et al., 2006). The mechanism of switchability generally requires specific reaction conditions, which can limit the range of applications for some of these surfactants. One of the promising classes of compounds that have been produced is viable in a wide range of systems and requires only that low pressure gasses be bubbled through the system in order to switch states. These compounds contain an amidine functional group and a long non-polar tail, giving an overall non-polar character. When exposed to gaseous CO₂, these compounds form an amidinium bicarbonate salt giving a polar head and non-polar tail, as seen in Figure 3. This reaction can then be reversed, or switched, by bubbling air, nitrogen or argon through the system, with the switchability being highly repeatable (Liu et al., 2006).

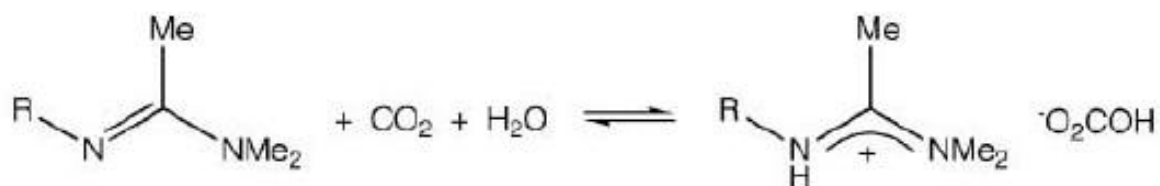


Figure 3 – Mechanism by which an amidinium-based switchable surfactant operates

1.2 Waxes – properties and production

A wax is recognized as an organic substance that is solid at ambient temperature but becomes a free-flowing liquid at elevated temperatures. Natural waxes are derived from plant, animal or mineral sources and are generally composed of esters of fatty acids and higher molecular weight alcohols, while synthetic waxes are generally composed of long alkyl chains and do not contain functional groups. Because different waxes vary so greatly in their compositions, they are classified by a myriad of properties. Multiple types of wax are often compounded together to form a product with various desired properties for specialized applications (Bennett, 1975). Waxes are found in a wide variety of products including adhesives, building materials, polishes, inks, cosmetics and waterproofing agents (American Fuel & Petroleum Manufacturers, 2009).

When thinking of natural waxes, beeswax is usually the first to come to mind and it has been used to make products like candles or sculptures for thousands of years, but more recently has been used on small scale in polishes and cosmetic items. The most industrially significant natural waxes are those derived from the petroleum refining process, and more specifically paraffin wax (Bennett, 1975; Bennett, 1956). Recent annual production of paraffin wax in North America is approximately 27500 barrels of oil or 2.75 billion pounds per year (American Fuel & Petroleum Manufacturers, 2009). Paraffin wax is a mixture of various isomers of saturated alkanes, as shown in Figure 4, with carbon numbers between 20 and 40.

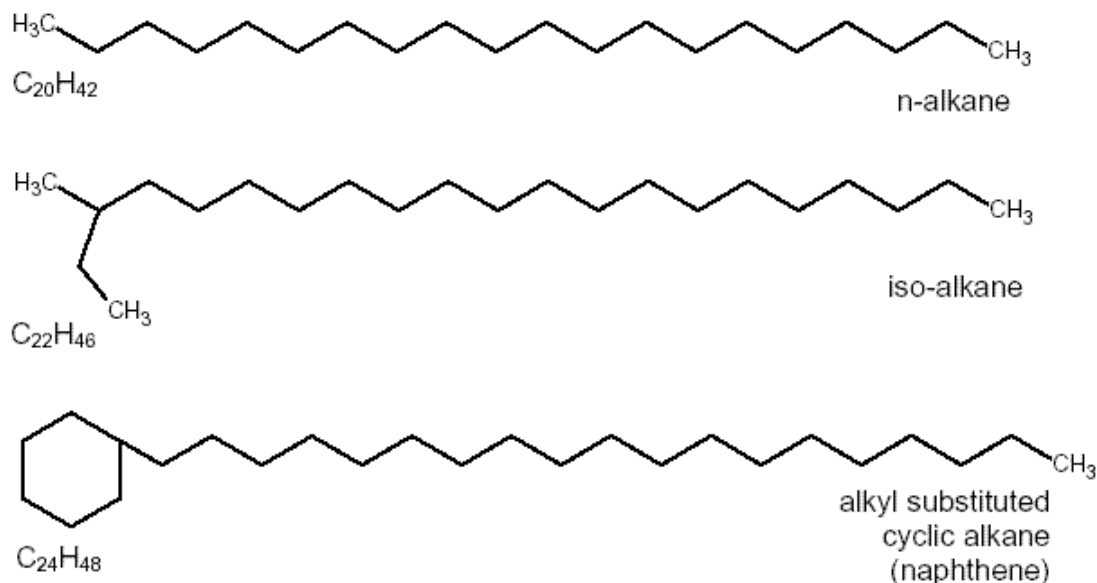


Figure 4 – Forms of hydrocarbons present in paraffin wax

Many different grades of paraffin wax are available, classified by composition or completeness of the refining process to make them. Major grades of paraffin wax on the market today include fully refined, semi-refined and crude scale waxes. The primary quality that differs between grades is the oil content, or amount of shorter chains present in the product, with refined waxes having an oil content of 0.5% or less, semi-refined having between 0.5% and 3% and crude scale waxes containing approximately 3% oil (Bennett, 1975). Oil content affects properties such as melting point, tensile strength, colour and odour. The properties of refined paraffin waxes are fairly consistent across manufacturers, but the properties of semi-refined and crude scale waxes tend to vary greatly depending on the manufacturer and location where petroleum feedstock was taken from (Bennett, 1975).

Paraffin wax is produced through an extensive process, starting with the distillation of petroleum feed stock to separate fractions via boiling point difference, giving fractions of lower gases, gasoline, naphtha, kerosene, gas-oil, wax or paraffinic distillates and asphaltic distillates,

from lightest to heaviest. Paraffinic distillates contain several different waxy compounds having the same boiling range, as well as some slightly light and higher boiling residues that must be removed through further processing. Wax distillates have wax content between 6-25%, with 15% being the average wax content (Bennett, 1956).

The first step in further processing the wax distillate is pressing, which involves filtering solid waxes from liquid oil at low temperatures, giving dewaxed oil and slack wax. The distillate is treated with acid to remove some impurities, washed with water and neutralized. It is then chilled to a certain temperature depending on the desired pour point for the separation causing the precipitation of waxy hydrocarbons with higher melting points. After the pressing process, slack wax containing approximately 35% oil is obtained (Bennett, 1975). The next step of the refinement process involves sweating or solvent pressing to further remove oil from the wax. The sweating process involves subjecting a solid cake of slack wax to very slight temperature increases, on the order of 2°F per hour, causing beads of oil to form on the surface of the wax which are then drained away. Sweating yields crude scale wax with oil content of approximately 5% and this wax is then treated again through the acid washing procedure described previously. The product wax can be resweated multiple times to produce different grades of crude scale with varying oil contents and melting temperatures. In solvent pressing, the slack wax is dissolved at a certain ratio of solvent to wax and is then cooled and filtered in a press, removing oil from the wax. Multiple pressing runs can be done to reduce the oil content to specific values.

Synthetic waxes including higher molecular weight alpha-olefins are made through a variety of processes, most notably through Fischer-Tropsch synthesis and Ziegler-Natta synthesis. They may also be formed as oligomeric products via other polymerization pathways. In Fischer-Tropsch processes synthesis gas containing hydrogen and carbon monoxide is passed

over metal-based catalysts, usually containing an iron or cobalt center (Housecroft & Sharpe, 2005). Waxes made through this synthetic route are compatible with mineral waxes and many other types of natural waxes, and are generally used in blends to increase the hardness and solidification temperature of the final product, rather than as a main fraction of a product (Bennett, 1975). The characteristics of Fischer-Tropsch products can be controlled by modifying process conditions like pressure or catalyst selectivity (Housecroft & Sharpe, 2005). The commercial viability of Fischer-Tropsch processes depends greatly on the price of petroleum feedstock used in traditional wax production via distillation. When the price of petroleum feedstock is low, the economics of the Fischer-Tropsch process are not sustainable for widespread application and because of this many industrial operations producing hydrocarbons through this process were shut down in the 1960s. Interest in Fischer-Tropsch hydrocarbons is growing once again due to concerns over the quantity of remaining oil reserves. Waxes synthesized through Ziegler-Natta processes use ethylene or low molecular weight terminal alpha-olefins as monomers to give products of various molecular weights. Waxy products with backbones ranging from 20 to 30 carbons in length represent only a very small fraction of the products coming out plants producing alpha-olefins and must be purified by separation before they can be used (Housecroft & Sharpe, 2005).

1.3 Emulsions

Colloids are ubiquitous throughout nature and find a wide range of applications in industry. A colloid is a mixture with one substance dispersed throughout another at the microscopic level. Mixtures can be classified based on their particle size and stability, going from largest to smallest particle size and lowest to highest relative stability at ambient temperatures, respectively. A general ranking of mixtures according to these factors would be as

follows: dispersion, general suspension, colloidal suspension, lyophobic suspension (suspensoid), lyophilic colloid (emulsoid), emulsion and finally solution, when the dispersed phase of the mixture is fully solvated and the system is homogeneous (Shinoda & Friberg, 1986). Colloids are given different names depending on the state of the phases within them. The different types are outlined in Table 1.

Table 1 - Classification of different colloid types

Phase		Dispersed phase		
		Gas	Liquid	Solid
Continuous phase	Gas	N/A, gases are mutually miscible	Liquid aerosol, e.g. mist	Solid aerosol, e.g. smoke
	Liquid	Foam, e.g. whipped cream	Emulsion, e.g. milk	Sol, e.g. blood
	Solid	Solid foam, e.g. aerogel	Gel, e.g. gelatin	Solid sol, e.g. cranberry glass

An emulsion is a specific type of colloid and is usually defined as a mixture of two immiscible liquids, such as oil and water. One liquid is dispersed as droplets into the other, as seen in Figure 5. The liquid which is broken up is called the dispersed phase, while the surrounding liquid is called a continuous phase or dispersing medium. The liquids are immiscible at standard conditions, and require a surfactant to form a stable emulsion (Bennett, 1968).

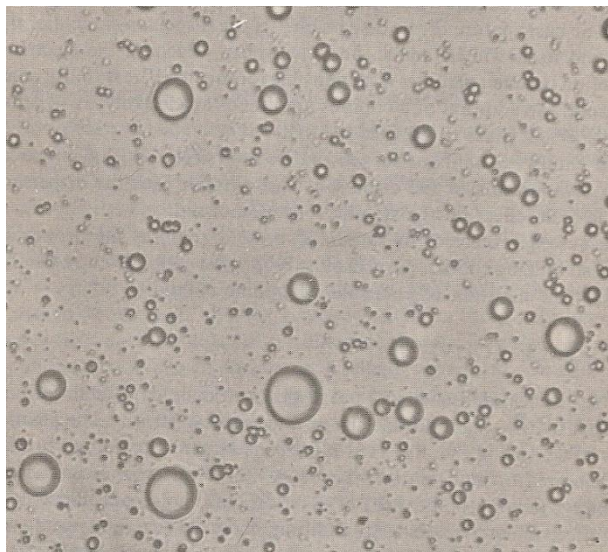


Figure 5 - Example of an oil-in-water emulsion

Emulsions with a continuous phase comprised of water or aqueous solution and a dispersed phase composed of oil or another non-polar substance are generally referred to as oil-in-water (O/W) emulsions. Emulsions with a continuous phase comprised of oil or another non-polar material and a dispersed phase composed of water or an aqueous solution are referred to as water-in-oil (W/O) emulsions. A drop of an O/W emulsion can spread when placed on the surface of an aqueous solution, while a drop of a W/O emulsion can coalesce under the same conditions. It is possible to change the type of emulsion through the process of inversion, which can be produced by changing the balance of components within the emulsion or through mechanical action such as pumping, or chemical action such as modifying the pH or ion concentration of the emulsion. Inversion can also occur if the emulsifying agent is relatively soluble in both phases of the emulsion. An emulsion that has undergone partial inversion after formation is referred to as a dual emulsion and will contain a small fraction of the continuous phase within the dispersed phase. Efforts are usually made to avoid the formation of dual emulsions, though there are select cases where a dual emulsion is desired.

In emulsions, the particle size of the dispersed phase is one of the most significant factors affecting stability. Particle size is affected by the phases present in the emulsion, the amount and strength of any surfactants present in the mixture and the processing conditions used to make the emulsion (Shinoda & Friberg, 1986). As the droplet size of an emulsion decreases, the total surface energy per volume increases as there is much more surface area present between the two phases of the emulsion. Surfactants work to lower the surface energy at the interface of the dispersed and continuous phases, allowing for more thermodynamically favorable configurations leading to stable emulsions with smaller droplet sizes.

When added to a mixture, surfactant molecules will tend to form small aggregates called micelles. Micelles are usually spherical in shape, but may also take ellipsoid or planar shapes. Surfactant molecules in the micelles will organize with their polar heads and non-polar tails in the same fashion as shown in Figure 6, depending on the nature of the continuous phase which they are dispersed into. As a solution becomes saturated with solvated surfactant, it will begin to form numerous micelles at a concentration referred to as the critical micelle concentration or CMC (Shinoda & Friberg, 1986). This point is where surfactants begin to become highly effective as emulsifying agents, and will generally lie at a concentration of less than 1% of the total matter within a mixture for most systems (Becher, 1957). The CMC of a surfactant in a mixture may be determined through a variety of measurements, including but not limited to measurements of electrical conductance, surface tension, light-scattering or viscosity.

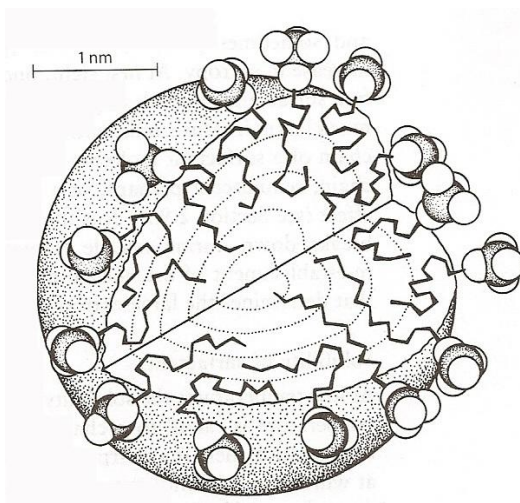


Figure 6 – Micelle structure showing organization of surfactant molecules (Barnes, 2005)

An example of the abrupt changes of various properties at the CMC is seen in Figure 7 from data presented by Preston for the surfactant sodium lauryl sulfate (Preston, 1948).

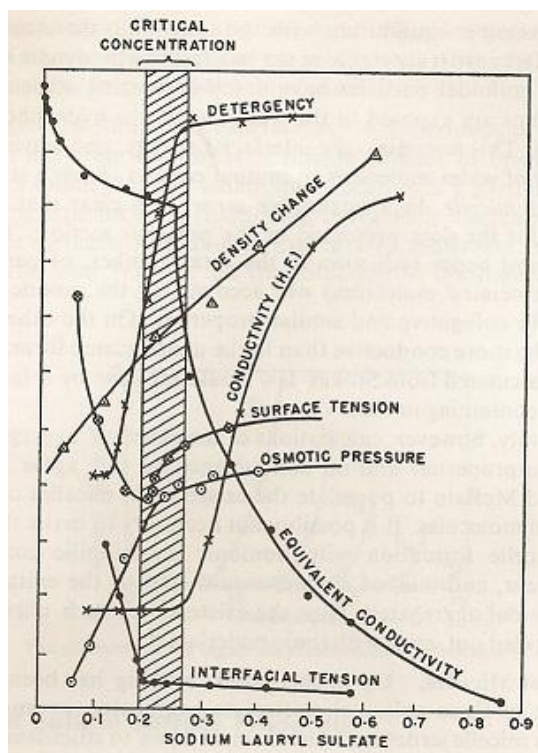


Figure 7 – Example of property changes at a critical micellar concentration for sodium dodecyl sulfate (Preston, 1948)

Stability is of paramount importance when considering the practicality of an emulsion and there are many conditions that can affect this characteristic. The role of a surfactant in an emulsion is to reduce the exceptionally large amount of interfacial energy found in the system, lowering the thermodynamic driving force that acts towards coalescence (Bennett, 1956). As an example, the surface tension of a droplet of olive oil in water in the absence of surfactant is 22.9 dynes/cm at 20° C. Adding 2% of a soap could reduce the surface tension to as little as 2 dynes/cm. If 10 cubic centimeters of olive oil were emulsified in water with 10 μm droplet size, the difference in interfacial energy would be 8.09 kg-cal for a system without any surfactant versus around 0.75 kg-cal for a system with a small amount of surfactant in it (Becher, 1957).

Several theories have been advanced to explain the ways that surfactants can contribute to the stability of emulsions. The various types of surfactants can promote stability via different mechanisms. Surfactants that have polar groups in their composition can contribute to emulsion stability through the formation of a Helmholtz electrical double layer when located at the interface between the oil and water phases of the emulsion (Becher, 1957; Barnes & Gentle, 2005). The ionic portion of the surfactant at the surface of a droplet will repel ions of the same charge and attract those that are oppositely charged, repelling other emulsion droplets. This also leads to the formation of a diffuse layer of ions with charge opposite to the head group of the surfactant around the surface of the droplet, as proposed by Guoy (Becher, 1957). The charge imbalance will decrease progressively from the surface of the droplet outward, until a charge balance is reached. At this point in the diffuse layer, there is zero electrical potential and the net charge in the diffuse layer balances the charge at the surface of the droplet. Further refinement of the diffuse layer theory by Stern suggests that a single ionic layer of finite thickness will surround the surface of the particle, with the diffuse layer extending outward from this initial

layer (Becher, 1957; Barnes & Gentle, 2005). The concept of the electrical double layer is illustrated in Figure 8.

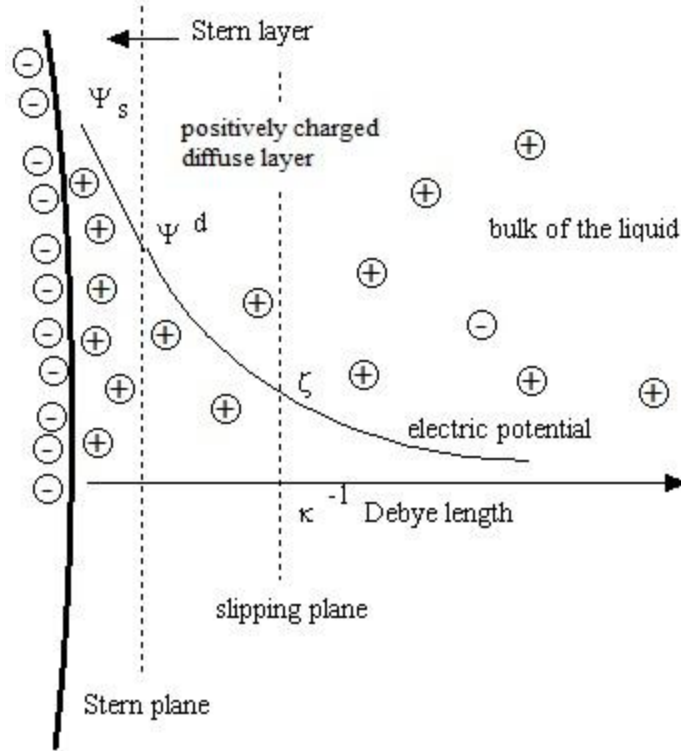


Figure 8 - Diagram showing surface charges and the presence of each part of the electrical double layer

In Figure 8, ψ_s represents the electrical potential at the Stern layer, ψ_d represents the potential of the diffuse layer and ζ represents the zeta potential, or potential at the slipping plane. The slipping plane is the boundary separates mobile fluid from fluid that is electrically bound to the surface of the droplet (Becher, 1957).

$$\kappa = \sqrt{\frac{8\pi n z^2 e^2}{\epsilon k T}} \quad (1)$$

The effective diameter of a particle is equal to the diameter of the particle plus $2/\kappa$, which is determined according to Eq. (1), where κ is the reciprocal of the distance from the surface of the droplet of a plane containing the most charge of the droplet, z is the valence of ions of the

opposite charge to the charge at the surface of the droplet, n is the concentration of ions in the solution at a distance from the double layer, e is the elementary charge, ϵ is the dielectric constant, k is the Boltzmann constant and T is absolute temperature (Becher, 1957). Increasing the concentration of ions in solution will decrease the thickness of the diffuse layer by a value proportional to $n^{-1/2}$, as the surface charge is more readily balanced by the increased ion concentration in solution (Barnes & Gentle, 2005).

Counteracting the repulsive force in this system is a small attractive force due to van der Waals' force between the oppositely charged diffuse ion layers and surface charge layers. These repulsive and attractive forces are subject to change as the distance between droplets changes. As one droplet approaches another, the repulsive forces will increase as the diffuse layers begin to overlap, until reaching a point where the attractive van der Waals' forces begin to overcome them, as seen in Figure 9 (Barnes & Gentle, 2005). The slope of the potential energy curve at a certain point determines whether the sum of forces between droplets is attractive or repulsive in nature. In order for droplets to flocculate, the potential barrier must be overcome by kinetic energy. This potential energy barrier is lowered by increasing the concentration of ions or the valency of ions, as per the Schulze-Hardy rule (Barnes & Gentle, 2005). It is therefore desirable to minimize the concentration of ions in an oil-in-water emulsion to reduce the rate of flocculation and subsequent coalescence.

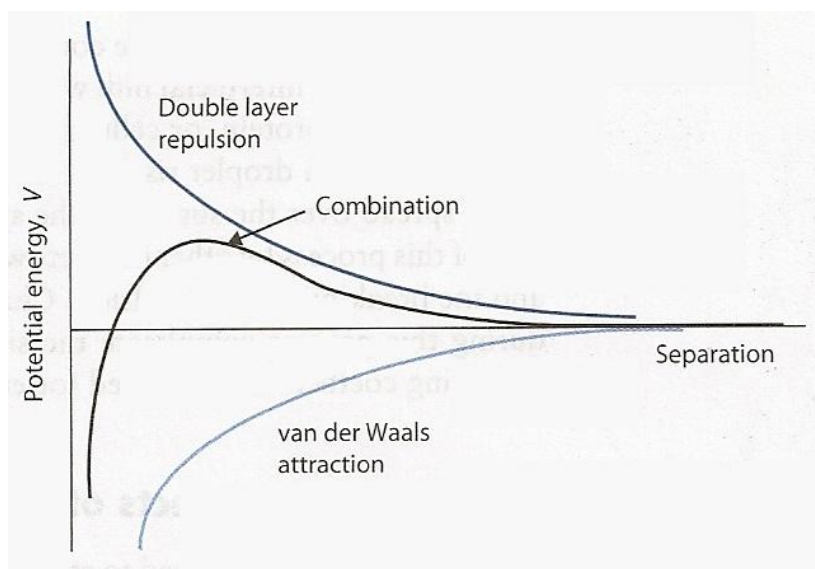


Figure 9 – Potential energy present between two emulsion droplets (Barnes, 2005)

Many commonly used polymeric surfactants are non-ionic. These surfactants do not have a specific charge associated with their head group and therefore do not contribute to stability through the formation of an electrical double layer. When there is no charge associated with the surfactant, changing the ion concentration of the emulsion does not change the effective size or range of the surfactant. As a consequence, non-ionic surfactants can be used much more effectively in non-aqueous systems than ionic surfactants (Napper, 1983). Polymeric surfactants function nearly the same way in dispersions of both solid particles and liquid droplets. The most effective polymeric surfactants are block or graft copolymers that have chain segments that are hydrophilic or lipophilic (Barnes & Gentle, 2005). Whichever chain segment is part of the continuous phase is the segment that will contribute to the stability of the emulsion through steric stabilization. The portion of the surfactant with an affinity towards the dispersion medium will be distributed as loops and tails in solution, while solid particles will have a portion of the surfactant adsorbed to their surface and liquid droplets will have a portion of the surfactant as loops and tails within the droplet, as seen in Figure 10 (Barnes & Gentle, 2005). Homopolymers

and random copolymers may also be used as surfactants, but are generally far less effective than block or graft copolymers. Polyvinyl alcohol or (PVA) is used very commonly in industry to help contribute to emulsion stability (Napper, 1983). Flocculation occurring in systems using polymeric surfactants is generally reversible through dilution of the emulsion, which is not the case for systems using ionic surfactants (Napper, 1983).

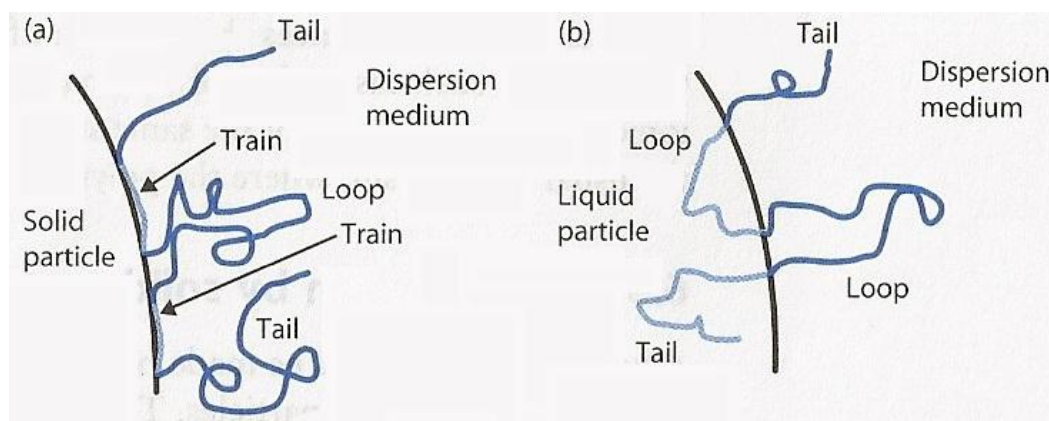


Figure 10 - Distribution of polymeric surfactant in liquid/liquid and liquid/solid colloids (Barnes, 2005)

There are several methods of categorizing the effectiveness of an emulsifier. The method most commonly used in industry is the calculation of a hydrophilic-lipophilic balance or HLB value. The HLB value for non-ionic emulsifiers can be crudely approximated using empirical equations and the molecular composition of the emulsifier in question (Becher, 1957). There are different calculation methods used to determine the HLB value for different types of emulsifiers, depending on their composition. For example, fatty acid esters of polyethylene oxide that give reliable saponification values use an equation that considers a ratio between the saponification value and acid number (or AN), but those that do not give a reliable saponification value use an equation that considers the weight percentage of different sections of the emulsifier molecule (Becher, 1957). More reasonable values for the HLB value can be determined from the solubility of the emulsifier in water and oil phases (Barnes & Gentle, 2005). As a rough

guideline, effective emulsifiers for water in oil emulsions will have HLB values between 3.5 and 6, while oil in oil emulsions will use an emulsifier with a HLB value between 8 and 18; however the type of emulsion formed using a specific emulsifier is not limited only to the HLB value of that emulsifier (Barnes & Gentle, 2005).

Unstable emulsions will show various modes of failure, including creaming, breaking and inversion. Creaming is a form of flocculation that occurs in oil in water emulsions. Creaming is caused by density differences between the oil and water phases of the emulsion, and does not involve coalescence of the droplets within the emulsion but is a necessary precursor for coalescence and breaking in an emulsion. Creaming is not always undesirable and may be used to facilitate a process, like when making butter. Milk is centrifuged in order to create more concentrated oil-in-water emulsion of butter fat in water, so that the cream may be churned and inverted to produce butter, which is a water-in-oil emulsion (Barnes & Gentle, 2005). Eq. (2) shows Stokes' law, which describes the frictional force on small spherical particles in a viscous fluid, and it can give information on the factors involved in governing the rate of creaming within an emulsion. It can be presented as:

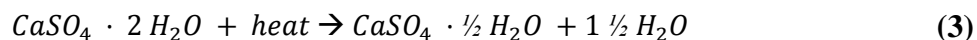
$$v = \frac{2gr^2(\rho_o - \rho_w)}{9\eta_w} \quad (2)$$

where g is the acceleration due to gravity, r is the radius of droplets within the emulsion, ρ_o and ρ_w are the density of the oil and aqueous phases and η_w is the viscosity of the aqueous phase (Bennett, 1956). From this, it can be seen that lowering droplet radius is an effective way of reducing the creaming rate, which is common practice in industry through operations such as homogenization.

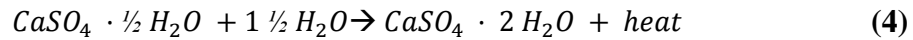
Breaking involves the coalescence of droplets and separation of an emulsion into two distinct phases, representing complete failure of the emulsion. The interfacial energy present in an emulsion is still slightly positive even with the presence of a surfactant and thus there is a thermodynamic drive to reduce total interfacial area via coalescence, as a means of lowering interfacial energy (Barnes & Gentle, 2005). The absolute energy difference will influence the rate of breaking, which must be controlled based on the desired lifetime of an emulsion. Inversion involves swapping the continuous phase of an emulsion from water to oil or vice versa. Inversion can occur as emulsion composition changes due to the addition or removal of material, or as properties such as temperature or pH or electrolyte balance are changed.

1.4 Gypsum wallboards

Drywall has nearly completely replaced antiquated wet plaster methods for interior and exterior surface finishing (Burke & Kingston, 1997). Drywall, or gypsum wallboard, is typically composed of a core containing an aqueous slurry of calcium sulfate hemihydrate (also known as calcined gypsum or stucco) that has been set and hardened, sandwiched between two sheets of cover paper. Stucco is produced by drying, grinding and calcining gypsum rock, and it is reported that as of 2000, 80% of the 23 million metric tons of gypsum produced annually are used in the production of drywall or other building materials (Wantling, 1999). Crude gypsum rock is passed through a drying kiln to remove free moisture and then ground in a roller mill until it reaches the desired fineness. The ground gypsum is then calcined, or relieved of its water of hydration through heating, according to Eq. (3) (Burke & Kingston, 1997).



This calcined gypsum is a less stable form of the 'land plaster' formed after grinding, but has the desired property of being highly reactive with water, allowing it to set quickly when it is used in an aqueous slurry. The setting reaction is the opposite of the calcination reaction, and proceeds according to Eq. (4) (Burke & Kingston, 1997).



The time required for the setting reaction to take place is dependent on the type of calciner used in the process, and can also be controlled by using additives called set retarders or set accelerators (Burke & Kingston, 1997). The setting reaction causes gypsum crystals to interlock forming a strong core structure. These crystals also interact with fibers of the facing paper used to line the gypsum boards and proper adhesion is important to ensure that a useful product is formed.

Wallboards are commercially manufactured through continuous processes operating at high throughput, with the aqueous slurry and other ingredients continuously being deposited between the cover paper sheets. As the slurry is deposited, the gypsum in the core composition reacts with water from the slurry and sets, forming a hardened board product. Boards are then cut to desired lengths and dried to remove excess water remaining from the hydration of the gypsum, yielding a strong building material (Patel & Finkelstein, 1998). Excess water is used during processing to decrease the viscosity of the slurry, in order to facilitate the uniform formation of boards. An example apparatus used for the continuous production can be seen in Figure 11 (Burke, 2000).

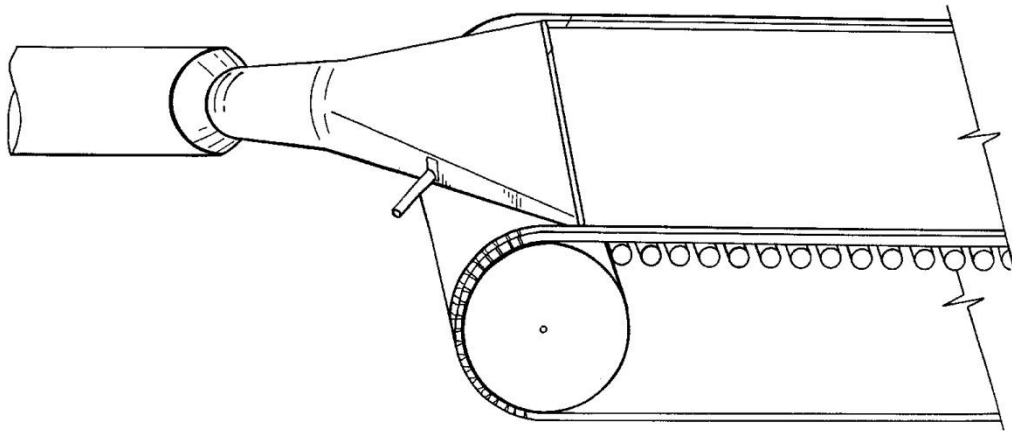


Figure 11 – Example industrial apparatus for continuous gypsum wallboard production (Burke, 2000)

In this example apparatus, gypsum slurry is discharged through a die and extruded onto a conveyor belt on which facing paper is being continuously supplied. A top conveyor belt supplies facing paper to the other side and sizes boards to the desired thickness. Downstream from the extrusion die is a hybrid dryer that incorporates both microwave and convective drying sections. Further downstream is an additional convective dryer that removes the excess water from the gypsum slurry in order to yield a dry board product. Next, additional process elements may be employed to further enhance the properties of the wallboard via the incorporations of various surface coatings. Finally, boards are trimmed and stacked and stored in a warehouse (Burke, 2000).

It has long been standard practice to include water repelling agents into gypsum board formulations in the form of an emulsion, as this allows for greater uniformity in the board properties. Adding water repelling agents in their non-emulsified form often has very little effect on the water repellency of gypsum boards (Camp, 1947). Typical emulsions used to impart water repellency to gypsum wallboards can contain more than one water repelling agent, and

there is an optimum formulation of the emulsion that will provide much better water repellency than either agent on its own. Figure 12 shows an example where water absorption values are compared between two boards using wax alone against using wax and asphalt as water repelling agents in combination at an optimum concentration. Figure 13 shows an example comparing the water absorption values obtained using wax and asphalt combinations ranging from 2.9 parts asphalt:1 part wax to 58 parts asphalt:18 parts wax (Camp, 1947).

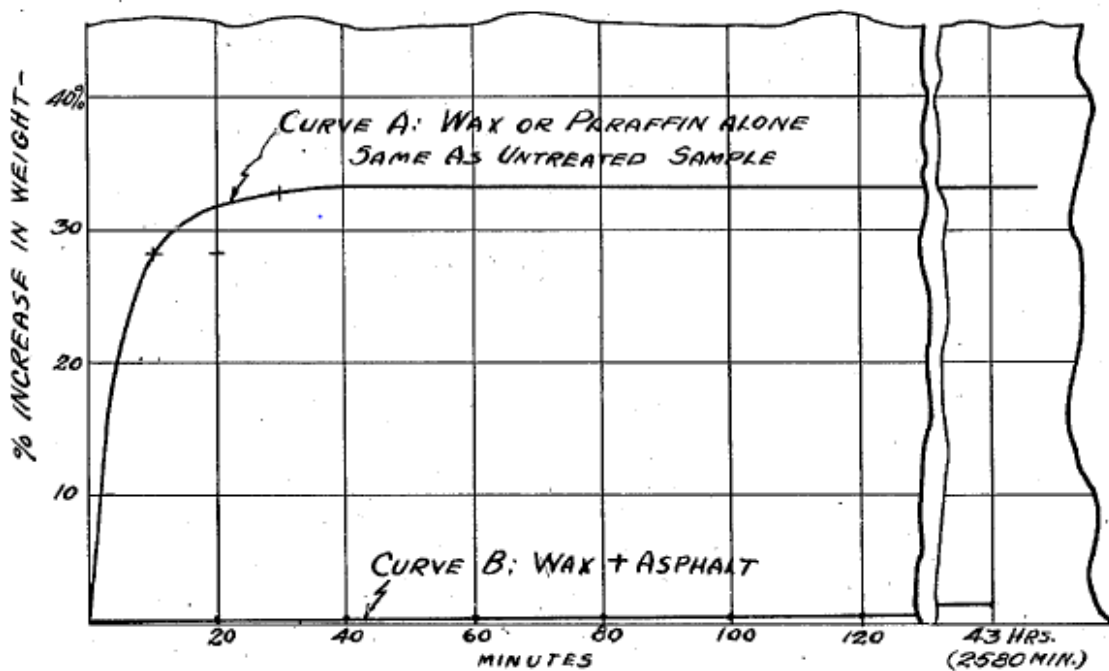


Figure 12 – Example comparing water absorbed by a sample of gypsum wallboard using an emulsion including only wax to a sample using an optimized mixture of wax and asphalt (Camp, 1947)

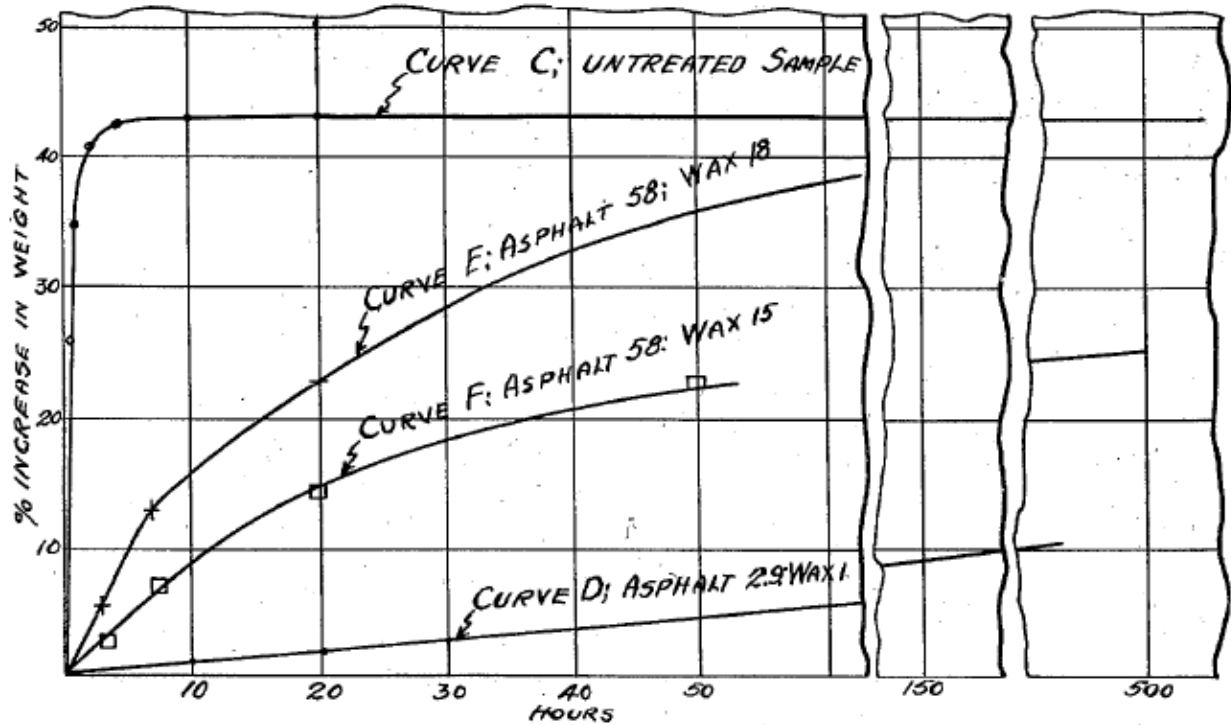


Figure 13 – Example comparing water absorption values obtained using a range of emulsions with compositions containing from 2.9 parts asphalt:1 part wax to 58 parts asphalt:18 parts wax (Camp, 1947)

From these examples, it can be seen that the water absorbed by a sample of gypsum wallboard made with an emulsion formulation outside of an optimum range can be nearly identical to that of an untreated sample after a certain length of time. Many emulsion formulations and compositions for making wallboards from gypsum are known in the art, each being tailored to the specific needs of their producers. Gypsum wallboards are often used in areas where they are exposed to wet or humid conditions, such as the exterior of buildings underneath siding and cladding, or in bathrooms. For these reasons, the boards often require the inclusion of a specialized emulsion in order to obtain manageable processing characteristics and also to impart water repellency to the final product. Water repellency is an important characteristic because gypsum, or stucco, is very hygroscopic in nature and water absorption can lead to weakening of the boards. To illustrate this, a sample of gypsum core immersed in water for two hours at room temperature can absorb up to 50 weight% water (Sellers et al., 1992). Emulsions used in gypsum

wallboards can contain many different hydrophobic elements to accomplish this goal, but waxes have become the preferred ingredient (Sinnige, 2005). The industry standard for water absorption in gypsum wallboards is approximately 5% by weight of water. While many emulsion compositions are able to reach this level of water repellency, the components used in them often have deficiencies and undesirable side-effects.

Wax-asphalt emulsions¹ were commonly used in the fabrication of gypsum boards; however these emulsions were subject to several problems (Greve & O'Neill, 1976). Wax-asphalt emulsions tend to be unstable and separate over time, giving a product that may be difficult or impossible to re-mix, becoming useless after standing for an extended period of time. This is of particular concern, as it is common practice in industry for emulsions to be produced in one location, transported and held in storage at another location for extended periods of time (Bornstein, 1995). Un-emulsified asphalt forms lumps in the boards and eventually bleeds out through the paper liner, giving off coloured and non-homogenous products. Additionally, the nature of the refining processes that yield asphalt leads to variation in the characteristics and qualities of emulsions that use asphalt as a hydrophobic ingredient (Sinnige, 2005). One approach to minimize these undesired side effects was to include additional components such as borate compounds or PVA to act as additional emulsifying agents in the formulation (Long, 1978). The use of other hydrophobic components, such as montan and lignite waxes, can reduce these problems slightly but not to a satisfactory level. Emulsions using these waxes can also cause build up of sludge in processing equipment used during emulsification (Sinnige, 1999). Siloxanes have also been investigated as water repelling agents, but their cost is prohibitive in industrial applications (Sinnige, 2005).

¹ Greve, D. R., O'Neill, E. D. Water-Resistant Gypsum Products. U.S. Patent 3,935,021, January 27, 1976.

Gypsum board formulations have been developed using emulsions consisting of water, hydrocarbon wax, PVA and emulsifying agents, leading to a reduction of the undesirable qualities (Sinnige, 2005; Sinnige, 1999). PVA is typically included not only to increase water repellency, but also to increase adhesion between the gypsum core and the facing paper (Bornstein, 1995). These emulsions are typically produced by forming a pre-blend of molten wax and non-aqueous emulsifying agents, which is mixed with a heated aqueous solution of PVA, stabilizers and additional emulsifying agents. The emulsion is rapidly cooled to form a stable emulsion with defined particle size before it is used in gypsum boards (Sinnige, 1999).

1.5 Research objectives and outlines

The main objective of this thesis project is to develop a process for modifying hydrophobic waxy materials or polymers for use as emulsifiers in water based formulations. The specific tasks associated with completing this objective are:

- To modify normal paraffins or synthetic hydrocarbon waxes, having a melting point less than 110 °C , with maleic anhydride;
- To develop a process for the modification of waxes that avoids the use of inert gases, high pressures, solvents and hazardous materials;
- To maximize the yield and minimize or eliminate any waste from the process;
- To provide a modified wax with properties desirable for creating stable oil-in-water emulsions;
- To optimize emulsion formulations such that using the new modified wax product yields emulsions that match or exceed the performance qualities of emulsions currently being produced using commercially available emulsifiers.

In order to achieve these goals, the following steps are taken:

- Develop and carry out a design of experiments in order to determine optimal conditions for the production of highly maleated waxes on a small laboratory scale;
- Apply the appropriate conditions to larger bench scale reactions in order to produce enough modified wax to carry out product testing in proprietary emulsion formulations;
- Test the efficacy of modified waxes in various proprietary emulsion formulations;
- Test the emulsion formulations made using modified waxes that have desirable qualities as replacements for commercially available emulsifiers in samples of gypsum wall boards and engineered wood products.

Chapter 2: Wax Maleation

2.1 Introduction

A great deal of focus has gone into the modification of various polymers via functionalization with polar or reactive monomers. Chemical functionalization can be used to improve characteristics such as paintability, adhesion or compatibility with other polymers in a blend or composite, or to create additional reactive sites on the polymer backbone (Sheshkali et al., 2007). Many different monomers such as glycidyl methacrylate, acrylic acid and diethyl maleate may be used to impart various functionalities to polyolefins, but one of the most common and important reactive modifiers is considered to be maleic anhydride (or MAH) (Sheshkali et al, 2005). Many commodity polymers can be functionalized with MAH; however polyethylene tends to show the highest grafting efficiency (Machado et al., 2001). Polymers that have been functionalized with MAH are often used as adhesives and compatibilizing agents (Heinen et al., 1996), but have also shown to be effective when used as emulsifiers. MAH grafting can occur through many different techniques, such as through a free-radical initiated reaction in a melt (Moad, 1999; Machado et al., 2000) or solution state (Yang et al., 2003), melt-grafting via ultrasonic (Zhang & Li, 2003) or thermomechanical (Qui & Takahiro, 2005) initiation as well as by photografting. Free-radical melt grafting is the most widely used method of modification, as it is generally the most viable in terms of economics and environmental impact (Sheshkali et al., 2007).

2.2 Wax maleation methods

2.2.1 Peroxide initiated grafting of maleic anhydride to wax backbones

It is widely known that the overall process of free radical grafting occurs through three steps: initiation, propagation and termination. The mechanisms of grafting MAH to a polyolefin backbone follow these general steps; however there are several side reactions that can contribute to some degree of uncertainty in the final product distribution (Yang et al., 2003). An overall reaction mechanism for the grafting of MAH to a linear polyethylene backbone is presented in Figure 14 (Sheshkali et al., 2007).

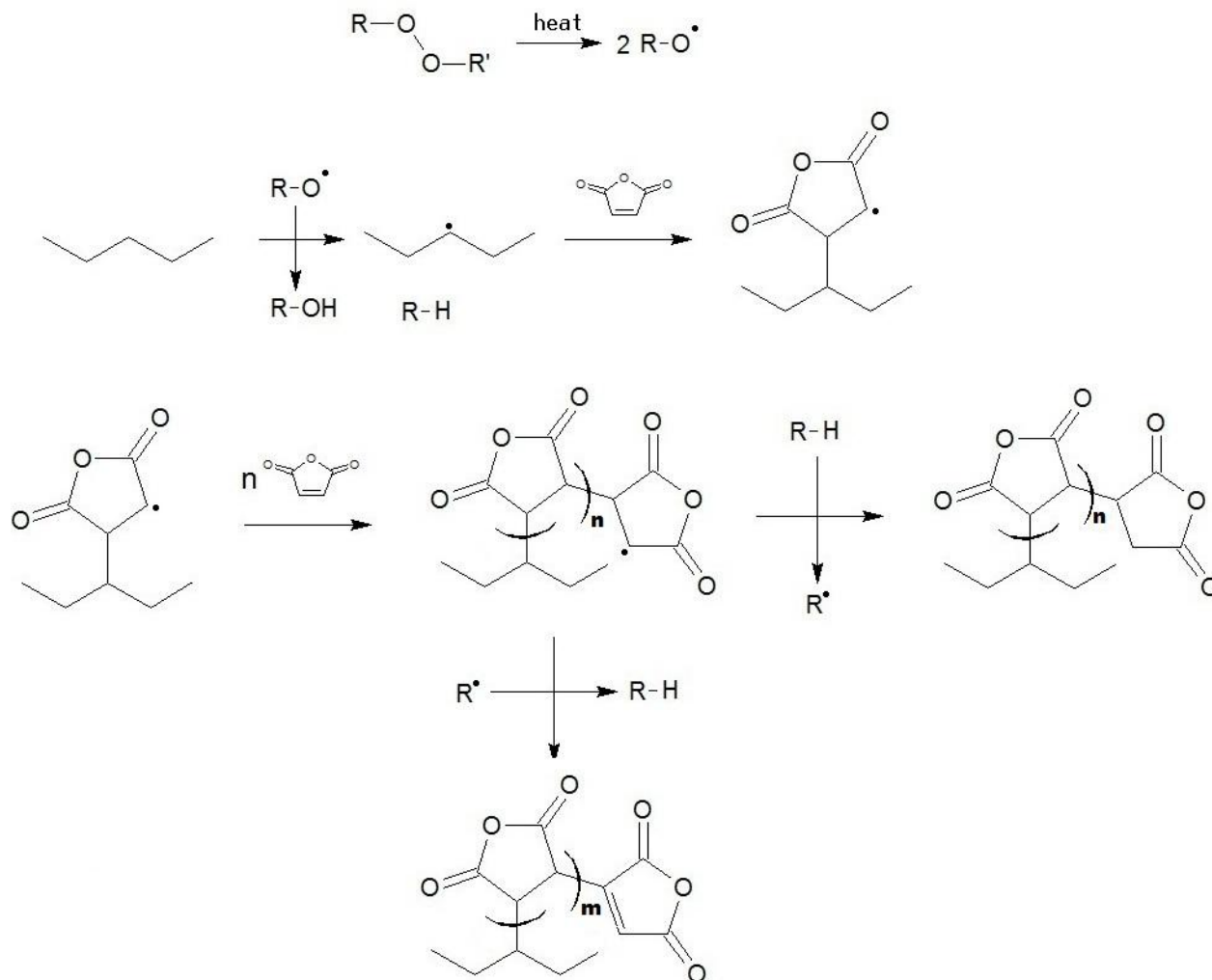


Figure 14 - Mechanism for grafting MAH to a polyethylene backbone

In the desired reaction where MAH is grafted onto a wax backbone the first step is initiation which occurs through the thermal homolysis of a peroxide initiator, producing free radicals which abstract hydrogen atoms from the wax. The next step occurs when the wax macroradical reacts with MAH to give a grafted product, resulting in a succinic anhydride (or SA) radical. Under certain conditions this radical can then undergo a propagation reaction, producing a homopolymer of MAH attached to the wax backbone. Alternatively, the macroradical can go on to abstract a hydrogen atom from another wax molecule and produce

another wax macroradical. Termination occurs via hydrogen abstraction or radical dismutation between two active species, though several side reactions can also occur. Possible side products, as shown in Figure 15, can include ungrafted homopolymers of MAH, crosslinked polymer species and occasionally bridged maleated polymer species. MAH is a strong electron acceptor, so termination reactions tend to move towards disproportionation and hydrogen abstraction rather than coupling, leaving an exceptionally small chance for the formation of bridged species (Yang et al., 2003).

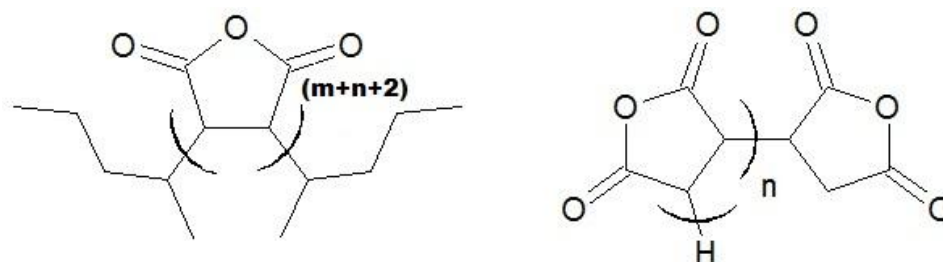


Figure 15 – Bridged side product formed through termination by coupling and homopolymerized MAH

The homopolymerization of free MAH occurs in nearly all peroxide initiated reactions of MAH grafting; however it can be controlled to a reasonable degree. In a system with polyethylene wax, crosslinking between wax molecules is a factor, increasing the average molecular weight of the final products and causing gellation in some cases (Sheshkali et al, 2005). In polypropene waxes, β -scission is dominant, reducing the average molecular weight of the final product (Shi et al., 2001). Paraffin wax is composed mostly of linear polyethylinic chains and thus may undergo a small increase in molecular weight during reaction without control over the reaction. One method of controlling the possible side reactions is to add a small amount of a Gaylord additive as a mediator. Gaylord additives are substances that are a nitrogen, phosphorous or sulfur containing electron donors and are a type of free radical transfer agent

(Sheshkali et al, 2005; Yang et al., 2001). Disadvantages to using these additives to control crosslinking side reactions include a reduction in the grafting degree of MAH and an increase in cost and complexity of the reaction system.

2.2.2 Thermal addition of maleic anhydride to wax backbones

Another method of functionalizing a wax backbone with MAH is through thermal addition. The modification progresses through well known chemistry, by the ene reaction. The ene reaction is a form of molecular addition involving the substitution of a substance containing a double bond on to an olefin containing an allylic hydrogen through an allylic shift of one double bond and, transfer of the allylic hydrogen and the formation of a chemical bond between the unsaturated moieties (Hoffman, 1969). The olefinic ene component usually contains at least one degree of unsaturation in its structure; however fully saturated compounds that exhibit a very high degree of ring strain can also fill this role. The conformation of the ene component is important in determining its reactivity as a primary hydrogen is abstracted most readily, followed by a secondary hydrogen and then tertiary hydrogen (Hoffman, 1969). Thus, the distribution of normal or internal double bonds in a wax backbone and the amount of branching present will determine the distribution of products from the ene reaction. An enophile will preferentially react with the least substituted allylic position of the ene component and the kinetics of the reaction are increased as the local substitution of the carbon-carbon double bond increases. Generally, the enophile is the electrophilic reagent in the ene reaction and reactivity can be improved by using a reagent with electron withdrawing substituents (Carey & Sundberg, 2007). For this reason, MAH with its dual carbonyl groups is one of the most common enophiles; however a staggeringly large variety of compounds may be used to impart various functionalities

(Hoffman, 1969). The mechanism of the reaction between MAH and an alpha-olefin is shown in Figure 16.

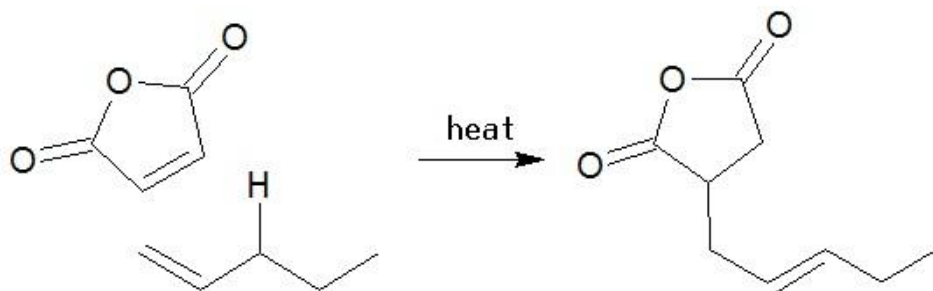


Figure 16 - Reaction mechanism of the ene reaction occurring between MAH and a-olefin

2.3 Materials used in experiments

In efforts to optimize the production of maleated waxes suited to the goals of this research, several different base waxes, peroxides and samples of MAH from different sources were used in experiments. The materials used in the following experiments and their providers are as follows:

- Potassium hydroxide (KOH) and maleic anhydride (99%) from Sigma Aldrich
- Maleic anhydride from Bartek (99.5%)
- Luperox DI *tert*-butyl peroxide (98%), Luperox P *tert*-butyl peroxybenzoate (98%) and Luperox A98 benzoyl peroxide from Sigma Aldrich
- Acetone, methanol and xylenes, all reagent grade, from Caledon
- IGI 1212U fully refined paraffin wax from The International Group, Inc.
- Prowax 563 slack wax from Imperial Oil
- AlphaPlus C30+ and AlphaPlus C30+ alpha-olefin waxes from Chevron Phillips

All reagents were used as received without any additional purification.

2.3.1 Comparison of waxes used in maleation experiments

Two types of paraffin waxes were used in grafting reactions to produce a maleated wax emulsifier. The first type is a fully refined paraffin wax, which comprises the bulk of the non-aqueous phase of emulsions used in gypsum wallboards. This wax has exceptionally low oil content and contains only linear and branched paraffin isomers of narrow molecular weight distribution. There are no cyclic paraffin isomers present, so the distribution of products generated is moderately well defined. The second type is a slack wax cut from an earlier stage in the wax refining process, and has significantly higher oil content. This wax contains linear, branched and cyclic isomers and also has a fairly broad molecular weight distribution. The products of grafting reactions using slack waxes are not as well defined as those using fully refined paraffin waxes.

Table 2 - Properties of paraffin waxes used in grafting experiments

Wax	Type	Oil Content (%)	Product distribution	Average Molecular Weight (g/mol)	PDI
IGI 1212U	Fully refined paraffin	<0.5	77.62 wt% linear 22.38 wt% branched	403	1.013
Imperial Prowax 563	Slack paraffin	4-10	27-32 wt% linear	534	1.309

Two types of synthetic alpha-olefin waxes were also used in thermal addition reactions to produce maleated wax emulsifiers. These waxes are very well defined in composition and have only one reactive site, which gives the benefit of having reaction products that are closer to uniformity.

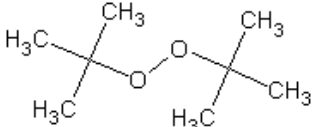
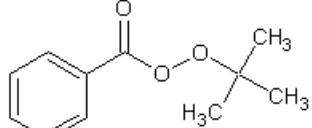
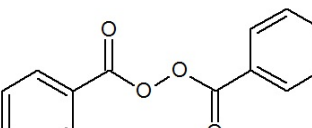
Table 3 - Properties of synthetic waxes used in thermal addition experiments

Wax	Oil Content (%)	Product Distribution	Average Molecular Weight (g/mol)
CP AlphaPlus C30+HA	1.9	75.4 wt% n-alpha-olefin 4.2 wt% linear internal olefin 19.4 wt% branched olefin	419
CP AlphaPlus C30+	1.9	71.4 wt% n-alpha-olefin 2.9 wt% linear internal olefin 24.7 wt% branched olefin	419

2.3.2 Comparison of peroxides used in grafting reactions

Three different peroxides were chosen for use in reactions at different temperatures so that peroxide decomposition rates and radical concentrations could be kept relatively constant (Arkema Inc., 2009).

Table 4- Properties of peroxides used in grafting experiments

Peroxide	Structure	Molecular Weight (g/mol)	Half-life Temperatures (°C)
<i>Tert</i> -butyl peroxide		146.23	1 hour – 149 10 hour – 129
<i>Tert</i> -butyl peroxybenzoate		194.23	1 hour – 122 10 hour – 104
Benzoyl peroxide		242.23	1 hour – 92 10 hour - 73

2.4 Experimental procedures

Several methods of modification were used in the study of the maleation of various waxes. For the paraffin and slack waxes, maleation took place via a free-radical initiated grafting approach. For the synthetic alpha-olefin waxes, maleation took place via thermally initiated ene reactions.

A design of experiments was initially carried out for the peroxide initiated systems in order to determine the optimal values of several variables. Variable ranges were chosen based on experiments conducted in literature, with parameters in desirable ranges. Experiments were carried out with variables in the following ranges:

- Reaction time varying between 1 – 12 hours per run;
- Reaction temperature varying between 70 – 160 °C;
- Maleic Anhydride loading from 2 – 20 weight % based on the weight of wax;
- Peroxide loading from 0.6 – 10 weight % based on the weight of wax.

Stirring was held constant throughout experiments of the same size scale. Initially, experiments were carried out with 100g of wax in a round bottom flask. When adequate results had been produced, experiments were then scaled up to 500g of wax and carried out in a one litre glass reaction vessel supplied by Ace Glass. For experiments carried out in round bottom flasks stirring was provided by a magnetic stir bar and heating was provided by a silicone oil bath. Experiments carried out in a glass reaction vessel were heated by using an Ace Glass heating mantle attached to a Love Instruments bench-top temperature controller with temperature being recorded by a J-type thermocouple and with stirring provided by an IKA dual-range mixer and a 4 blade impeller with blades at a 45° pitch.

After peroxide initiated grafting to give maleated waxes had been extensively studied, thermal maleation was investigated. Experimental parameters were chosen based on the optimal values obtained in peroxide grafting experiments and on the chemistry of the ene reaction. Thermal maleation experiments were carried out using alpha-olefin waxes as the wax backbone, a reaction time of eight hours, reaction temperature of 200°C and MAH loading of 18.7 wt%. The MAH addition temperature was varied between room temperature and 200°C, and reactor configuration and MAH sources were investigated during the experiments.

2.4.1 Free-radical maleation of paraffin waxes

Several experimental configurations were examined during the optimization of conditions for making modified waxes via free-radical maleation. Several semi-batch approaches were tested, producing varying results. The peroxide addition methods are ordered in terms of complexity as follows: bulk addition being the simplest approach; pulse addition being in the middle; and the continuous addition method being the most complex of the three. The MAH addition method uses much of the same approach as the peroxide addition methods, with some slight variation.

2.4.1.1 Bulk peroxide addition method

The simplest of the reaction methods employed was the bulk addition method and is referred to as such because the peroxide in the system is added all at once. In this method, molten wax at approximately 100 °C was added to the reaction vessel. The desired amount of peroxide and solid MAH pellets were then added to the vessel immediately after adding the wax. Stirring was started after all reactants were introduced into the vessel and the vessel was sealed. In some cases, the reaction vessel was degassed with nitrogen but it was not always necessary to do so. After degassing was started, the reaction mixture was brought up to the desired

temperature and stirred continuously to the end of the reaction. 'Time zero' was marked as the point where the reaction mixture reached the desired temperature, usually after about 30-40 minutes. The reaction was allowed to progress for the desired period of time and then the products were removed from the reactor and purified through one of several washing techniques. Each.

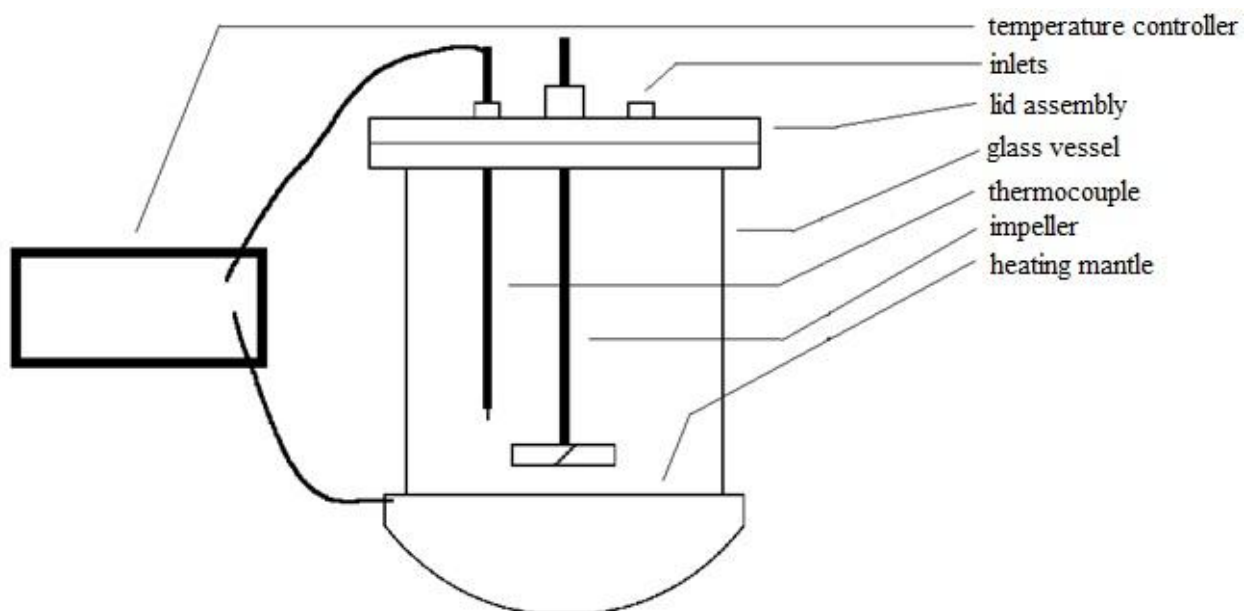


Figure 17 shows an example of the experimental apparatus used in this approach.

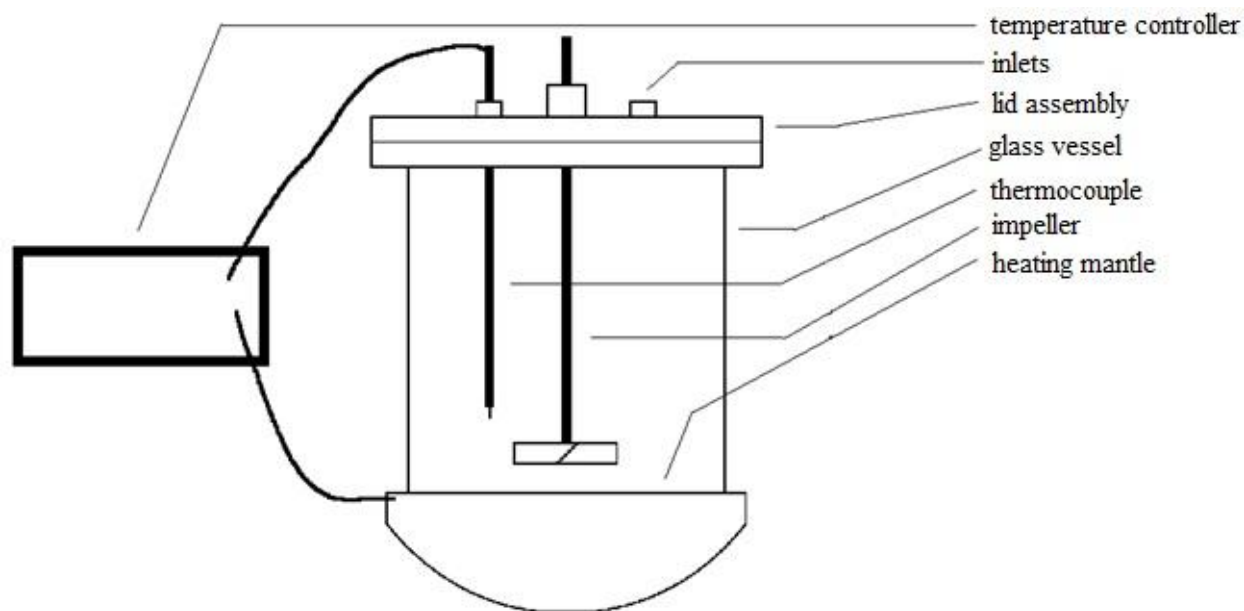


Figure 17 - Apparatus used in bulk addition method

2.4.1.2 Pulse Peroxide addition method

The next reaction method in terms of complexity is the pulse addition method. In this system, peroxide was added over time through several evenly spaced and evenly measured doses. As before, molten wax was added to the reaction vessel. The desired amount of solid MAH was added to the vessel immediately after adding the wax. The vessel was sealed and stirring was then started. The reaction vessel was then brought up to the desired temperature and stirred continuously to the end of the reaction. In some cases, the reaction vessel was then degassed with nitrogen, but again, it was not always necessary to do so. Once the degassed reaction vessel stabilized at the desired temperature, the first portion of peroxide was added to the reaction mixture, and this was marked as 'time zero'. The peroxide was split into four even portions and added at time intervals depending on the desired reaction time. After the desired reaction time had been reached, the products were removed from the reaction vessel and purified. The apparatus used in this method is the same as that used in the bulk addition method.

2.4.1.3 Continuous peroxide addition method

The final method of peroxide addition is the continuous addition method. In this system, peroxide was added evenly over the course of a reaction by pumping with Cole Parmer peristaltic pump. Molten wax was added to the reaction vessel and the desired amount of solid MAH pellets was added to the vessel immediately after. The vessel was sealed and stirring was then started. The reaction vessel was then brought up to the desired temperature and stirred continuously to the end of the reaction. The reaction vessel contents and peroxide were then degassed with nitrogen and peroxide pumping was started. Peroxide was pumped in to the mixture at a constant rate over the entire course of the reaction, which was dependant on the desired reaction time. After all the peroxide was pumped into the reaction vessel, the products were removed and purified. Figure 18 shows an example of the experimental apparatus used in this approach.

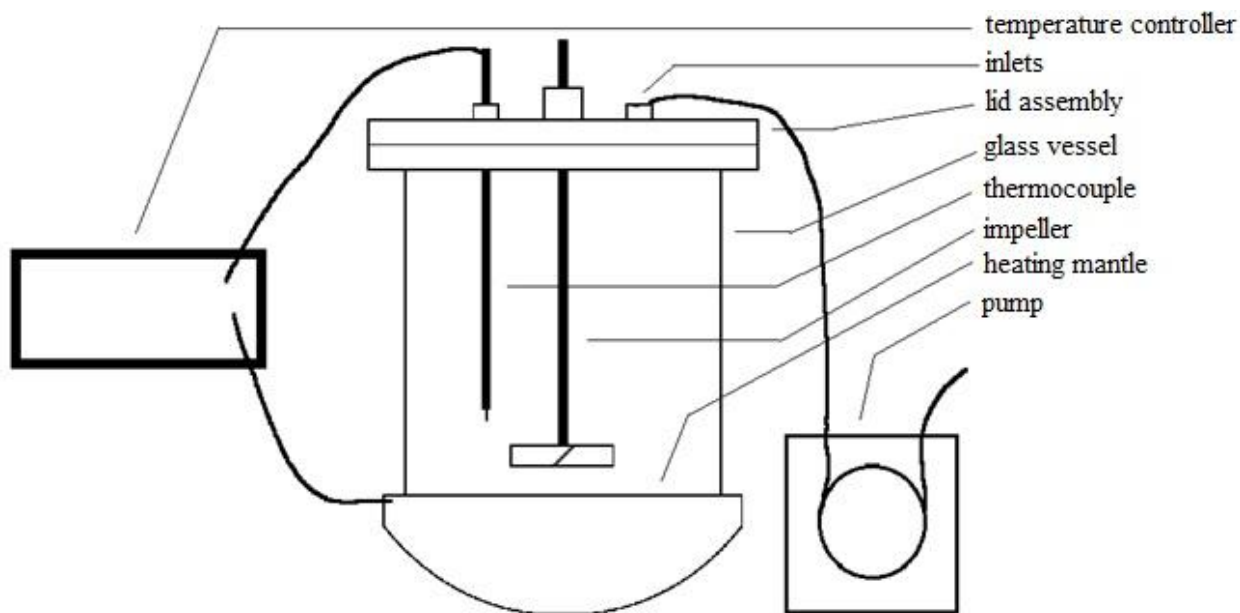


Figure 18 - Apparatus used in continuous peroxide addition method

2.4.1.4 Maleic anhydride addition method

A slightly different approach was used in the MAH addition method. Peroxide was introduced in one large portion at the beginning of the reaction and then the MAH was added slowly over time. Molten wax was added to the reactor and brought up to the desired temperature. Peroxide was then added to the reaction vessel and stirring was started. No degassing was required in this method. The temperature was stabilized and the mixture was allowed to remain at the reaction temperature for one hour. Solid MAH was then added to the reaction mixture in several small, evenly spaced portions, similar to the peroxide pulse addition method. After the desired reaction time had been reached, the product was removed from the vessel and then purified. The apparatus used in this method is the same as that used in the bulk addition method.

2.4.1.5 Ball milling method

In this approach, a planetary ball mill was used as an alternative apparatus. Small stainless steel reaction vessels of approximately 100mL volume were filled with the desired amount of wax and MAH. Several small stainless steel ball bearings were added to each vessel and the vessels were sealed. Samples were not degassed during the reaction. After the vessels were sealed, they were heated to the appropriate temperature and then placed inside the ball mill apparatus, which then spun them to promote mixing and internal heating via friction caused by the ball bearings within the vessels. The temperature of the reaction mixture was occasionally checked and adjusted accordingly if the mixture began to cool slightly. After the reaction had been run for the desired period of time, the product was purified by one of several washing techniques (refer to Section 2.4.3).

2.4.2 Thermal maleation of alpha-olefins

The thermal addition of maleic anhydride to alpha-olefins was investigated with the intention of simplifying process conditions and reducing reaction costs. Experiments were initially conducted in a reaction vessel that was open to the atmosphere. This allowed unreacted MAH to leave the reactor via sublimation, saving the washing the final product. Further experiments were later conducted in a reaction vessel that was sealed to the atmosphere, with the interest of recapturing the sublimated MAH.

2.4.2.1 Thermal maleation in an open system

For thermal maleation in an open system, solid pellets of alpha-olefin wax were added to the reaction vessel, and then depending on the desired conditions, MAH was added to the system either at room temperature or once the vessel had been heated to the desired reaction temperature. A lid with several unsealed openings was used to cover the reactor, allowing MAH to escape via sublimation during the reaction. The vessel was heated to the desired temperature and stirring was started once all the wax had melted. After the desired period of reaction time, the products were removed from the vessel. Figure 19 shows an example of the experimental apparatus used in this approach.

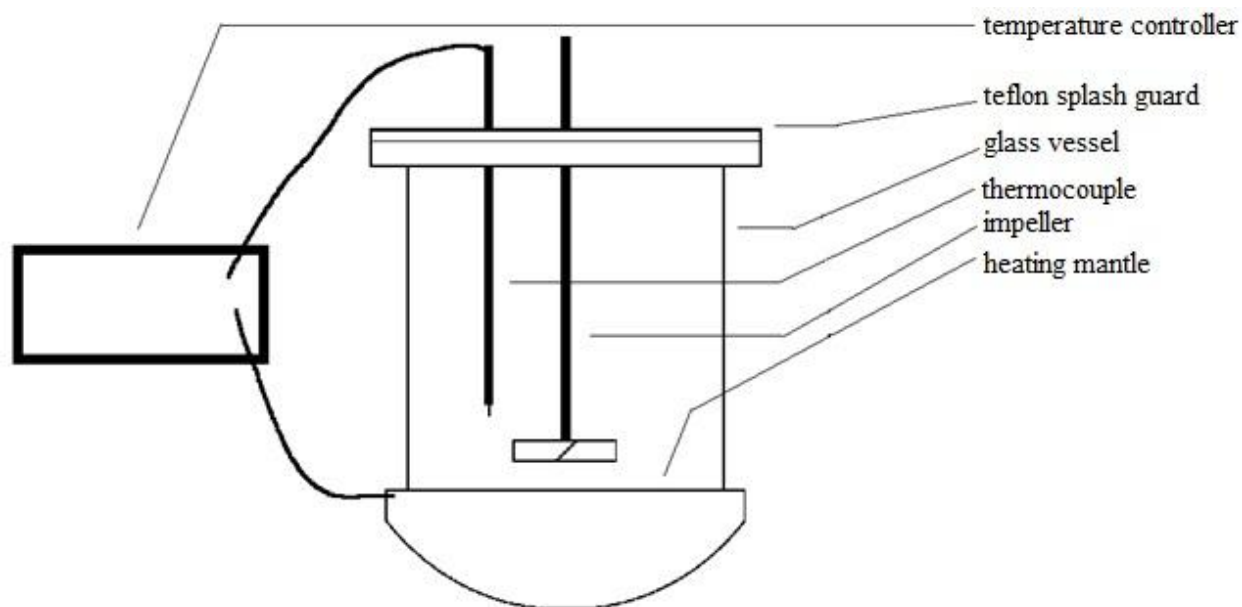


Figure 19 - Apparatus used in an 'open' thermal maleation system

2.4.2.2 Thermal maleation in a closed system

The procedure for thermal maleation in a closed system was typically the same as that in the open system. A lid that was sealed to the atmosphere was used to simulate more real world conditions and to test for any difference in grafting degree when MAH was not allowed to sublime from the vessel. In some experiments, a recapture system was attached to the lid, consisting of a heat traced line leading to a condenser setup to test the possibility of recapturing unused MAH. Figure 20 shows an example of the experimental apparatus used in this approach.

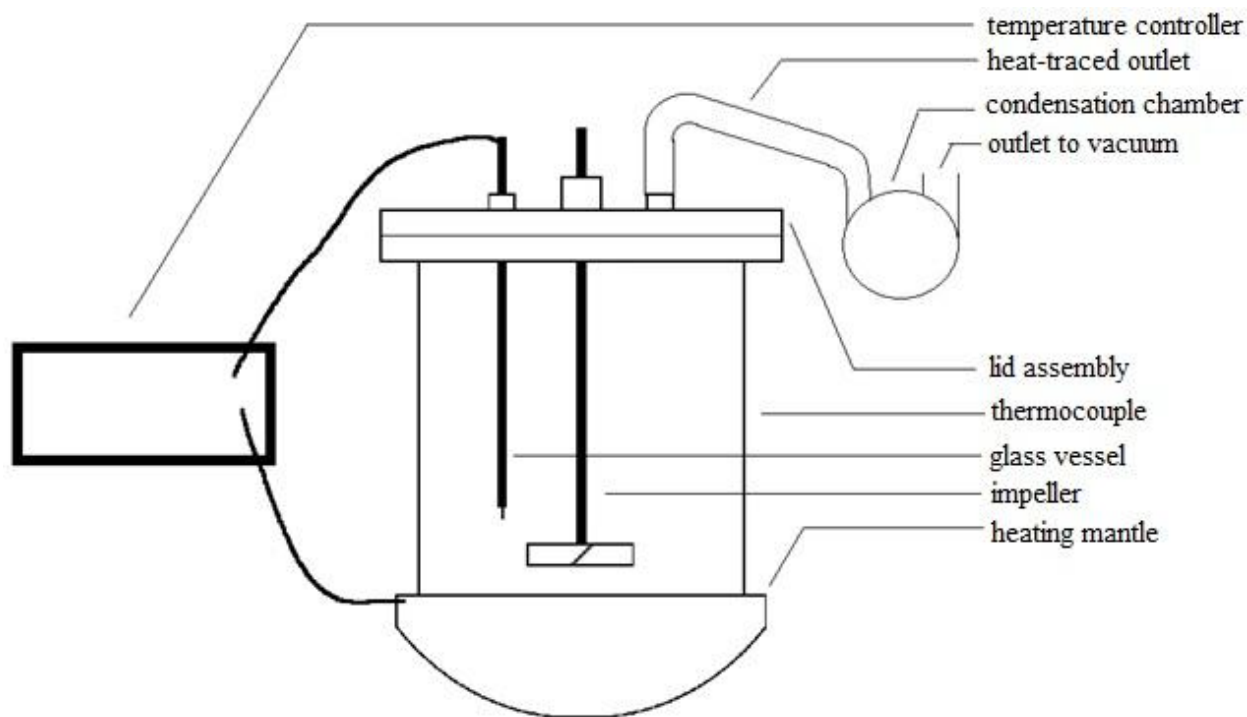


Figure 20 - Apparatus used in a 'closed' thermal maleation system

2.4.3 Product purification methods

Simple product purification steps were taken in order to obtain an accurate representation of the degree of grafting in each of the modified wax samples. Acetone washing, water washing and vacuum purification were used in order to remove any undesired components from the final product, such as unreacted MAH and peroxide. During purification by washing with acetone, molten wax samples were added to acetone and stirred to ensure adequate dispersion of the wax. Samples were left overnight and then vacuum filtered through a Buchner funnel, rinsed several times with additional acetone and the collected filtrate was dried overnight in a vacuum oven. During purification by washing with water, wax was added to a water bath that was at a temperature just higher than the melting point of the modified wax, typically around 70°C, and was allowed to stir for several hours. The mixture was then cooled and the solidified modified wax was removed from the top. The aqueous solution was vacuum filtered through a Buchner

funnel and the filtrate was washed several times with additional water. The collected product was then dried overnight in a vacuum oven. During purification by vacuum, the product wax was taken from the reaction vessel and placed directly in a vacuum oven overnight.

2.4.4 Quantification of grafting extent via acid number titration

AN tests were used in order to determine the extent of maleation for each of the modified polymer samples. Tests were conducted according to ASTM Standard Test D974. For each AN test, one gram of modified wax was measured and dissolved into 40mL of hot xylenes. After the wax was dissolved, 3-4 drops of a phenolphthalein solution in methanol were added. A 0.1M solution of KOH in methanol was loaded into a burette and the sample was titrated until the end point was reached, which was shown by a marked colour change of the solution from clear and nearly colourless to pink. The volume of the KOH solution added was recorded and then the AN was calculated from Eq. (5), where V_B is the volume of base solution used in the titration in mL, C_B is the concentration of the base solution in mol/L, MW_{KOH} is the molecular weight of KOH in g/mol and m_{wax} is the mass of the wax sample in the titration in g.

$$AN = \frac{V_B C_B MW_{KOH}}{m_{wax}} \quad (5)$$

AN can be related to the more commonly used measurement of “degree of grafting” (or DG) through Eq. (7). Grafting efficiency (or GE) can be calculated through Eq. (7), where MAH loading is the amount of MAH by weight of wax in the reaction.

$$DG = \frac{V_B C_B MW_{MAH}}{2 \cdot m_{wax} \cdot 1000} \times 100\% \quad (6)$$

$$GE = \frac{V_B C_B MW_{MAH}}{2 \cdot m_{wax} \cdot 1000 \cdot MAHloading} \times 100\%^2 \quad (7)$$

2.5 Results and discussion of wax maleation methods

2.5.1 Products formed via peroxide initiation methods

The initial set of experiments to determine optimal reaction ranges was carried out via the peroxide pumping method using tert-butyl peroxide with variable ranges previously described. After optimal values were determined, experiments were expanded to incorporate other peroxide addition methods and different peroxides to further expand on the scope of wax maleation. The collected results of the peroxide grafting experiments are seen in Figure 21.

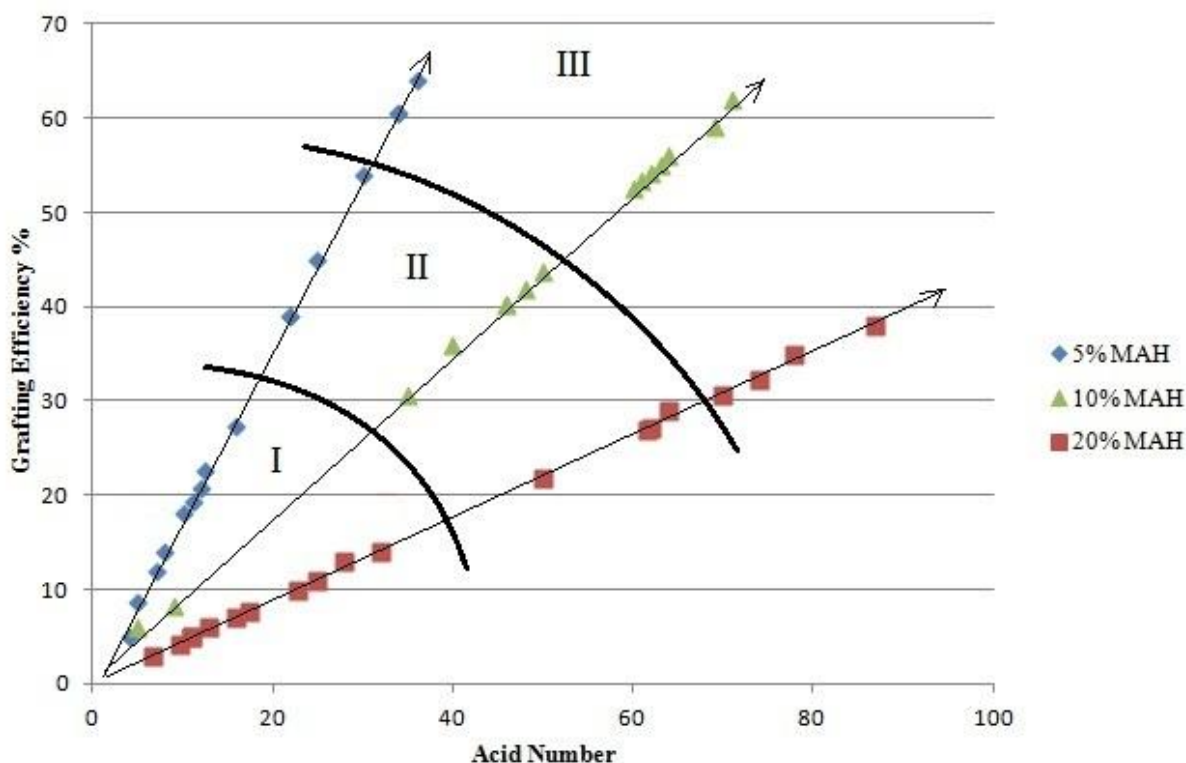


Figure 21 - Collected results of wax grafting experiments with region I representing the continuous peroxide addition experiments, region II representing the pulse peroxide addition and region III representing the bulk addition of peroxide and MAH addition reaction methods

Several trends can be observed from this set of data. It was noted that the graph could be divided into sections based on the method of peroxide addition that was used during each experiment. In Figure 21, region I represents the continuous peroxide pumping and ball milling addition methods, region II represents the pulse peroxide addition method and region III represents the bulk addition of peroxide and MAH addition methods. While there are some outliers for each section, this trend is generally accurate. Within each region of the graph, the amount of peroxide used in the reaction increases as the line moves to the right for each MAH loading amount. As the amount of peroxide in the reaction increases, the AN of the maleated wax does as well and the grafting efficiency with respect to MAH in the reaction also rises. Table 5 shows a comparison of the average values of AN, degree of grafting and grafting efficiency as well as evaluations of the robustness and sensitivity of each method and the purity of the product obtained through each method with MAH loading of 20% and using TBP as the initiator.

Table 5 - Comparison of average values for 20% MAH loading for each reaction method, across varying reaction conditions

Method	Average Acid Number	Average Efficiency (%)	Average Degree of Grafting (wt%)	Precision	Sensitivity	Purity
Bulk Peroxide Addition	48.4	21.2	4.2	Medium	Medium	Low
Pulse Peroxide Addition	43.7	19.1	3.8	Lowest	High	Low
Continuous Peroxide Addition	22.5	10.1	2.0	Low	High	Low
MAH Addition	77.7	33.9	6.8	Highest	Low	High
Ball Milling	32	14	2.8	High	Low	Low

It can be seen that the MAH addition method yielded the highest overall level of grafting, had the highest robustness, lowest sensitivity and the highest product purity. Precision is described based on the variance between AN measurements for samples for each category, so a low value of precision will correspond to high sample variance, and a high value of precision will correspond to a low sample variance. Sensitivity is based on the performance of the reaction when experiments are conducted with or without first degassing with nitrogen. The formation of homopolymerized MAH or other impurities in the presence of oxygen corresponds to high sensitivity. Purity is based on the difference between the AN of the product when measured after washing with acetone and when measured without additional washing, as well as the presence of gelation or ungrafted homopolymers of MAH.

Experiments conducted by the peroxide pumping method were very sensitive to air, often resulting in gelation and a high degree of free homopolymerized MAH. One example of this can be seen in Figure 22. Homopolymerized MAH appeared as a red precipitate almost immediately after the pumping of peroxide was started. In just 30 minutes a crosslinked product could be observed as a separated layer of darker wax at the bottom of the reaction vessel.

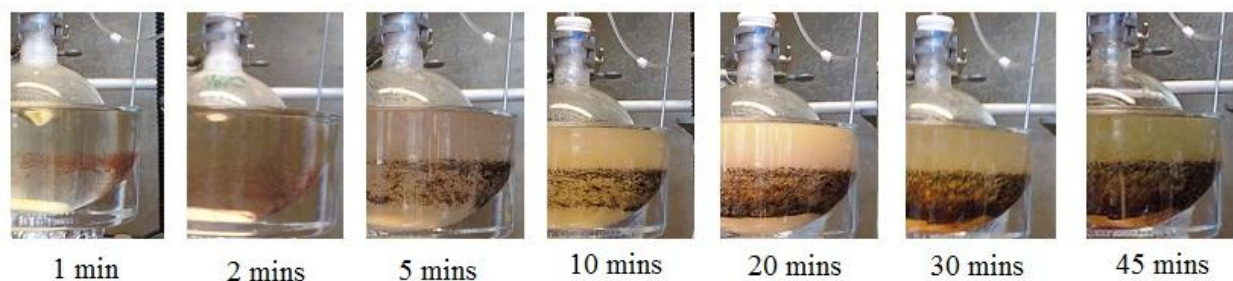


Figure 22 - Time lapse showing reaction progression of a continuous peroxide pumping experiment

Figure 23 and Figure 24 show the grafting results of experiments using the bulk peroxide addition method, TBP as the initiator, reaction temperature of 160 °C and reaction time of 10

hours. Both AN and grafting efficiency increased as the amount of peroxide in the system was increased for MAH loading amounts of 10% and 20% by weight of wax in the system. The slope of the AN graph is larger, approximately doubled, for the reaction with 20% MAH loading when compared to the reaction with 10% MAH loading. The slopes of the efficiency graphs are the same at both loading levels. From this it can be said that the rate at which MAH grafting occurs is first order with respect to MAH concentration. The slopes of the graphs for acid number and grafting efficiency both drop as the amount of peroxide in the reaction increases. With respect to radical concentration, the rate of termination is second order, while the rate of MAH grafting is first order or less (Sheshkali et al., 2007). As the concentration of peroxide increases, the rate at which termination reactions occur increases faster than the rate at which MAH grafting reactions occur.

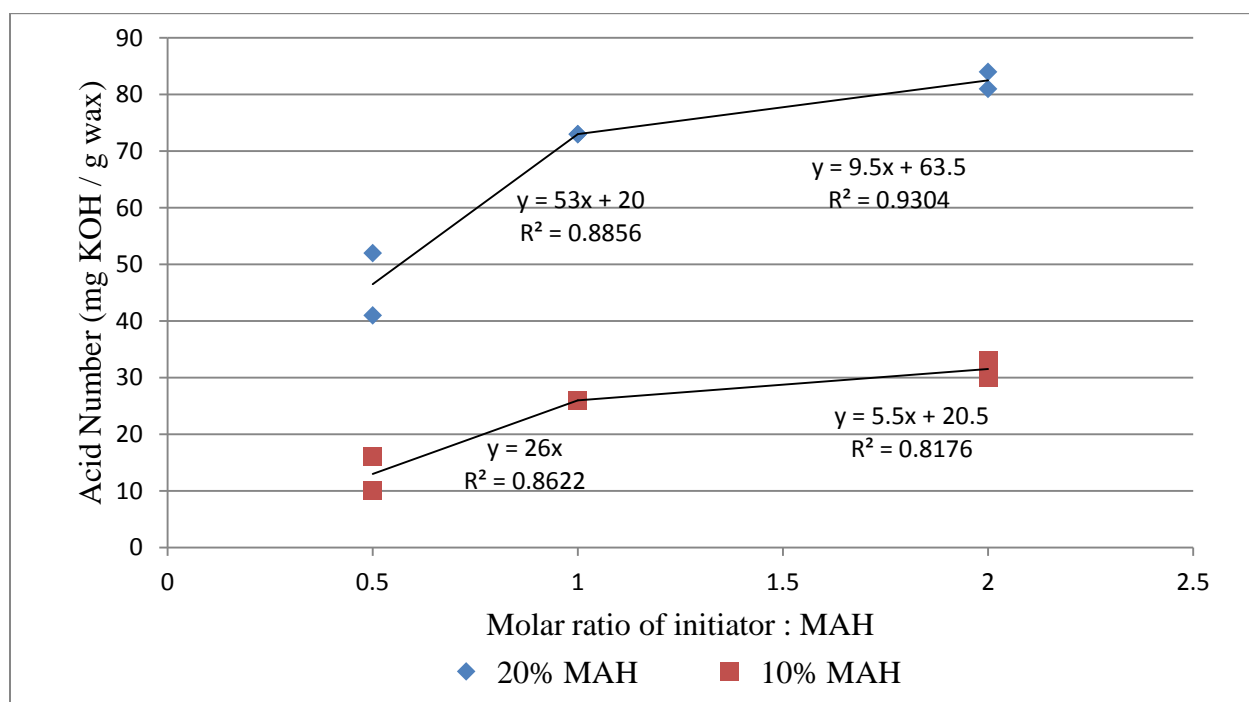


Figure 23 – Acid number vs. molar ratio of initiator TBP to MAH in the product formulation at 160 °C, bulk addition of peroxide reaction method

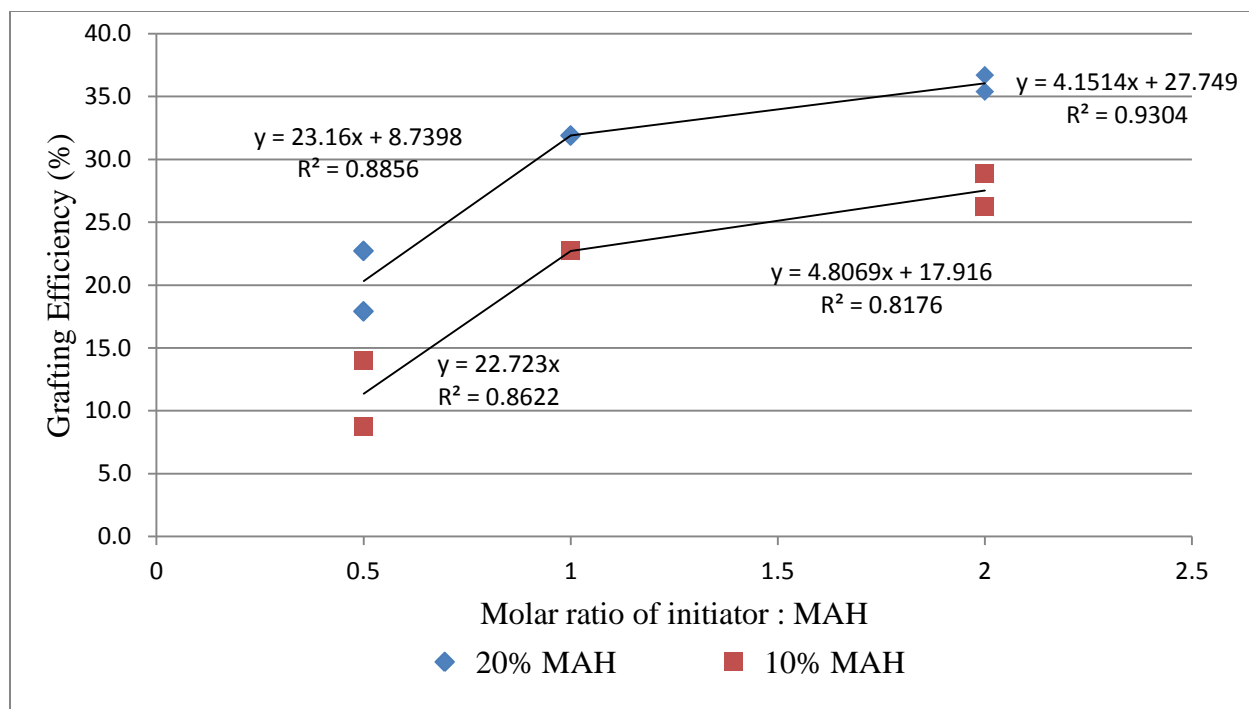


Figure 24 – Grafting efficiency vs. molar ratio of initiator TBP to MAH in the product formulation at 160 °C, bulk addition of peroxide reaction method

Figure 25 and Figure 26 show the results experiments using the bulk peroxide addition method, TBPB as the initiator, reaction temperature of 130 °C and reaction time of 10 hours. At the 20% MAH loading level, similar trends are observed in both AN and grafting efficiency as in the data shown in Figure 23 and Figure 24 for experiments carried out with TBP as the initiator.

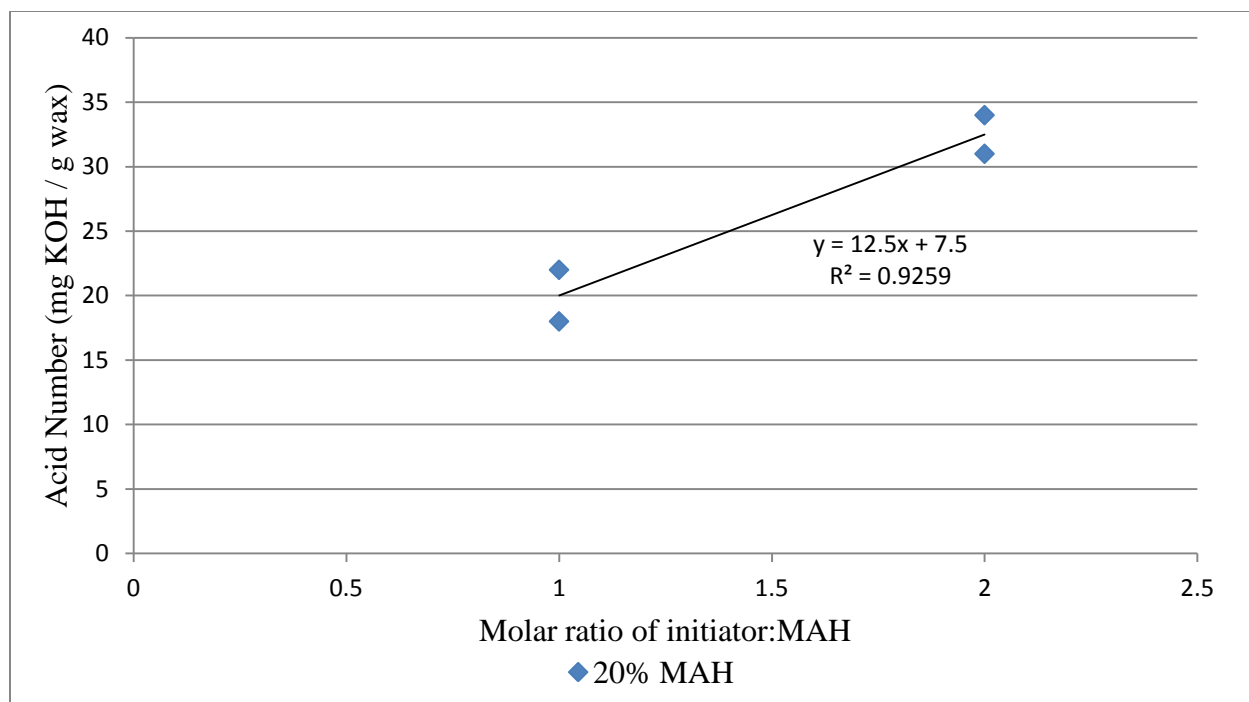


Figure 25 - Acid number vs. molar ratio of initiator TBPB to MAH in the product formulation at 130 °C, bulk addition of peroxide reaction method

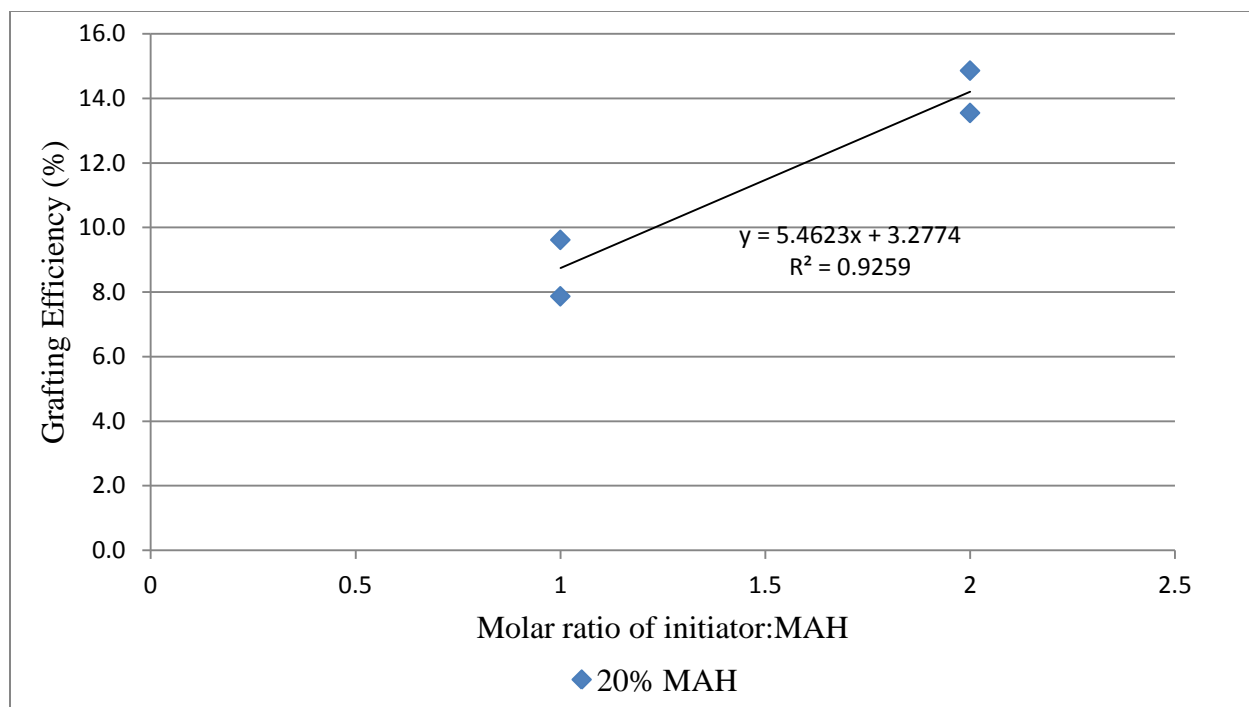


Figure 26 - Grafting efficiency vs. molar ratio of initiator TBPB to MAH in the product formulation at 130 °C, bulk addition of peroxide reaction method

Figure 27 and Figure 28 show the grafting results of experiments using the MAH addition method, TBP as the initiator, reaction temperature of 160 °C and reaction time of 10 hours. Contrary to the bulk peroxide addition method, the slope of the graph of AN results for 10% MAH loading is higher than the slope of the graph of AN results for 20% MAH loading.

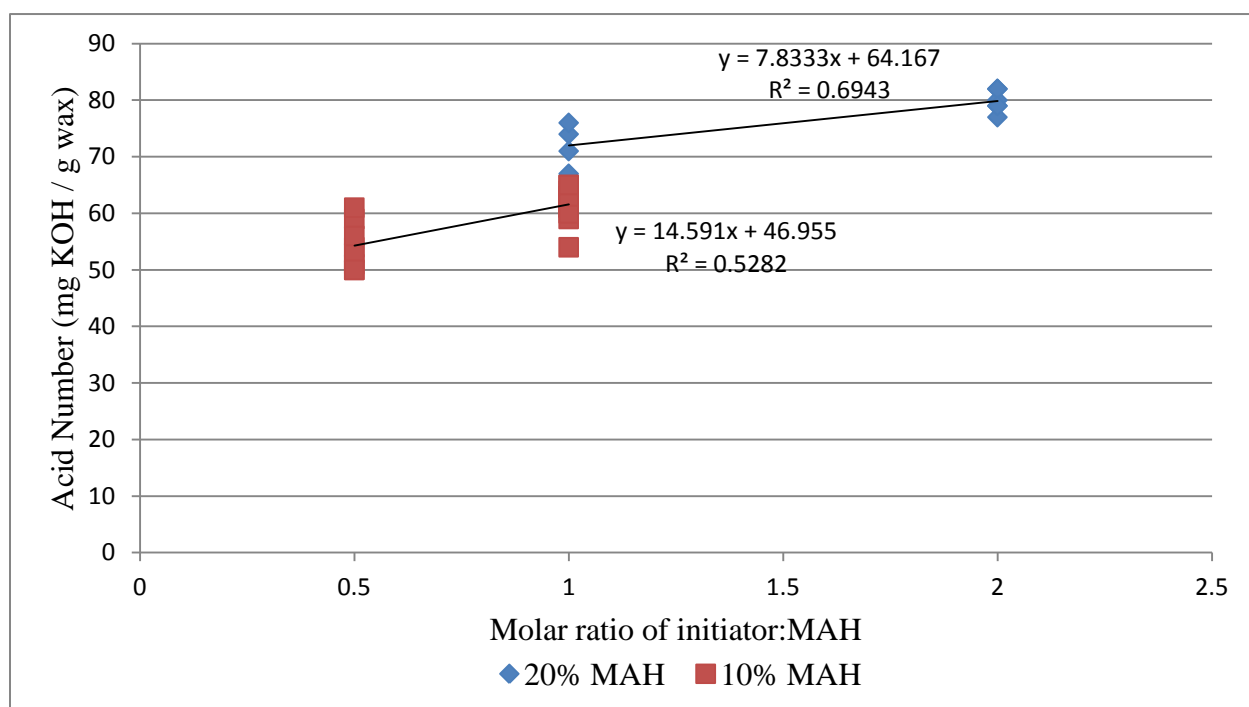


Figure 27 – Acid number vs. molar ratio of initiator TBP to MAH in the product formulation at 160 °C, MAH addition reaction method

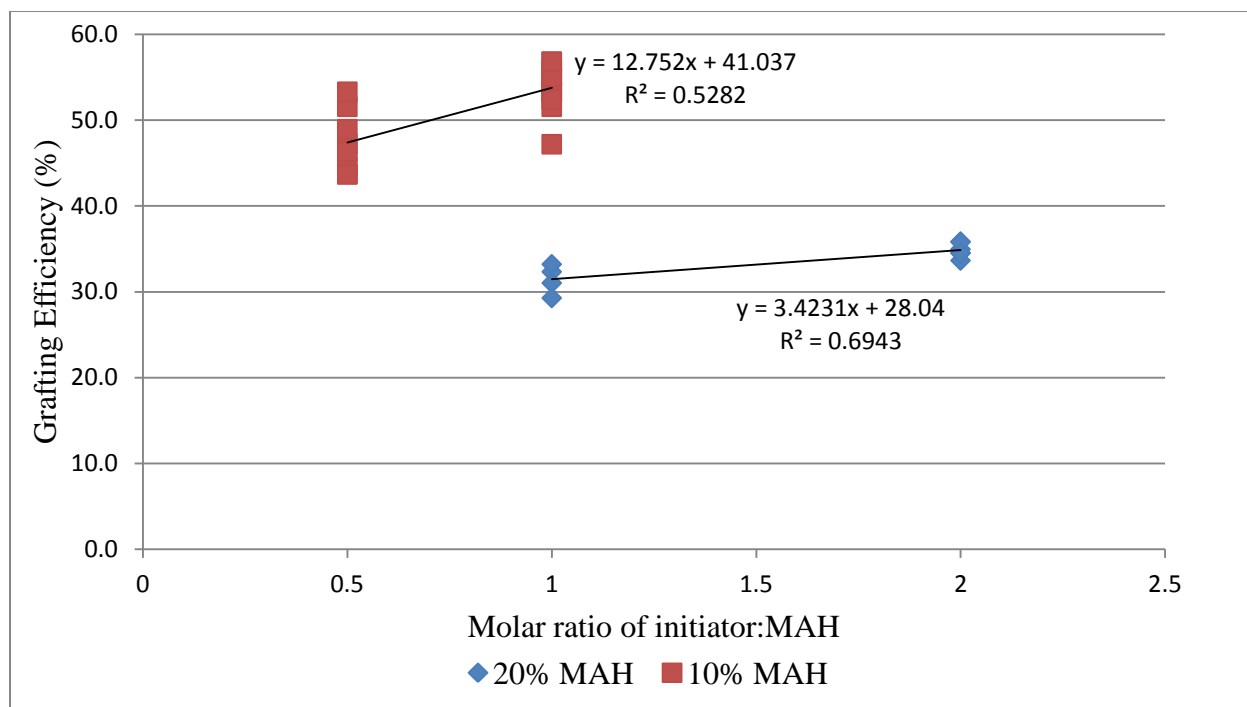


Figure 28 – Efficiency vs. molar ratio of initiator TBP to MAH in the product formulation at 160 °C, MAH addition reaction method

The difference in the grafting results obtained through the different grafting methods can be explained, in part, by considering the relative concentrations of each reagent in the reaction mixture. The concentration of active peroxide radicals produced can be determined through a peroxide half-life decomposition equation (Hiemenz & Lodge, 2007), Eq. (8), where $[P]_t$ is the concentration of active peroxide radicals at time t , $[P]_0$ is the initial concentration of peroxide, f is the peroxide decomposition efficiency parameter and $t_{1/2}$ is the half-life time of the peroxide at the reaction temperature.

$$[P]_t = 2 f [P]_0 \frac{1^{t/t_{1/2}}}{2} \quad (8)$$

In the peroxide pumping method, peroxide is slowly introduced and has the lowest overall residence time, therefore at the completion of the experiment there will be a significant fraction of peroxide that has not decomposed and become an active radical. Accordingly, the

pulse addition method will have a slightly lower portion of non-activated peroxide at reaction completion, while the peroxide in the bulk and MAH addition approaches will have essentially non-activated peroxide at reaction completion. With more active radicals in the reactive system, it follows that the rate of grafting will increase.

With respect to peroxide type (Figure 23 and Figure 24 for TBP versus Figure 25 and Figure 26 for TBPB), grafting improved as the half-life temperature of the peroxide initiator increased, not only because of the higher reaction temperature but also because of the increase of the activity of the peroxide radicals generated after initiator decomposition. Initiators with higher half-life decomposition temperatures contain more energetic O-O bonds, in turn producing radicals that are less stable and more reactive when the bond homolysis occurs. Examining the structures of the radicals, shown in Figure 29, it can be seen that peroxybenzoyl radicals are more stable due to the electrophilic nature of the resonant structure than tert-butyl radicals containing an electron-donating t-butyl group (Clayden et al., 2001).

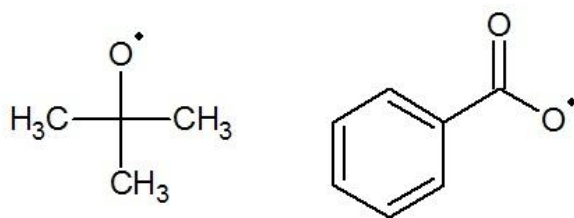


Figure 29 - *t*-Butyl and peroxybenzoyl radicals formed in grafting reactions

The initial concentration of MAH relative to the concentration of peroxide in the reaction system can be ordered from highest to lowest as such: peroxide pumping method; pulse addition method; bulk addition and ball milling methods; and finally the MAH addition method. This can explain the abundance of homopolymerized MAH produced in the continuous addition method and the relative absence of the same in the MAH addition method. Lower initial MAH

concentrations will push the system to produce a greater abundance of wax macroradicals that will go on to produce a grafted wax product, while higher initial MAH concentrations will increase the rate at which homopolymerized MAH is produced.

The progression of the grafting reaction was tracked by drawing samples from a reaction periodically. In Figure 30, it can be seen that the largest part of the grafting reaction is completed within the first four hours and the grafting extent continues to rise very slowly after that. This is important as it allows for optimization of a commercial process to produce this wax, allowing for greater throughput of a product made in a batch process.

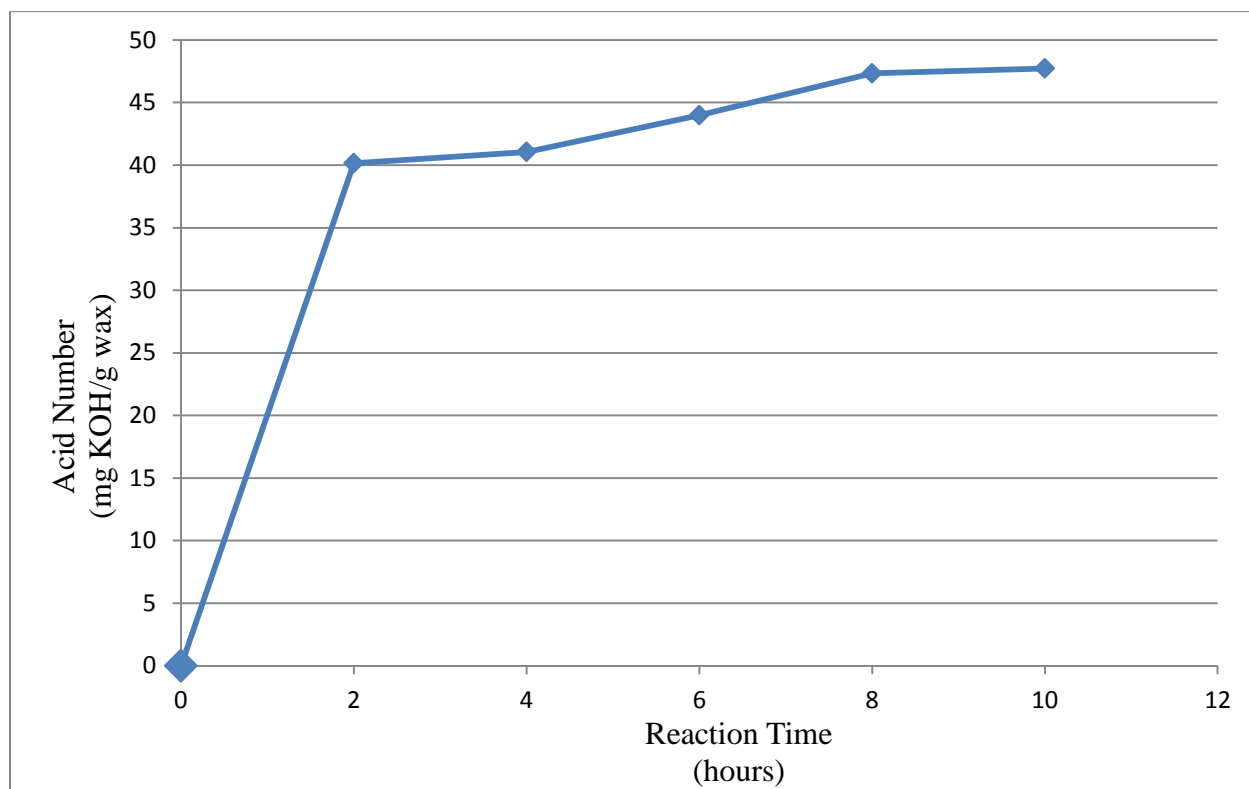


Figure 30 – Grafting over time experiment – 10% MAH by weight of wax, 1:1 mol ratio TBP:MAH, 160 °C

2.5.1.1 Thermal stability of waxes produced via peroxide initiation

The thermal stability of products formed through peroxide initiated grafting was also investigated. In a commercial setting these waxes would be stored in tanks in a molten state, around a temperature of 100 °C, in order to facilitate their use and eliminate the large amount of preparation time required to melt the grafted wax on-demand. As such, it is important that the wax does not undergo any change when it is held at this temperature for an extended period of time. In order to test this, samples of wax from a completed reaction were held at a temperature of 100 °C in a drying oven with measurements being taken every 24 hours. From Figure 31 it can be seen that the waxes produced through peroxide initiated grafting are chemically stable when held at a temperature of 100 °C for extended periods of time.

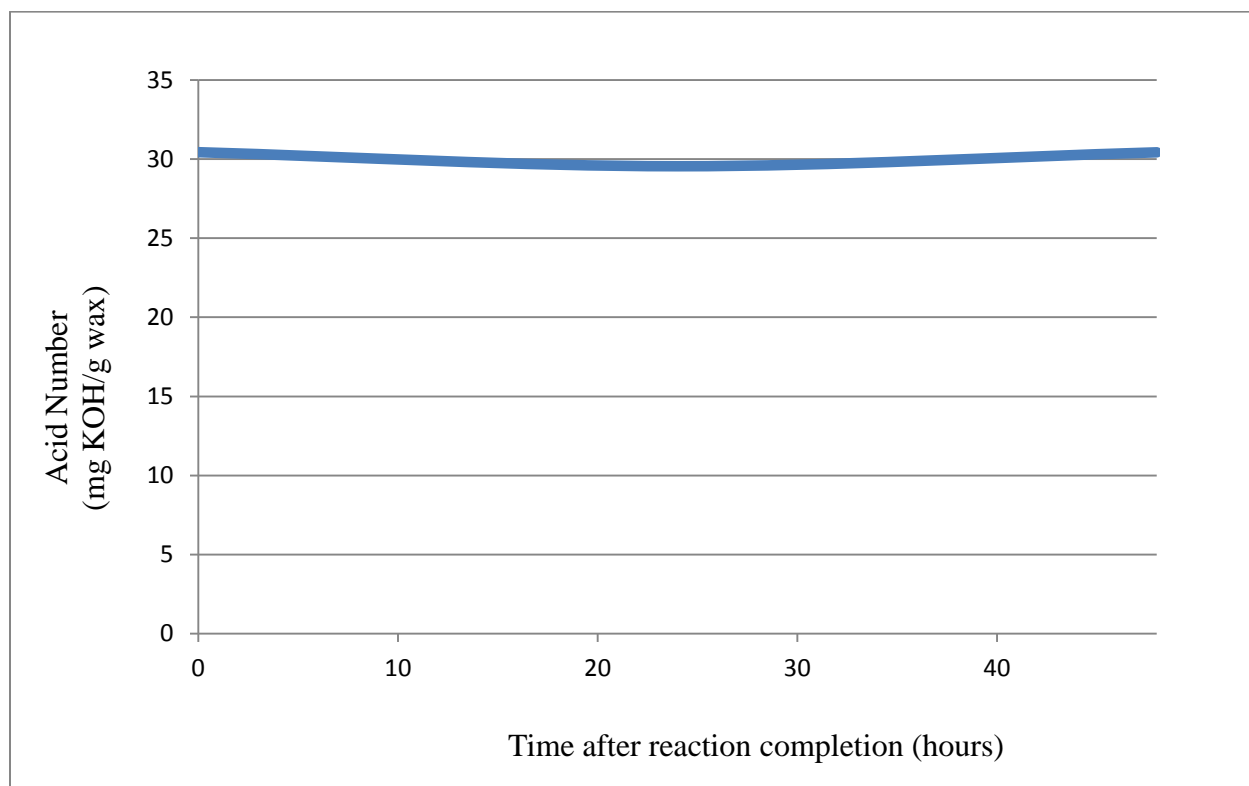


Figure 31 – Thermal stability experiment - 10% MAH by weight of wax, 1:1 mol ratio TBP:MAH, 160 °C

2.5.1.2 Characterization of waxes produced via peroxide initiation

From the overall reaction mechanism for the grafting of MAH to paraffin waxes, Figure 14, it can be seen that there are several possible grafted products from the reaction, which are shown in Figure 32.

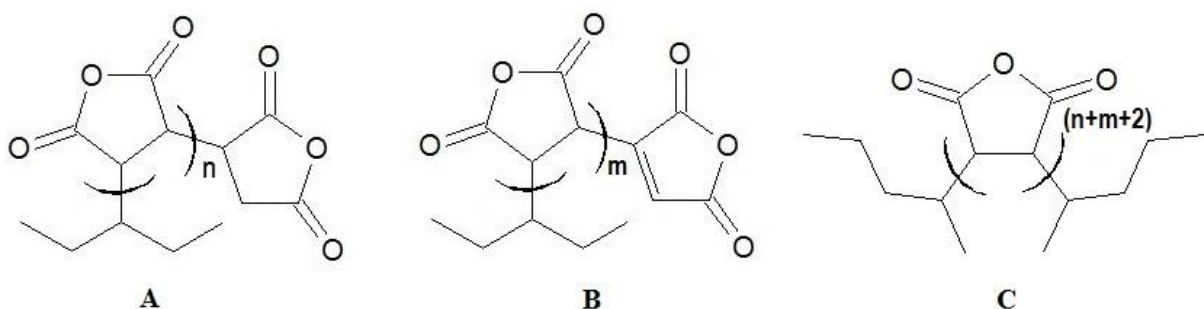


Figure 32 – Possible products of radical termination reactions

Low molecular weight polyethylene, which can be said to be similar in structure to paraffin wax, has been characterized through the use of ^{13}C and ^1H NMR, as well as FTIR spectra. The conditions that produce different distributions of the products shown in Figure 32 were determined through grafting experiments with $[2,3-^{13}\text{C}_2]$ maleic anhydride, from literature, using similar reaction conditions. Structures **A** and **B** are both present in the final products from the peroxide initiated grafting of MAH to low molecular weight polyethylene with both oligomeric ($m, n \geq 1$) and monomeric ($m, n = 0$) saturated SA termini (**A**) or unsaturated MAH termini (**B**). In the case of MAH loading lower than 2 wt% (corresponding to a 0.3 MAH:TBP molar ratio), **B** is found only as a single graft ($m = 0$) (Heinen et al., 1996; Yang et al., 2003).

In both low molecular polyethylene and paraffin wax the fraction of secondary carbons is much greater than the fraction of tertiary carbons (Zhu et al., 2004). Hydrogen abstraction from a tertiary carbon occurs more readily than from a secondary carbon (Russel, 2001), and accordingly a secondary carbon radical will in turn perform hydrogen abstraction more readily

than a tertiary radical. Statistically, hydrogen abstraction from tertiary carbons by peroxide initiator radicals is negligible, so the grafting of MAH occurs nearly completely on secondary carbons. Because MAH is a strong electron acceptor, a large portion of the single-graft MAH species will terminate via hydrogen abstraction, yielding a single grafted SA product (**A**, $n = 0$). Remaining MAH macroradicals will go on to form multi-graft MAH radical species and multi-grafted SA products (**A**, $n \geq 1$) accordingly. A six-membered ring transition state is formed, as shown in Figure 33 (Yang et al., 2001). In the presence of a high degree of tertiary carbons (e.g. in an ethylene/propylene copolymers or slack waxes with a high degree of branched components) the transition state formed will be less reversible, due to the stability of radicals centered on tertiary carbons, and the products will favour a single-graft type SA (**A**, $n = 0$) (Machado et al., 2001; Heinen et al., 1996).

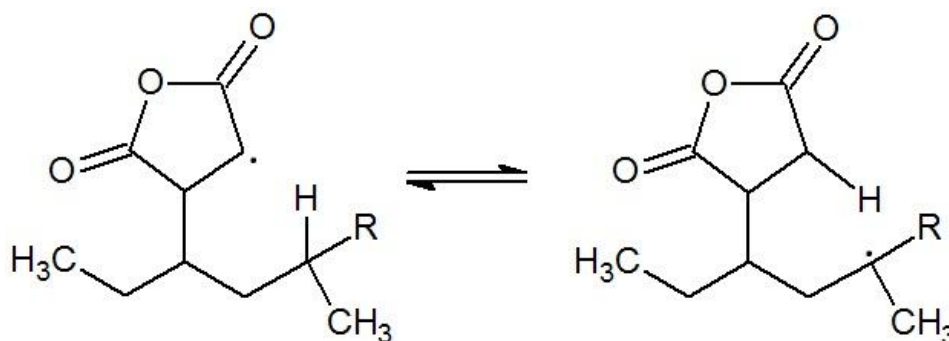


Figure 33 - Six-membered ring transition state formed between MAH and backbone polymer, R= H or alkyl group

In order to explain the production of unsaturated MAH terminated products (**B**), termination by disproportionation and hydrogen abstraction between two radical species must be considered. The mechanism of termination by disproportionation between two SA macroradicals of length $n + 1$ and $m + 1$ will yield a combination of **A** with a graft length of $n + 1$ and **B** with a graft length of $m + 1$, or **A** with a graft length of $m + 1$ and **B** with a graft length of $n + 1$ with equal probability. Hydrogen abstraction between two radicals resulting in disproportionation can

occur with an alkyl radical abstracting a hydrogen from a terminal succinic radical, yielding **B** with a graft length of $m + 1$ and a regenerated alkane, or with the opposite interaction yielding **A** with a graft length of $n + 1$ and an alkene side product. The former of these two disproportionation mechanisms is much more likely to happen due to the stability of the additional tertiary radical formed on the SA radical (Yang et al., 2003). Termination by combination between two SA radicals to yield **C** is negligible because MAH is a very strong electron acceptor.

Combining these factors, it can be said that for systems with a lower initial concentration of MAH than initiator, primarily single graft species of **A** and **B** will be formed. Due to the relative abundance of alkyl-centered radicals, longer grafts of MAH become unlikely, so there is a very small chance of producing **A** with a graft length of $n \geq 1$, and there is essentially no chance of forming **B** with a graft length $m \geq 1$. When the initial concentration of MAH is higher than that of the initiator, the opposite trend is true, where it is more likely that **A** and **B** will be formed with $n \geq 1$ and $m \geq 1$.

Therefore, it is highly likely that the products formed through the continuous addition and pulse addition of peroxide, as well as products formed through the bulk addition of peroxide at a low molar ratio of initiator:MAH will be of forms **A** and **B** with $n \geq 1$ and $m \geq 1$. Products formed through the bulk addition of peroxide at a high molar ratio of initiator:MAH as well as products formed through the MAH addition method will be of forms **A** with $n \geq 0$ and **B** with $m=0$.

To confirm grafting, FTIR spectra were taken using a Nicolet 510 FTIR spectrometer and then analyzed. Several model compounds, shown in Table 6 were compared to the experimental

products in order to evaluate the type of MAH grafts present in the products. Figure 34 shows the FTIR spectrum for a grafted wax sample using the MAH addition method at a MAH loading level of 10% by weight of wax and a 1:1 molar ratio of TBP:MAH at 160 °C, and the peak assignments for this spectrum are shown in Table 7.

Table 6 - FTIR peak assignments of model compounds used to evaluate MAH grafting types

Compound	Peak	Assignment
Paraffin	2927, 2855, 1378	C-H stretches
Poly(maleic anhydride)	1851	Asymmetric C=O stretch
	1780	Symmetric C=O stretch
n-Octadecylsuccinic anhydride	1867	Asymmetric C=O stretch
	1792	Symmetric C=O stretch

The spectrum of n-octadecylsuccinic anhydride was chosen because it is a very close analogue to a single graft product with a linear backbone (**A**, $n = 0$). The peaks assigned to poly(maleic anhydride) can be said to be analogous to those that would be found in long graft-chain products **A** and **B** with $n > 1$ and $m > 1$. The spectrum of paraffin wax is used as a baseline to determine peaks corresponding to the backbone of the grafted products.

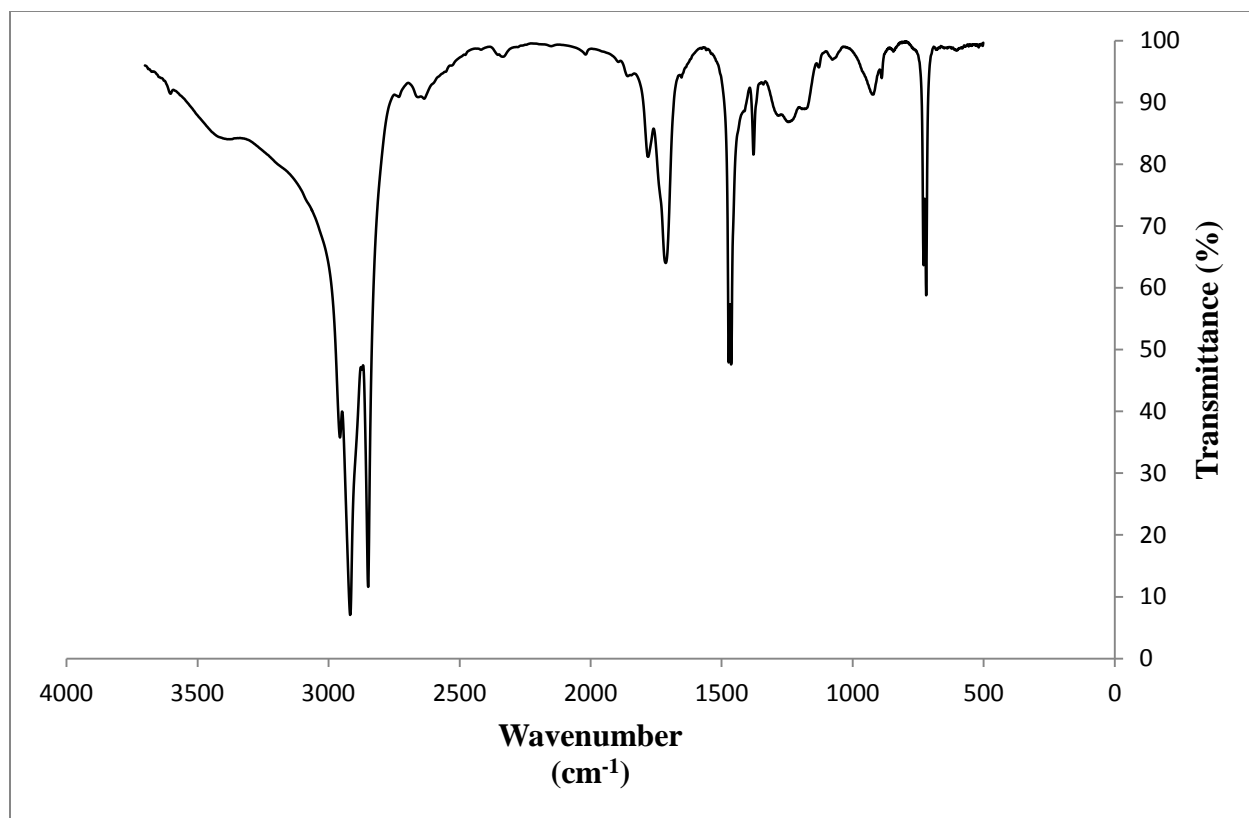


Figure 34 - FTIR spectrum of 10% MAH loading / 1:1 TBP / 60 AN

Table 7 - Peak assignment for MAH loading spectrum

Peak (cm ⁻¹)	Assignment
1859	Asymmetric C=O stretch
1780	Symmetric C=O stretch
1713	Acetone
2956, 2917, 2848, 1463-1472, 719-729	Paraffin wax

The peaks present in Figure 34 corresponding to the symmetric and asymmetric carbonyl shifts of grafted MAH groups are between the reference values for n-octadecylsuccinic anhydride and poly(maleic anhydride). This slight downward wavelength shift signifies that the graft length is longer than a single graft, but not an extended chain, therefore the product likely contains a mixture of single-graft **A** and **B**, with a small amount of multiple-graft (n and m ~ 1)

A and **B**, which is the expected result from comparison with experiments from literature (Yang et al., 2003). The wavelength shift can be explained by examining the resonance structure of MAH, shown in Figure 35. The dipole moments present in the resonance structure of MAH will allow for interaction between the grafted groups of different chains and as the graft length of MAH increases this interaction becomes more prevalent. These interactions lead to a reduction of the bond order of the carbonyl groups producing a downward wavelength shift (Pavia et al., 2001).

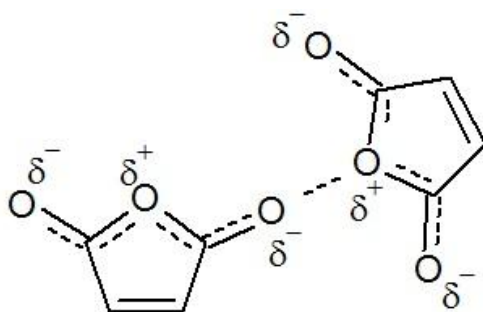


Figure 35 - Resonance structure and interactions of maleic anhydride

Slack wax was briefly examined as a possible starting material, but was quickly dismissed as it became apparent that the distribution of products formed from such a poorly defined starting material was too broad to have any practical application. The products of maleation reactions using slack wax had a very deep brown colour as opposed to the light yellow-brown colour of the products formed when using refined paraffin wax. Even when using refined paraffin wax it has been shown that there are a wide variety of products formed through the peroxide initiated grafting of MAH that not only vary in MAH graft length but also in the position of MAH grafts along the wax backbone. This difference in isomerization can lead to reduced surfactant properties as the head and tail groups of the molecule become less well defined.

2.5.2 Products formed via thermal addition methods

After thoroughly examining methods of modification involving peroxide initiated grafting of MAH to a paraffin wax backbone, the thermal addition of MAH to an alpha-olefin wax was examined. It was hoped that the defined chemistry of the reaction would lend itself to creating a modified wax with surfactant properties greater than those produced using peroxide initiation on a refined paraffin wax. Table 8 shows the collected results of thermal addition experiments conducted at a reaction temperature of 200°C for 8 hours using MAH loading of 18.7 wt% of the total formulation and the remainder being alpha-olefin wax.

Table 8 - Results of thermal addition experiments conducted at a reaction temperature of 200°C for 8 hours. 18.7 wt% MAH loading

Sample #	Wax Type	MAH Source	Acid Number (acetone)	Acid Number (unwashed)	Reaction Efficiency	MAH addition temperature	Lid configuration
1	C30+HA	Sigma	72	-----	66	200 °C	Open
2	C30+HA	Sigma	77	79	70	RT	Open
3	C30+	Sigma	82	83	75	RT	Open
4	C30+HA	Industrial	49	-----	45	200 °C	Open
5	C30+HA	Industrial	76	77	70	200 °C	Open
6	C30+HA	Industrial	73	76	67	200 °C	Open
7	C30+HA	Industrial	54	56	50	200 °C	Open
8	C30+HA	Industrial	91	117	83	200 °C	Closed
9	C30+HA	Sigma	108	110	99	200 °C	Closed
10	C30+HA	Sigma	96	116	88	200 °C	Closed
11	C30+HA	Industrial	92	110	84	90 °C	Closed
12	C30+HA	Sigma	84	101	77	RT	Closed
13	C30+HA	Sigma	92	105	83	RT	Closed
14	C30+HA	Industrial	93	96	85	RT	Open
15	C30+HA	Sigma	95	109	87	RT	Closed
16	C30+HA	Sigma	102	103	94	RT	Open
17	C30+HA	Sigma	102	108	94	RT	Closed
18	C30+HA	Sigma	119.5	123	-----	RT	Closed

The effects of changing each variable are summarized in Table 9, showing the average AN for both acetone washed and unwashed samples, as well as the average reaction efficiency.

Table 9 - Comparison of the effects of each experimental variable on the AN of products with experiments conducted at a reaction temperature of 200°C for 8 hours, with 18.7 wt% MAH loading

Variable	Value	Average AN (acetone wash)	Average AN (unwashed)	Average Efficiency
MAH Source	Sigma	90	100	83
	Industrial	82	92	75
Wax temperature when MAH is added	200 °C	82	92	71
	Room temp.	89	96	82
Lid configuration	Open	79	81	72
	Closed	94	110	86

Changing the source of MAH and the MAH addition temperature did not yield any significant differences in AN. Changing the lid configuration, however, can have a large effect on the addition of MAH. At a reaction temperature of 200 °C, the vapour pressure of MAH is approximately 100 kPa (Huntsman International LLC, 2001), and even a slight vacuum such as that present in a fume-hood may be enough to draw MAH vapour out of the system, reducing overall efficiency of the reaction. This is the case for the open system where only a Teflon splash-guard was used to cover the reactor. Accordingly, it can be seen that the average of the AN of acetone washed products is essentially the same as the average AN of unwashed samples of the same products and product purification occurs naturally as MAH vapours are drawn out of the reactor. In the case of the closed lid configuration, the system is air-tight and it is seen that the difference in the two values of AN is significant. The high vapour pressure of MAH at the temperature of reaction can be used advantageously to give a product with a relatively low level of unreacted MAH left within, as well as allow for the recovery of MAH by extraction by vacuum and subsequent condensation of the vapour. The process of the thermal addition reaction over time was measured, the results of which are shown in Figure 36. It can be seen that

the bulk of thermal addition of MAH to alpha-olefins occurs within the first two to four hours of the reaction time, as was the case for the peroxide initiated grafting of MAH to refined paraffin wax backbones, though the rate does not drop as sharply as in the peroxide initiated grafting experiments.

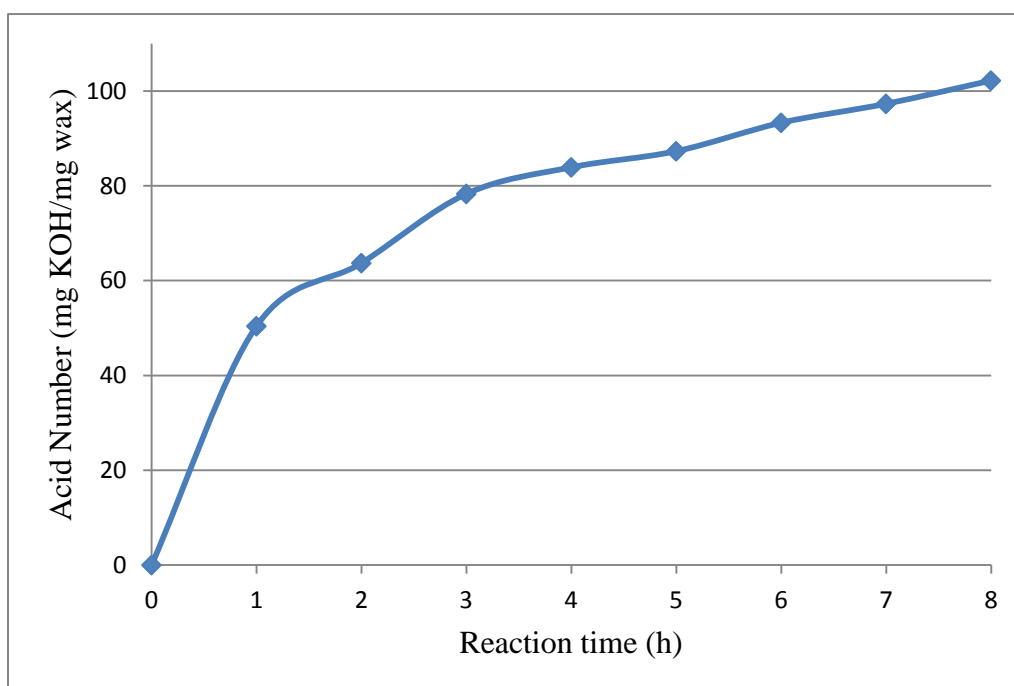


Figure 36 - Reaction progression for thermal addition of MAH, sample #17

2.5.2.1 Calculation of maximum theoretical acid number in thermal addition reactions

For emulsifiers made with alpha-olefins through a thermal reaction, the theoretical maximum AN for a sample can be calculated using the formulation of the sample and the chemistries that are known for the thermal addition reaction and the titration of the emulsifier. The standard formulation of the alpha-olefin based emulsifier includes 500g wax and 115g MAH, which is roughly a 1:1 mole ratio of the two components. The average molecular weight of the wax can be approximated by using a molecular weight profile provided by Chevron Phillips, as seen in Table 10.

Table 10 - Important properties of CP 30+HA wax

Property	Value
Carbon Number C ₂₄₋₂₈ , wt%	4.45
Carbon Number C ₃₀₊ , wt%	95.55
n-Alpha-Olefins, wt%	75.4
Linear Internal Olefins, wt%	4.2
Branched Olefins, wt%	19.4

Assuming a chain length of 26 carbons for the chains listed as C₂₄₋₂₈ and assuming a chain length of 30 carbons for the chains listed as C₃₀₊, the average molecular weight is calculated to be approximately 418.1 g/mol. The total amount of chains with sites available for reaction via the addition of MAH is 99% of chains by weight. The addition of MAH proceeds via the ene reaction in 1:1 stoichiometry, giving an average molecular weight for the final product of 516.16 g/mol. ANs are determined through acid-base titration proceeding according to ASTM test D974-11. The reaction for the titration yielding the potassium salt of the hydrolyzed wax-maleic acid compound is shown in Figure 37.

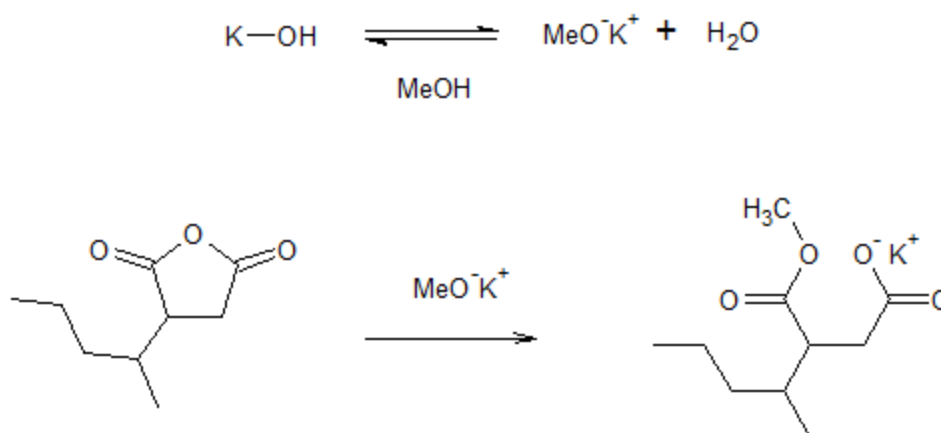


Figure 37 - Titration reaction to determine acid number of emulsifier

Under aqueous conditions the titration reaction requires two moles of potassium hydroxide to reach completion; however when methanol is used as the solvent for the potassium

hydroxide solution only one mole is required as there is no additional proton to be abstracted after esterification of the MAH group. Generally, methoxide anions will react with water to produce methanol and a hydroxide anion but methanol is present in large excess compared to the water formed by the solvation of potassium hydroxide, so it is likely that potassium methoxide is the reactive species in the titration reaction. This is a basic reaction that is used to great extent in the production of biodiesel (Lotero et al., 2005).

Reaction efficiency based on the amount of MAH in the system is calculated by determining the AN for each sample and compared to the maximum theoretical AN, which is calculated to be 109 mg KOH/g wax. Measured AN may come out slightly higher than this value if there are slight amounts of residual MAH left in the product, slight oxidation of the double bonds in the modified alpha-olefin product and because of measurement inaccuracies associated with the AN test.

2.5.2.2 FTIR Characterization of modified waxes produced through thermal maleation

FTIR spectra were taken for several samples of modified C30+HA products as well as the unmodified C30+HA wax, shown in Figure 38.

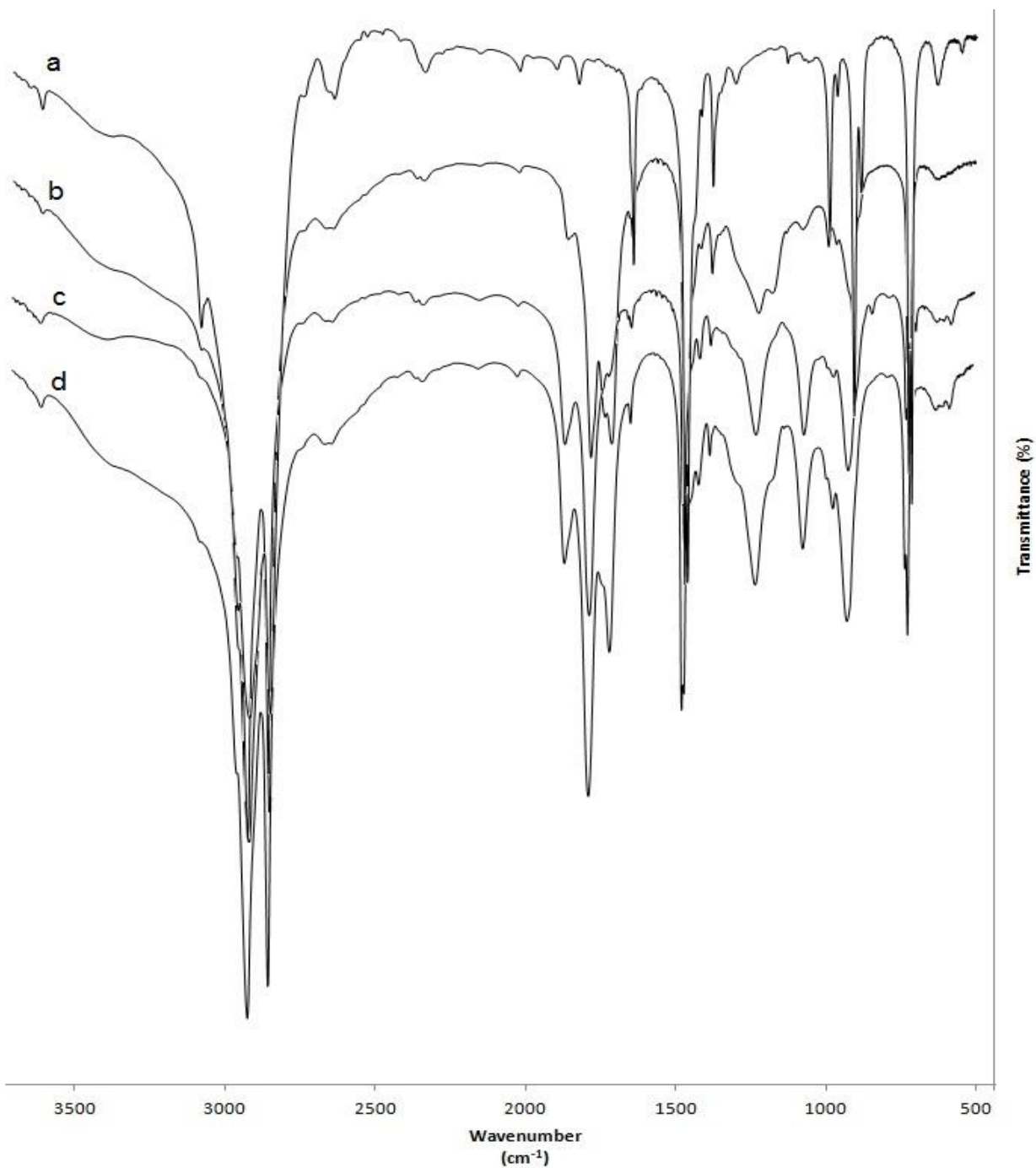


Figure 38 - FTIR spectra taken from unmodified C30+HA wax (a), sample #1 (table 8) - 72 AN (b), sample #18 washed with acetone - 119.5 AN (c) and sample #18 unwashed - 123 AN (d)

Table 11 - Peak assignments for FTIR taken from products of thermal addition reactions

Compound	Peak wavenumber (cm ⁻¹)	Assignment
Unmodified C30+HA alpha-olefin wax (a)	3077 2916, 2848 2635 1642 1463 991, 910, 866	sp ² C-H stretch (n- α -olefin) sp ³ C-H stretch Linear internal or branched internal olefin C-H stretch C=C stretch CH ₂ bend Vinyl out-of-plane bending
Sample #1, 72 AN, acetone washed (b)	3078 2918, 2849 1859, 1781 1712 1641 1464 944, 910	sp ² C-H stretch sp ³ C-H stretch graft C=O acetone C=C stretch CH ₂ bend Vinyl out-of-plane bending
Sample #23, 119.5 AN, acetone washed (c)	2918, 2850 1861, 1783 1712 1641 1472 1068	sp ³ C-H stretch graft C=O acetone C=C stretch CH ₂ bend C-O stretch (OH from oxidation)
Sample #23, 123 AN, unwashed (d)	2918, 2849 1863, 1783 1639 1472 1069	sp ³ C-H stretch graft C=O C=C stretch CH ₂ bend C-O stretch (OH from oxidation)

The peak assignments in Table 11 help to confirm the reaction of MAH with the alpha-olefin. In the baseline spectrum for the unmodified C30+HA wax (**a**), there are significant peaks at 3077 cm⁻¹ and 1642 cm⁻¹ that are due to sp² C-H stretching and C=C stretching associated with

the double bonds present in alpha-olefins. As the AN of the product increases, **(b-d)** these peaks shrink, while peaks around 1859 cm^{-1} and 1781 cm^{-1} which are characteristic of C=O stretching in grafted anhydride groups grow in intensity. In the spectrum of the unwashed sample of #23, **(d)**, the C=O stretching bands are shifted slightly to 1863 cm^{-1} and 1783 cm^{-1} because of a very small amount of residual MAH in the product.

Chapter 3: Emulsion Formulations for use in Gypsum Wallboards

3.1 Experimental procedures

3.1.1 Emulsion preparation

Emulsions for use in gypsum wallboards are prepared as needed for board testing, according to standard formulations. An aqueous mixture of water PVA was made and heated to 95 °C. After all the PVA was dissolved, Ultrazine NA (a sodium lignosulfate dispersing agent) was added to the mixture and the temperature was maintained. At the same time, a mixture of fully refined paraffin wax, oxidized polyethylene wax and maleated wax emulsifier was prepared and heated to approximately 110 °C. Both the aqueous and wax mixtures were stirred well separately to ensure that they were homogeneous. Potassium hydroxide, Ultrazine NA (a sodium lignosulfate dispersing agent) and Tamol 731A (a dispersing agent) were added to the aqueous mixture, which was then mixed at high speed with a Silverson laboratory dispersing apparatus and the wax mixture was slowly added in to it to create an oil-in-water emulsion. After the emulsion was mixed at high shear for several minutes, it was cooled in a water bath until it had reached room temperature. The emulsion was finger-tested (rubbed between thumb and forefinger) for the appearance of any grit or grain that would suggest instability in the emulsion. The emulsion was also tested for pH and viscosity. A shear test was conducted on a portion the emulsion, where it was subjected to high shear in the Silverson laboratory disperser for three minutes, in order to simulate the shear forces present due to pumping in industrial applications. Melment 17G (a fluidizing and water reducing agent) was mixed into the emulsion. A slump test was performed by adding a small amount of the emulsion to an aqueous slurry of hemi-hydrate gypsum to determine the water demand of the slurry, with the emulsion present.

3.1.2 Evaluation of emulsion stability

Emulsions are tested for both shear and storage stability. As mentioned previously, shear stability tests are conducted with a Silverson laboratory disperser and help to determine the performance of the emulsion during pumping in an industrial setting. Storage stability is evaluated over time by observing the completed emulsions and is an important characteristic, as these emulsions are made on site and then transported to external production facilities to be incorporated into gypsum wallboards. Emulsions are stored for 48 hours after they are made and any visible separation of the aqueous and wax phases or formation of hardened wax layers is noted. Emulsions that have separated slightly but can be easily reincorporated back into a single phase are considered acceptable.

3.1.3 Gypsum wallboard preparation

Gypsum wallboard samples were prepared according to internal standards used by Norjohn Ltd. Formulations include water, hemihydrate gypsum, a small portion of a wax emulsion, foaming agents and setting agents. The samples are heated to dryness in a convection oven and then cooled to room temperature overnight. The cooled and dried board samples are weighed and then immersed in a water bath for 2 hours. After the boards were removed from the water, surface moisture is removed and then the boards are weighed again to determine the water absorption of each sample.

3.2 Results and discussion of emulsion production

Extensive testing was done to determine the reaction conditions that produce emulsifiers that function well according to the needs of the system at hand. The formulations and performance characteristics of selected emulsion samples are shown in Table 12 and Table 13.

The complete listing of formulations and performance characteristics can be found in the appendix, in Table 24 and Table 25.

Table 12 - Selected formulations of experimental emulsion formulations

Emulsion Sample #	Wax sample #	Wash	AN (AC)	Paraffin (wt %)	Exp wax (wt %)	OPE (wt %)	Water additives (wt %)	+	KOH (wt %)
1	-----	-----	48	32	1.289	1.273	65.163		0.273
7	5	AC	84	32	2.562	0	65.163		0.273
8	5	AC	84	32	1.289	1.273	65.163		0.273
9	5	AC	84	32	1.012	0	65.163		0.273
10	17	UW	80	32	2.562	0	65.163		0.273
11	5	AC	84	32.36	2.2	0	65.163		0.273
12	5	AC	84	31.562	3	0	65.163		0.273
13	5	AC	84	31.562	3	0	65.163		0.273
14	5	AC	84	32	2.562	0	65.163		0.273
15	5	AC	84	31.562	3	0	65.163		0.273
16	5	AC	84	31.562	3	0	65.163		0.273
32	82	UW	50	32.562	2	0	65.163		0.273
33	1	AC	39	31.964	2.6	0	65.163		0.273
34	82	UW	50	32.562	2	0	65.163		0.273
35	13	H2O	48	32.562	2	0	65.163		0.273
46	85	AC	60	33.362	1.2	0	65.163		0.273
47	85	AC	60	33.36	1.2	0	65.163		0.273
48	85	AC	60	32.56	2	0	65.163		0.273
55	85	AC	60	33.36	1.2	0	65.163		0.273
63	110	UW	72	33.762	0.8	0	65.163		0.273
64	110	UW	72	33.762	1.6	0	65.163		0.273
65	110	UW	72	33.762	1.2	0	65.163		0.273
66	110	UW	72	32.962	0.8	0.8	65.163		0.273
82	117	UW	117	32.291	1	1.273	65.163		0.273
83	118	UW	110	32.291	1	1.273	65.163		0.273
84	119	UW	116	32.291	1	1.273	65.163		0.273
85	120	UW	110	32.291	1	1.273	65.163		0.273
86	121	UW	101	32.291	1	1.273	65.163		0.273
87	122	UW	105	32.291	1	1.273	65.163		0.273

Table 13- Selected results of emulsion performance testing

Emulsion Sample #	Wash	AN (AC)	Solids (%)	Visc (cP)	pH	Finger	shear	storage	Tested in boards
1	control	48	40-42	300	8 -10	pass	pass	pass	yes
7	AC	84	-----	167.6	7.88	pass	fail	fail	no
8	AC	84	-----	-----	-----	fail	-----	-----	no
9	AC	84	-----	-----	-----	fail	-----	-----	no
10	UW	80	42.65	295.2	7.07	pass	pass	pass	yes
11	AC	84	-----	-----	-----	-----	-----	-----	no
12	AC	84	42.74	230.4	8.6	pass	fail	fail	no
13	AC	84	42.99	236.4	8.43	pass	fail	pass	no
14	AC	84	42.81	373.2	8.46	pass	fail	pass	no
15	AC	84	41.68	281	9.84	pass	pass	pass	yes
16	AC	84	42.11	95.1	9.76	pass	pass	pass	yes
32	UW	50	44.25	245.4	9.02	pass	pass	pass	yes
33	AC	39	37.54	2244	10.39	pass	pass	pass	yes
34	UW	50	42.29	194.4	8.64	pass	pass	pass	yes
35	H2O	48	-----	-----	-----	fail	-----	-----	no
46	AC	60	39.4	199.7	11.46	pass	pass	pass	yes
47	AC	60	41.47	233.1	8.56	pass	pass	pass	yes
48	AC	60	41.47	233.1	8.56	pass	pass	pass	yes
55	AC	60	42.19	208		pass	pass	thick	yes
63	UW	72	40.23	140	11.42	pass	pass	pass	yes
64	UW	72	42.11	167.5	10.42	pass	pass	pass	yes
65	UW	72	42.57	167.1	10.93	pass	pass	pass	yes
66	UW	72	41.46	159.1	10.99	pass	pass	pass	yes
82	UW	117	41.42	435	8.59	pass	pass	pass	yes
83	UW	110	41.82	552	8.59	pass	pass	pass	yes
84	UW	116	41.58	802	8.48	pass	pass	pass	yes
85	UW	110	41.61	245	8.46	pass	pass	pass	yes
86	UW	101	41.49	233	8.56	pass	pass	pass	yes
87	UW	105	41.38	271	8.6	pass	pass	pass	yes

Emulsion samples using a wide variety of experimental waxes were tested and compared to a control emulsion using a commercially available emulsifier, with an AN of approximately 48 mg KOH / g wax. The control emulsion has a solids content between 40% and 42%, viscosity up to 300 cP, pH between 8 and 10, will not feel gritty or produce coagulated wax in a finger test, pass a shear test with a minimum time of two minutes and thirty seconds and will show only

minimal separation that can be easily reincorporated when stored for extended periods of time. Gypsum emulsions made with formulations based on these control samples are highly sensitive to impurities, and often fail in the presence of residual MAH which may be present in unwashed samples of modified wax. As such, wax samples that were washed with acetone and then used in emulsions performed better than those that were washed with water or vacuum, or left unwashed. In the case of the emulsifiers produced using thermal addition, it has been shown that the amount of residual MAH left in the wax was much lower and thus washing was generally not necessary to produce emulsions with desirable performance characteristics. This is highly advantageous for applications in an industrial setting, as it not only removes costly and time consuming purification and solvent separation steps from the maleation process, but is also a great deal more environmentally friendly.

Emulsifiers made by peroxide initiated grafting using TBP were much more successful than those made using TBPB, even with similar levels of grafting. This is likely due to the variation in active radical species present for the different peroxides. TBP homolyzes to produce two identical radical species while TBPB homolyzes to give two different active radical species, which may have different activities or adversely affect emulsion performance if there is any peroxide residue left in the emulsifier. It was found that, in general, emulsions using waxes that were made using peroxide initiated grafting methods did not perform as well as those made using the thermal addition of MAH to alpha-olefins when the AN of the modified waxes was similar. There are several reasons for this, the first of which is the lack of uniformity in the products of peroxide initiated reactions. These grafted waxes can have MAH graft chains located anywhere along their wax backbones, so emulsifiers made through this method will have a wide variety of tail-group shapes and lengths. The possibility for MAH graft lengths longer than one unit further

extends the variation in these emulsifiers. By contrast, the products made through thermal initiated addition can only have MAH added to one location on the wax chain and addition occurs in 1:1 stoichiometry. The waxes are well defined in composition, so variation in the emulsifiers is minimal. Additionally, the extended graft length of the peroxide initiated products can affect local ionic strength as the surface charge will be less evenly distributed when compared to the thermal addition products which have MAH chain lengths of one.

3.3 Gypsum wallboard results

Emulsions that had desirable performance characteristics were tested in samples of gypsum wallboards. The results of these tests are shown in Table 14.

Table 14 - Results of gypsum wall board samples created with experimental emulsifiers

Emulsion Sample #	Wash	AN (AC)	Exp wax (wt%)	OPE (wt%)	Slump (inches)	Water absorption (%)	Control WA (%)
1	-----	48	1.289	1.273	6.75	~10	
10	UW	80	2.562	0	6.5	22.6	9.3
15	AC	84	3	0	6.75	36.9	9.3
16	AC	84	3	0	6.825	33.7	9.3
32	UW	50	2	0	6.825	21.8	9.3
33	AC	39	2.6	0	6.825	32.6	9.3
34	UW	50	2	0	6.75	23.7	9.3
46	AC	60	1.2	0	6.75	19.8	9.3
47	AC	60	1.2	0	6.5	19.9	9.3
48	AC	60	2	0	6.75	18.7	9.3
55	AC	60	1.2	0	6.75	13.7	9.3
63	UW	72	0.8	0	7.625	12.2	8.8
64	UW	72	1.6	0	8	10.9	8.3
65	UW	72	1.2	0	8	10.3	8.3
66	UW	72	0.8	0.8	7.75	8.4	8.8
82	UW	117	1	1.273	7.5	10.3	10.1
83	UW	110	1	1.273	7.5	8.8	10.1
84	UW	116	1	1.273	7.25	8.8	10.1
85	UW	110	1	1.273	7.5	5.6	5.5
86	UW	101	1	1.273	7.75	5.5	5.5
87	UW	105	1	1.273	7.5	5.4	5.5

It was found that the emulsions made with waxes produced through peroxide initiated grafting did not perform at an acceptable level in gypsum wallboards, while those that were made through thermal addition were able to perform as well or better than control emulsions. The best result for peroxide initiation gave a water absorption value of 13.7% versus a control of 9.3% with experimental emulsifier loading of 1.2 wt%, while the best result for thermal addition gave a water absorption value of 5.4% versus a control of 5.5% with experimental emulsifier loading of 1 wt%. It can be seen that the AN and loading amount of the emulsifier in the emulsion are not the only contributing factors to gypsum wallboard performance. The structure and residual impurities found in unwashed emulsifiers can also have a significant contribution on emulsion performance in gypsum wallboards. The presence of excess free ions in the emulsion from residual MAH will decrease the overall hydrophobic activity of the emulsion and increase the water absorption of gypsum wallboards. By the same mechanism, excessive emulsifier loading can contribute to increased water absorption. Samples produced with 3 wt% of an acetone washed emulsifier with AN produced the highest levels of water absorption. The choice of modified wax did not seem to have any significant effect on the slump value of the emulsion, which is an indicator of the water demand for rehydrating the stucco used in board production.

3.4 Additional applications of experimentally obtained maleated waxes

In collaboration with my colleague, Nels Grauman Neander, research was also done into the use of these emulsifiers in emulsion formulations for engineered wood products, such as wooden chip-board. It was found that the emulsifiers formed with peroxide initiated grafting performed adequately in these emulsions but only at high loading, such that successful samples use an emulsifier loading of approximately 4 wt% versus a control value of 1.7 wt%. The emulsifiers formed with the thermal addition of MAH to alpha-olefins showed exceptional

performance at loading values of approximately 1.5 wt% versus a control value of 1.7 wt%. For the latter case, a 24 hour water absorption value of 43.13% and 24 hour thickness swell value of 23.29% was achieved versus a control with values of 50.29% and 26.28% for water absorption and thickness swell, respectively.

3.5 Cost analysis for application with an industrial partner

The cost difference of plant operation using new experimental emulsifiers versus the emulsifiers currently being used by Norjohn Emulsions has been calculated for both the emulsions used in gypsum boards and engineered wood products. Estimated yearly production values for each emulsion are approximately 900,000 kg/year for gypsum wallboards and 9,000,000 kg/year for engineered wood products. The yearly requirements and base cost for each ingredient are listed in Table 15 and Table 16.

Table 15 - Yearly requirements for each ingredient in an industrial process

Emulsion	Ingredient	Loading (wt%)	Yearly Requirement (kg/year)
Gypsum	Ceramer 67	1.291	11,619
	Oxidized Polyethylene Wax	1.273	11,457
	Experimental Wax	1.0	9,000
Engineered Wood Product	Pristerine	1.7	153,000
	Experimental Wax	1.5	135,000

Table 16 - Cost of ingredients used in emulsion production

Chemical	Industrial Price (\$/kg)
Maleic anhydride	1.5
C30+HA alpha-olefin	1.87
Paraffin wax	3.00
Slack wax	1.25
Pristerine (EWP emulsifier)	3.44
Ceramer 67 (gypsum emulsifier)	7.45
Oxidized polyethylene wax (gypsum emulsifier)	3.3

From the ingredient requirements, it is calculated that a reactor volume of approximately 800 L is required to accommodate the required daily emulsifier production of 552.85 kg. Theoretical reactor properties are listed in Table 17.

Table 17 - Sample dimensions of reactor required to produce emulsifier

Property	Measurement
Inner diameter	32.5 inches
Height	117.1 inches
Wall thickness	0.2 inches
Insulation	Fiberglass, 2 inches

From these dimensions, the cost of heating the reactor and wax to a reaction temperature of 200 °C can be calculated to be approximately 0.182 \$/kg. The cost of chemicals to make an emulsifier using 18.7 wt% MAH and 81.3 wt% C30+HA alpha-olefin is approximately \$1.80/kg, giving a total material and energy cost of \$1.82/kg. By replacing commercially available emulsifiers with this experimentally derived emulsifier in both gypsum and engineered wood product emulsions, a cost savings of roughly \$336,000 per year can be achieved. Capital investment costs should be minimal, roughly \$50,000 or less for the scale presented in this evaluation.

Chapter 4: Conclusions and Recommendations

4.1 Conclusions

In this project, several methods of adding MAH to a wax backbone were investigated. It was determined that high AN maleated waxes could be produced with high repeatability through both peroxide initiated grafting of MAH to refined paraffin wax and thermal addition of MAH to alpha-olefin wax. The best experimental method was determined to be the thermal addition of MAH to C30+HA wax in a closed system, giving a high purity emulsifier that is made with reaction efficiency up to 99%.

Emulsions made with experimentally produced emulsifiers showed acceptable properties for solids content, viscosity, pH, shear stability and storage stability when compared to control emulsions made with commercially available emulsifiers using equivalent or lower emulsifier loading levels for use in gypsum wallboards. Emulsions were tested in board samples and it was determined that for emulsifiers made using peroxide initiated grafting, the reduction in water absorption was not adequate in gypsum emulsions. For emulsifiers made using thermal addition of MAH, it was determined that the reduction in water absorption was equivalent or better at 1% emulsifier loading than in control samples at 1.29% emulsifier loading.

References (Bibliography)

- American Fuel & Petroleum Manufacturers. Wax Facts. <http://www.afpm.org/Wax-Facts/> (accessed Sept 15, 2009)
- Arkema Inc. Luperox Organic Peroxides: General Catalog. <http://www.arkema-inc.com/literature/pdf/320.pdf> (accessed Nov 15, 2009).
- Barnes, G. T., Gentle, I., R., *Interfacial Science: An Introduction*; Oxford University Press, New York, U.S.A., 2005.
- Becher, P., *Emulsions: Theory and Practice*; Reinhold Publishing Corporation, New York, U.S.A., 1957
- Bennett, H., Ed. *Commercial Waxes*; Chemical Publishing Company, Inc., 1956.
- Bennett, H., *Industrial Waxes Volume 1: Natural & Synthetic Waxes*; Chemical Publishing Company, 1975.
- Bennett, H., Bishop Jr., J. L., Wulfinghoff, M. F., *Practical Emulsions Volume 1: Materials and Equipment*; Chemical Publishing Company, Inc., New York, U.S.A., 1968.
- Bornstein, L. Water-Resistant Gypsum Compositions and Emulsion for Making Same. U.S. Patent 5,437,722, August 1, 1995.
- Burke, W. R. Gypsum Wallboard Core, and Method and Apparatus for Making the Same. U.S. Patent 6,699,429, May 10, 2000.
- Burke, W. R.; Kingston, L. W. Gypsum Wallboard and Method of Making Same. U.S. Patent 5,879,825, January 7, 1997.
- Camp, T. P. Water-Resistant Gypsum Products and Process of Making. U.S. Patent 2,432,963, December 16, 1947.
- Carey, F. A., & Sundberg, R. J. *Advanced Organic Chemistry Part B: Reactions and Synthesis*; Springer: Charlottesville, U.S.A., 2007.
- Clayden, J., Greeves, N., Warren, S., Wothers, P. *Organic Chemistry*; Oxford University Press, New York, U.S.A., 2001.
- Greve, D. R., O'Neill, E. D. Water-Resistant Gypsum Products. U.S. Patent 3,935,021, January 27, 1976.
- Hiemenz, P. C., Lodge, T. P. *Polymer Chemistry*; CRC Press: Boca Raton, U.S.A., 2007.

Master's Thesis – M. Rattle; McMaster University – Chemical Engineering

Heinen, W.; Rosenmüller, C. H.; Wenzel, C. B.; de Groot, H. J. M.; Lugtenburg, J.
Macromolecules, **1996**, *29*, 1151-1157.

Housecroft, C. E., Sharpe, A. G., *Inorganic Chemistry*; Pearson Education Limited, Essex, England (2005).

Huntsman International LLC. Maleic Anhydride Customer Guide.
http://www.huntsman.com/performance_products/media/ma_customer_guide-2001.pdf
(accessed Mar 2011).

Liu, Y.; Jessop, P. G.; Cunningham, M.; Eckert, C. A.; Liotta, C. L. *Science*, **2006**, *313*, 958.

Long, W. J. Water-Resistant Gypsum Composition and Products, and Process of Making Same.
U.S. Patent 4,094,694, June 13, 1978.

Lotero, E.; Liu, Y.; Lopez, D. E.; Suwannakarn, K.; Bruce, D. A.; Goodwin, Jr., J. G. *Ind. Eng. Chem. Res.* **2005**, *44*, 5353-5363.

Machado, A.V., Covas, J. A., van Duin, M., *Polymer*, **2001**, *42*, 3649-3655.

Machado, A. V.; van Duin, M.; Covas, J. A. *J. Polym. Sci. Part A Polym. Chem.* **2000**, *38*, 3919-3932.

Moad, G., *J. Prog. Polym. Sci.*, **1999**, *24*, 81-142.

Napper, D. H., *Polymeric Stabilization of Colloidal Dispersions*; Academic Press Inc.: London, U.K. 1983.

Oh, Y. S.; Dahlgren, R. M.; Russell, G. D. Shampoo Compositions. U.S. Patent 4,704,272, July 10, 1985.

Patel, J. M., Finkelstein, R. S. Gypsum Wallboard and Method of Making Same. U.S. Patent 5,879,446, August 21 1998.

Pavia, D. L., Lampman, G. M., Kriz, G. S. *Introduction to Spectroscopy*; Thomson Learning, Inc: U.S.A. 2001.

Preston, W. C., *J. Phys. & Colloid Chem.*, **1948**, *52*, 84.

Qui, W., Takahiro, H., *Macromol. Chem. Phys.* **2005**, *206*, 2470-2482.

Russel, K. E. *Prog. Polym. Sci.*, **2001**, *27*, 1007-1038.

Sellers, D. G., Altman, F. A., Richards, T. W. Method of Manufacturing a Water-Resistant Gypsum Composition. U.S. Patent 5,135,805, August 4, 1992.

Sheshkali, Z.; Assempour, H.; Nazockdast H., *J. Appl. Polym. Sci.*, **2007**, *105*, 1869-1881.

Shi, D.; Yang, J.; Yao, Z.; Wang, Y.; Huang, H.; Jing, Wu.; Yin, J.; Costa, G. *Polymer*, **2001**, *42*, 5549-5557

Shinoda, K., Friberg, S., *Emulsions and Solubilization*; John Wiley & Sons, New York, U.S.A., 1986.

Sinnige, L. A. Wax Emulsion Composition for Imparting Water Repellency to Gypsum. U.S. Patent 5,968,237, October 19, 1999.

Sinnige, L. A. Wax Emulsion Formulation and Gypsum Composition Containing Same. U.S. Patent 6,890,976 B2, May 10, 2005.

Tadrous, Th. F., Ed. *Surfactants*; Academic Press: Orlando, U.S.A., 1984.

Tomoshige, T., Furuta, H., Tachi, A., Kawamoto, N. Highly Maleated Wax and Process for Producing the Same. U.S. Patent 4,315,863, February 16, 1982.

Wantling, S. J. Water-Resistant Gypsum Composition. U.S. Patent 6,165,261, June 10, 1999.

Yang, J., Yao, Z., Shi, D., Huang, H., Wang, Y., Yin, J., *J. Appl. Polym. Sci.*, **2001**, *79*, 535.
H. M. R. Hoffman, *Angew. Chem. Int. Ed. Engl.*, **1969**, *8*, 556.

Yang, L., Zhang, F., Endo, T., Takahiro, H., *Macromolecules*, **2003**, *36*, 4709-4718.

Zhang, Y.; Li, H. *J. Polym. Eng. Sci.*, **2003**, *43*, 774-782.

Zhu, Y.; Zhang, R.; Wei, J. *J. Polym. Sci. Part A Polym. Chem.*, **2004**, *42*, 5714-5724 .

Appendix A: Raw Data for Wax, Emulsion and Board Samples

A.1. Wax Data

Table 18 - Raw data from experiments using bulk addition of peroxide

Initiator Used	Sample #	MAH (wt % by wt of wax)	Mol ratio MAH : Init	mol ratio init:MAH	Temp (°C)	Time (hours)	AN (mg KOH/g wax)	GE (%)
TBP	1	20	2	0.5	160	10	41	17.9
TBP	2	20	2	0.5	160	10	52	22.7
TBP	3	20	1	1	160	10	73	31.9
TBP	4	20	0.5	2	160	10	81	35.4
TBP	5	20	0.5	2	160	12	84	36.7
TBP	6	10	0.5	2	160	12	33	28.8
TBP	7	10	0.5	2	160	10	30	26.2
TBP	8	10	2	0.5	160	10	10	8.7
TBP	9	10	2	0.5	160	11	16	14.0
TBP	10	10	1	1	160	11	26	22.7
TBP	11	5	1	1	160	10	9	15.7
TBP	12	5	1	1	160	10	11	19.2
TBPB	13	20	0.5	2	130	10	34	14.9
TBPB	14	20	0.5	2	130	14	31	13.5
TBPB	15	20	1	1	130	14	22	9.6
TBPB	16	20	1	1	130	10	18	7.9

Table 19 - Raw data of experiments using pulse addition of peroxide

Initiator Used	Sample #	MAH (wt % by wt of wax)	Mol ratio MAH : Init	mol ratio init:MAH	Temp (°C)	Time (hours)	AN (mg KOH/g wax)	GE (%)
TBP	17	20	1	1	160	10	84	36.7
TBP	18	20	1	1	160	10	61	26.7
TBP	19	20	1	1	160	10	31	13.5
TBP	20	20	1	1	160	10	64	28.0
TBP	21	20	1	1	160	10	20	8.7
TBP	22	20	1	1	160	10	33	14.4
TBP	23	20	1	1	160	10	18	7.9
TBP	24	20	1	1	160	10	21	9.2
TBP	25	20	1	1	160	10	76	33.2
TBP	26	20	1	1	160	10	29	12.7

Table 20 - Raw data of experiments using continuous addition of peroxide

Initiator Used	Sample #	MAH (wt % by wt wax)	Mol ratio MAH : Init	mol ratio init:MAH	Temp (°C)	Time (hours)	AN (mg KOH/g wax)	GE (%)
TBP	27	5	5	0.2	160	0.5	10	17.5
TBP	28	5	1	1	160	10	25	43.7
TBP	29	20	5	0.2	70	0.5	11	4.8
TBP	30	20	1	1	160	10	gelation	0.0
TBP	31	20	1	1	70	0.5	13	5.7
TBP	32	20	5	0.2	160	10	78	34.1
TBP	33	20	1	1	160	0.5	32	14.0
TBP	34	5	5	0.2	70	0.5	4	7.0
TBP	35	5	5	0.2	70	10	7	12.2
TBP	36	5	1	1	160	0.5	22	38.5
TBP	37	20	5	0.2	70	10	11	4.8
TBP	38	20	1	1	70	10	16	7.0
TBP	39	20	5	0.2	160	0.5	28	12.2
TBP	40	5	1	1	70	0.5	5	8.7
TBP	41	5	1	1	70	10	gelation	0.0
TBP	42	5	5	0.2	160	10	16	28.0
TBP	43	5	0.2	5	160	0.5	33	57.7
TBP	44	10	0.2	5	160	0.5	40	35.0
TBP	45	20	0.2	5	160	0.5	gelation	0.0
TBP	46	5	0.2	5	160	1	36(partial gelation)	0.0
TBP	47	5	0.2	5	160	1.5	gelation	0.0
TBP	48	5	0.4	2.5	160	0.5	30	52.4
TBP	49	5	1	1	160	0.5	22	38.5
TBP	50	5	0.2	5	160	0.5	34	59.4
TBP	51	5	0.2	5	160	0.5	34	59.4
TBP	52	5	1	1	160	5	16	28.0
TBP	53	5	1	1	160	10	12	21.0
TBP	54	5	1	1	160	10	gelation	0.0
TBP	55	5	1	1	160	10	gelation	0.0
TBP	56	25	3	0.3333333	160	10.5	32.6	11.4
TBP	57	25	3	0.3333333	160	12.5	gelation	0.0
TBP	58	5	1	1	160	0.5	12.5	21.8
TBP	59	2.5	1	1	160	0.5	5	17.5
TBP	60	7.5	1	1	160	0.5	5	5.8
TBP	61	10	1	1	160	0.5	9	7.9
TBP	62	20	1	1	120	10	6.7	2.9

Initiator Used	Sample #	MAH (wt % by wt wax)	Mol ratio MAH : Init	mol ratio init:MAH	Temp (°C)	Time (hours)	AN (mg KOH/g wax)	GE (%)
TBPB	63	20	0.5	2	100	10	24.9	10.9
TBPB	64	20	1	1	100	10	9.6	4.2
TBPB	65	20	1	1	130	0.5	22.7	9.9
TBPB	66	20	1	1	120	0.5	17.4	7.6

Table 21 - Raw data of experiments using MAH addition

Initiator Used	Sample #	MAH (wt % by wt wax)	Mol ratio MAH : Init	mol ratio init:MAH	Temp (°C)	Time (hours)	AN (mg KOH/g wax)	GE (%)
TBP	67	20	0.5	2	160	10	82	35.8
TBP	68	20	0.5	2	160	10	79	34.5
TBP	69	20	0.5	2	160	10	80	35.0
TBP	70	20	0.5	2	160	10	77	33.6
TBP	71	20	0.5	2	160	10	82	35.8
TBP	72	20	0.5	2	160	10	79	34.5
TBP	73	20	1	1	160	10	74	32.3
TBP	74	20	1	1	160	10	71	31.0
TBP	75	20	1	1	160	10	67	29.3
TBP	76	20	1	1	160	10	76	33.2
TBP	77	10	1	1	160	10	64	55.9
TBP	78	10	1	1	160	10	61	53.3
TBP	79	10	1	1	160	10	59	51.6
TBP	80	10	1	1	160	10	63	55.1
TBP	81	10	1	1	160	10	62	54.2
TBP	82	10	1	1	160	10	54	47.2
TBP	83	10	1	1	160	10	65	56.8
TBP	84	10	1	1	160	10	61	53.3
TBP	85	10	1	1	160	10	60	52.4
TBP	86	10	2	0.5	160	10	59	51.6
TBP	87	10	2	0.5	160	10	50	43.7
TBP	88	10	2	0.5	160	10	51	44.6
TBP	89	10	2	0.5	160	10	54	47.2
TBP	90	10	2	0.5	160	10	53	46.3
TBP	91	10	2	0.5	160	10	50	43.7
TBP	92	10	2	0.5	160	10	56	48.9
TBP	93	10	2	0.5	160	10	61	53.3
TBP	94	10	1	1	160	10	63	55.1

Initiator Used	Sample #	MAH (wt % by wt wax)	Mol ratio MAH : Init	mol ratio init:MAH	Temp (°C)	Time (hours)	AN (mg KOH/g wax)	GE (%)
TBP	95	10	1	1	160	10	65	56.8
TBPB	96	20	0.5	2	130	10	86	37.6
TBPB	97	20	0.5	2	130	10	79	34.5
TBPB	98	10	1	1	130	10	63	55.1
TBPB	99	10	1	1	130	10	64	55.9
TBPB	100	10	1	1	130	10	66	57.7
TBPB	101	10	1	1	130	10	61	53.3
TBPB	102	10	1	1	130	10	60	52.4

Table 22 - Raw data of experiments using ball milling approach

Initiator Used	Sample #	MAH (wt % by wt wax)	Mol ratio MAH : Init	mol ratio init:MAH	Temp (°C)	Time (hours)	AN (mg KOH/g wax)	GE (%)
BPO	103	2.5	1	1	80	6	6.8	23.8
BPO	104	2.5	1	1	80	6	8.6	30.1
BPO	105	5	1	1	80	2	8	14.0
BPO	106	5	1	1	80	2	9.2	16.1
BPO	107	5	1	1	80	6	10	17.5
BPO	108	5	1	1	80	6	7	12.2
BPO	109	20	0.5	2	80	6	32	14.0

Table 23 - Raw data for experiments using thermal addition of MAH to alpha-olefins at 200 °C for 8 hours,

Sample #	Wax type	MAH source	AN	Unwashed AN	Efficiency	MAH add'n temp (°C)	Lid config
110	OlefinC30+HA	Sigma	72	-----	66.05505	200	open
111	OlefinC30+HA	Sigma	76.9	78.5	70.55046	RT	open
112	olefinC30+	Sigma	81.9	79.4	75.13761	RT	open
113	olefinC30+HA	Ind	49	-----	44.95413	200	open
114	OlefinC30+HA	Ind	76.3	77.4	70	200	open
115	olefinC30+HA	Ind	73	76	66.97248	200	open
116	OlefinC30+HA	Ind	54	56	49.54128	200	open
117	OlefinC30+HA	Ind	90.5	117	83.02752	200	closed
118	OlefinC30+HA	Sigma	108.5	110	99.54128	200	closed
119	OlefinC30+HA	Sigma	96.2	116	88.25688	200	closed
120	OlefinC30+HA	Ind	92	110	84.40367	90	closed

Sample #	Wax type	MAH source	AN	Unwashed AN	Efficiency	MAH add'n temp (° C)	Lid config
121	OlefinC30+HA	Sigma	84.4	101	77.43119	RT	closed
122	OlefinC30+HA	Sigma	91.5	105	83.94495	RT	closed
123	OlefinC30+HA	Ind	93	96.3	85.3211	RT	open
124	OlefinC30+HA	Sigma	95.4	109.1	87.52294	RT	closed
125	OlefinC30+HA	Sigma	102.7	103.1	94.22018	RT	open

Eq. (7) corresponds to the calculation of degree of grafting (DG), which is analogous to AN and more traditional in that it quantifies the amount of grafted MAH as a weight percentage; however AN is the measurement that is typically used in the emulsion industry. Eq. (7) corresponds to the calculation of grafting efficiency (GE).

$$DG = \frac{V_B C_B MW_{MAH}}{2 \cdot m_{wax} \cdot 1000} \times 100\% \quad (6)$$

$$GE = \frac{V_B C_B MW_{MAH}}{2 \cdot m_{wax} \cdot 1000 \cdot MAHloading} \times 100\%^2 \quad (7)$$

A.2. Calculation of theoretical acid number for 1:1 thermal grafting

$$C_{KOH\ soln} = 0.1\ M = \frac{1.0 \times 10^{-4}\ mol}{mL} = 5.61 \frac{mg}{mL}$$

1g emulsifier = 0.00194 mol = 19.4 mL KOH sol'n to neutralize

$$AN = \frac{V_{base} [B] MW_{KOH}}{m_{emulsifier}}$$

$$AN = \frac{(19.4\ mL)(0.1\ M) \left(\frac{56.1\ g}{mol} \right)}{1\ g\ emulsifier}$$

$$AN = 108.834 \frac{mg\ KOH}{g}$$

A.3. Emulsion data

Table 24 - Raw data for formulations of emulsions to be used in gypsum wallboards

SAMPLE #	Wax sample #	Wash method	AN (Ace)	Paraffin	Exp wax	OPE	Water + additives	KOH
1	-----	-----	48	32	1.289	1.273	65.163	0.273
2	50	AC	34	31.66	3.116	0	65.163	0.273
3	50	AC	34	31.556	3.192	0	65.163	0.273
4	52	AC	16	29.03	6	0	65.163	0.273
5	58	AC	12.5	27.06	7.5	0	65.163	0.273
6	53	AC	12	26.848	8.9	0	65.163	0.273
7	5	AC	84	32	2.562	0	65.163	0.273
8	5	AC	84	32	1.289	1.273	65.163	0.273
9	5	AC	84	32	1.012	0	65.163	0.273
10	17	UW	80	32	2.562	0	65.163	0.273
11	5	AC	84	32.36	2.2	0	65.163	0.273
12	5	AC	84	31.562	3	0	65.163	0.273
13	5	AC	84	31.562	3	0	65.163	0.273
14	5	AC	84	32	2.562	0	65.163	0.273
15	5	AC	84	31.562	3	0	65.163	0.273
16	5	AC	84	31.562	3	0	65.163	0.273
17	102	AC	55	30.2	4.36	0	65.163	0.273
18	102	AC	55	30.2	4.26	0	65.163	0.545
19	102	H2O	55	31.4	3.158	0	65.163	0.545
20	102	H2O	55	31.4	3.158	0	65.163	0.82
21	97	UW	70	31.562	3	0	65.163	0.4
22	101	UW	61	31.562	3	0	65.1634	0.4
23	102	H2O	70	30.562	4	0	65.1634	0.545
24	84	H2O	61	32.964	1.6	0	65.163	0.273
25	1	AC	39	31.564	3	0	65.163	0.273
26	84	H2O	61	32.964	1.6	0	65.163	0.273
27	96	AC	80	33.364	1.2	0	65.163	0.273
28	84	H2O	61	33.064	1.5	0	65.163	0.273
29	1	H2O	39	31.564	3	0	65.163	0.273
30	84	H2O	61	33.064	1.5	0	65.163	0.273
32	82	UW	50	32.562	2	0	65.163	0.273
33	1	AC	39	31.964	2.6	0	65.163	0.273
34	82	UW	50	32.562	2	0	65.163	0.273
35	13	H2O	48	32.562	2	0	65.163	0.273
36	13	H2O	48	31.562	3	0	65.163	0.273
37	82	UW	50	32.562	2	0	65.163	0.273
38	82	UW	50	32.762	1.8	0	65.163	0.273
39	82	UW	50	32.962	1.6	0	65.163	0.273
40	85	AC	60	32.962	1.6	0	65.163	0.273
41	85	AC	60	32.562	2	0	65.163	0.273
42	85	AC	60	33.362	1.2	0	65.163	0.273
43	77	UW	64	32.562	2	0	65.163	0.273
44	77	UW	64	32.962	1.6	0	65.163	0.273

SAMPLE #	Wax sample #	Wash method	AN (Ace)	Paraffin	Exp wax	OPE	Water + additives	KOH
45	85	AC	60	33.162	1.4	0	65.163	0.273
46	85	AC	60	33.362	1.2	0	65.163	0.273
47	85	AC	60	33.36	1.2	0	65.163	0.273
48	85	AC	60	32.56	2	0	65.163	0.273
49	85	AC	60	33.36	1.2	0	65.163	0.273
50	85	AC	60	32.56	2	0	65.163	0.273
51	85	AC	60	33.562	1	0	65.163	0.273
52	77	UW	60	31.562	3.4	0	65.163	0.273
53	85	AC	60	33.762	0.8	0	65.163	0.273
54	77	UW	60	31.562	3	0	65.163	0.273
55	85	AC	60	33.36	1.2	0	65.163	0.273
56	88	AC	51	33.36	1.2	0	65.163	0.273
57	77	UW	54	33.36	1.2	0	65.163	0.273
58	85	AC	60	33.962	0.6	0	65.163	0.273
59	85	AC	60	33.862	0.7	0	65.163	0.273
60	85	AC	60	33.862	0.7	0	65.163	0.273
61	85	AC	60	33.562	1	0	65.163	0.273
62	85	AC	60	33.762	0.8	0	65.163	0.273
63	110	UW	72	33.762	0.8	0	65.163	0.273
64	110	UW	72	33.762	1.6	0	65.163	0.273
65	110	UW	72	33.762	1.2	0	65.163	0.273
66	110	UW	72	32.962	0.8	0.8	65.163	0.273
67	110	UW	72	32	1.291	1.273	65.163	0.273
68	111	UW	72	32	1.291	1.273	65.163	0.273
69	111	UW	72	32	0.641	1.923	65.163	0.273
70	111	UW	72	32	1.923	0.641	65.163	0.273
71	111	UW	72	32	1.291	1.273	65.163	0.273
72	110	UW	72	32	1.291	1.273	65.163	0.273
73	111	V	72	32	1.291	1.273	65.163	0.273
74	111	UW	72	32	1.923	0.641	65.163	0.273
75	111	UW	72	32	0.641	1.923	65.163	0.273
76	114	UW	72	32	1.291	1.273	65.163	0.273
77	114	UW	72	32	0	2.564	65.163	0.273
78	114	UW	72	32	0.641	1.923	65.163	0.273
79	114	UW	72	32	1.291	1.273	65.163	0.273
80	114	UW	72	32	1.291	1.273	65.163	0.273
81	111	AC	72	31.773	0.68	1.882	65.163	0.5
82	117	UW	117	32.291	1	1.273	65.163	0.273
83	118	UW	110	32.291	1	1.273	65.163	0.273
84	119	UW	116	32.291	1	1.273	65.163	0.273
85	120	UW	110	32.291	1	1.273	65.163	0.273
86	121	UW	101	32.291	1	1.273	65.163	0.273
87	122	UW	105	32.291	1	1.273	65.163	0.273

Table 25 - Raw data for emulsion performance

SAMPLE #	Wax sample #	Wash	AN (Ace)	Solids (%)	Visc (cP)	pH	Finger	shear	storage
1	-----	-----	48	40-42	300	8 - 10	pass	pass	pass
2	50	AC	34	42.08	146.4	8.32	pass	pass	fail
3	50	AC	34	42.03	288	9.01	pass	pass	fail
4	52	AC	16	39.44	1254	9.4	pass	pass	fail
5	58	AC	12.5	38.99	1410	10.08	pass	pass	fail
6	53	AC	12	40.63	624	10.2	pass	pass	fail
7	5	AC	84	-----	167.6	7.88	pass	fail	fail
8	5	AC	84	-----	-----	-----	fail	-----	-----
9	5	AC	84	-----	-----	-----	fail	-----	-----
10	17	UW	80	42.65	295.2	7.07	pass	pass	pass
11	5	AC	84	-----	-----	-----	-----	-----	-----
12	5	AC	84	42.74	230.4	8.6	pass	fail	fail
13	5	AC	84	42.99	236.4	8.43	pass	pass	pass
14	5	AC	84	42.81	373.2	8.46	pass	pass	pass
15	5	AC	84	41.68	281	9.84	pass	pass	pass
16	5	AC	84	42.11	95.1	9.76	pass	pass	pass
17	102	AC	55	-----	-----	7.51	fail	-----	-----
18	102	AC	55	-----	-----	12.08	fail	-----	-----
19	102	H2O	55	-----	-----	-----	fail	-----	-----
20	102	H2O	55	-----	-----	12.2	fail	-----	-----
21	97	UW	70	39.35		8.98	fail	-----	-----
22	101	UW	61	-----	540	9.82	fail	-----	-----
23	102	H2O	70	-----	-----	-----	fail	-----	-----
24	84	H2O	61	42.35	218.7	9.94	pass	pass	fail
25	1	AC	39	43.7	291	8.83	pass	fail	fail
26	84	H2O	61	51.54	522	9.73	pass	fail	fail
27	96	AC	80	41.21	452	12.21	pass	pass	fail
28	84	H2O	61	37.35	1154	9.78	pass	pass	fail
29	1	H2O	39	44.11	262.8	9.46	pass	pass	fail
30	84	H2O	61	41.64	55.5	10.03	pass	pass	fail
32	82	UW	50	44.25	245.4	9.02	pass	pass	pass
33	1	AC	39	37.54	2244	10.39	pass	pass	pass
34	82	UW	50	42.29	194.4	8.64	pass	pass	pass
35	13	H2O	48	-----	-----	-----	fail	-----	-----
36	13	H2O	48	-----	-----	-----	fail	-----	-----
37	82	UW	50	42.02	164.4	8.43	pass	pass	pass
38	82	UW	50	42.41	174.4	9.54	pass	pass	pass
39	82	UW	50	42.29	177.9	9.62	pass	pass	pass
40	85	AC	60	40.78	118.2	9.51	pass	pass	pass
41	85	AC	60	41	212.7	11.1	pass	pass	pass
42	85	AC	60	-----	-----	-----	fail	-----	-----
43	77	UW	64	41.47	233.1	8.56	pass	pass	-----
44	77	UW	64	41.56	237	11	pass	pass	pass
45	85	AC	60		216	9.22	fail	-----	-----
46	85	AC	60	39.4	199.7	11.46	pass	pass	pass

SAMPLE #	Wax sample #	Wash	AN (Ace)	Solids (%)	Visc (cP)	pH	Finger	shear	storage
47	85	AC	60	41.47	233.1	8.56	pass	pass	pass
48	85	AC	60	41.47	233.1	8.56	pass	pass	pass
49	85	AC	60	41.56	237	11	pass	pass	pass
50	85	AC	60	41.56	237	11	pass	pass	pass
51	85	AC	60	41.23	288	10.71	pass	pass	
52	77	UW	60	-----	-----	-----	fail	-----	-----
53	85	AC	60	41.1	229.2	10.53	pass	pass	
54	77	UW	60	-----	-----	-----	fail	-----	-----
55	85	AC	60	42.19	208		pass	pass	thick
56	88	AC	51	-----	-----	-----	fail	-----	-----
57	77	UW	54	-----	-----	-----	fail	-----	-----
58	85	AC	60	-----	-----	-----	fail	-----	-----
59	85	AC	60	-----	-----	-----	fail	-----	-----
60	85	AC	60	-----	-----	-----	fail	-----	-----
61	85	AC	60	40.57	254.4	11.45	pass	pass	pass
62	85	AC	60	41.73	234	12	pass	pass	pass
63	110	UW	72	40.23	140	11.42	pass	pass	pass
64	110	UW	72	42.11	167.5	10.42	pass	pass	pass
65	110	UW	72	42.57	167.1	10.93	pass	pass	pass
66	110	UW	72	41.46	159.1	10.99	pass	pass	pass
67	110	UW	72	42.63	228.6	9.84	pass	pass	pass
68	111	UW	72	-----	-----	-----	fail	-----	-----
69	111	UW	72	41.88	218.1	9.65	pass	pass	pass
70	111	UW	72	-----	-----	-----	fail	-----	-----
71	111	UW	72	-----	-----	-----	fail	-----	-----
72	110	UW	72	44.86	198	9.75	pass	pass	pass
73	111	V	72	-----	-----	-----	fail	-----	-----
74	111	UW	72	40.2	249.6	9.12	pass	pass	pass
75	111	UW	72	41.31	224	10.6	pass	pass	pass
76	114	UW	72	41.38	HIGH	8.46	fail	-----	-----
77	114	UW	72	41.74	235.5	10.63	pass	pass	pass
78	114	UW	72	41.37	222.9	9.6	pass	pass	pass
79	114	UW	72	40.8	180	8.06	pass	pass	pass
80	114	UW	72	41.5	204	7.95	pass	pass	pass
81	111	AC	72	-----	-----	-----	fail	-----	-----
82	117	UW	117	41.42	435	8.59	pass	pass	pass
83	118	UW	110	41.82	552	8.59	pass	pass	pass
84	119	UW	116	41.58	802	8.48	pass	pass	pass
85	120	UW	110	41.61	245	8.46	pass	pass	pass
86	121	UW	101	41.49	233	8.56	pass	pass	pass
87	122	UW	105	41.38	271	8.6	pass	pass	pass

Appendix B: FTIR Reference Spectra

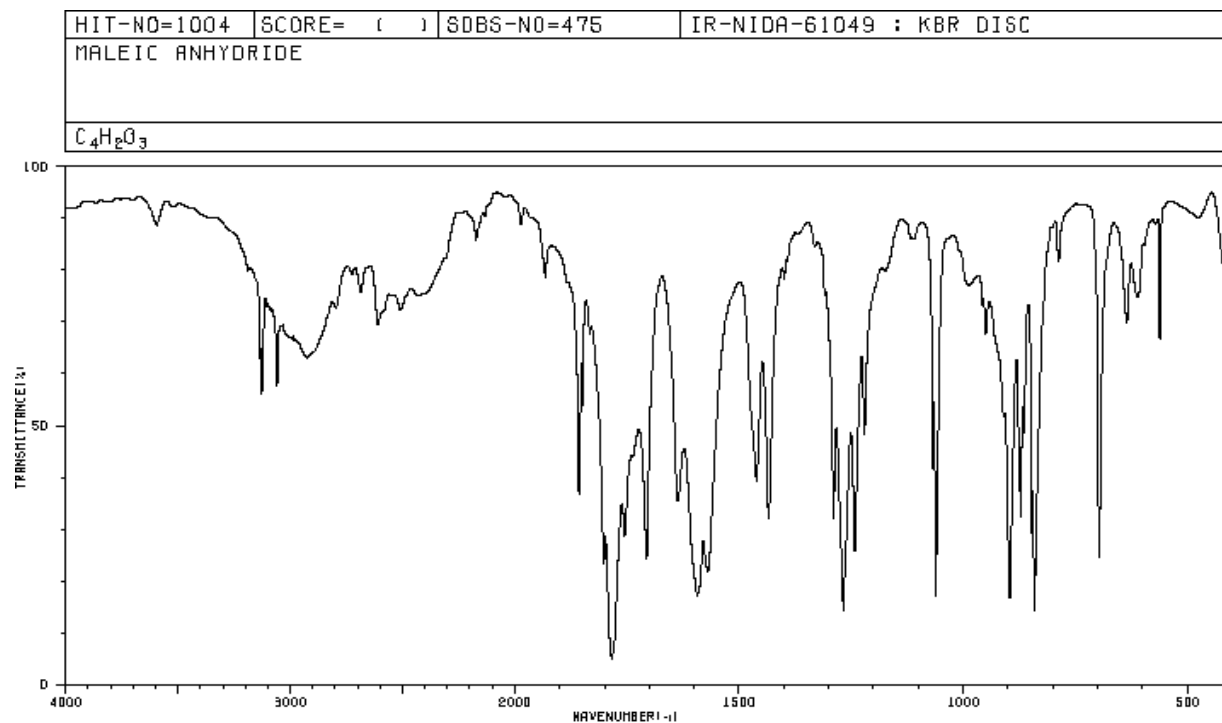


Figure 39 - Reference FTIR spectrum of maleic anhydride

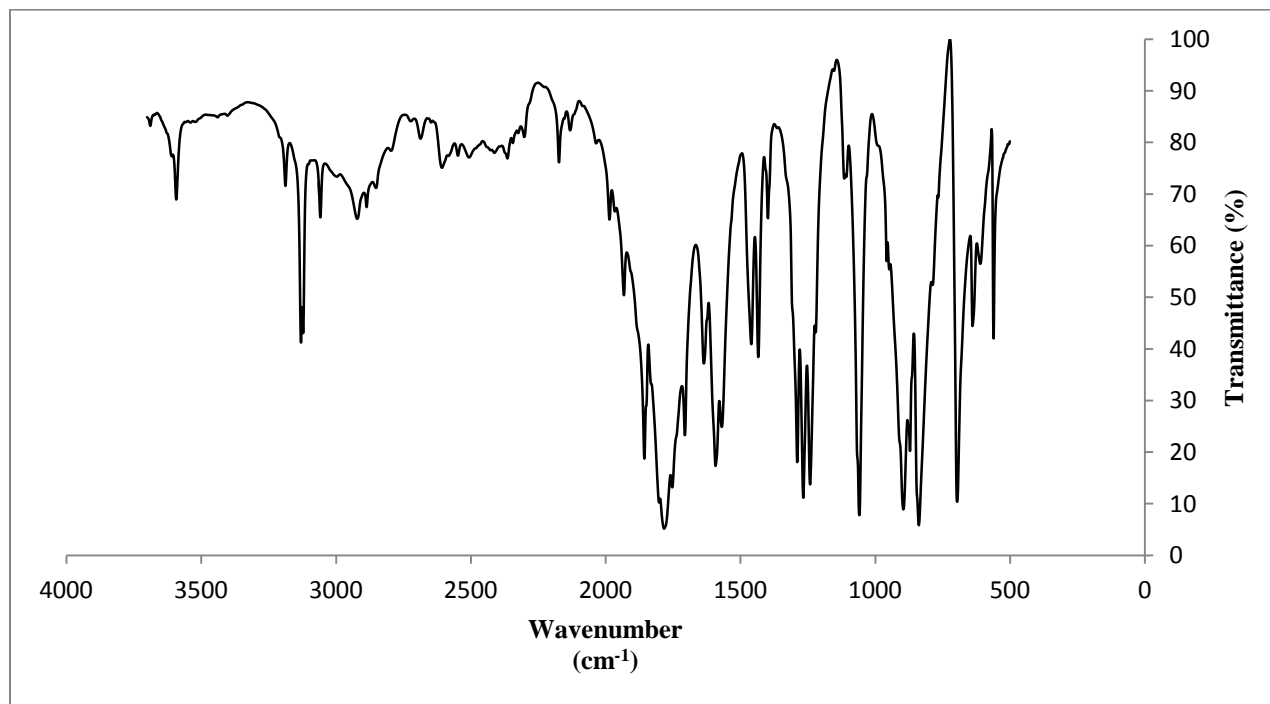


Figure 40 - FTIR Spectrum of maleic anhydride recaptured from thermal grafting experiments

By comparing Figure 39, a reference spectrum of MAH, with Figure 40 which shows an experimentally obtained FTIR spectrum of recaptured MAH that has been removed from the reaction mixture by vacuum during thermal maleation, it can be seen that no change occurs in the structure of the maleic anhydride before it is removed from the reaction mixture. Therefore, MAH could be recycled to increase the overall efficiency of the maleation process.

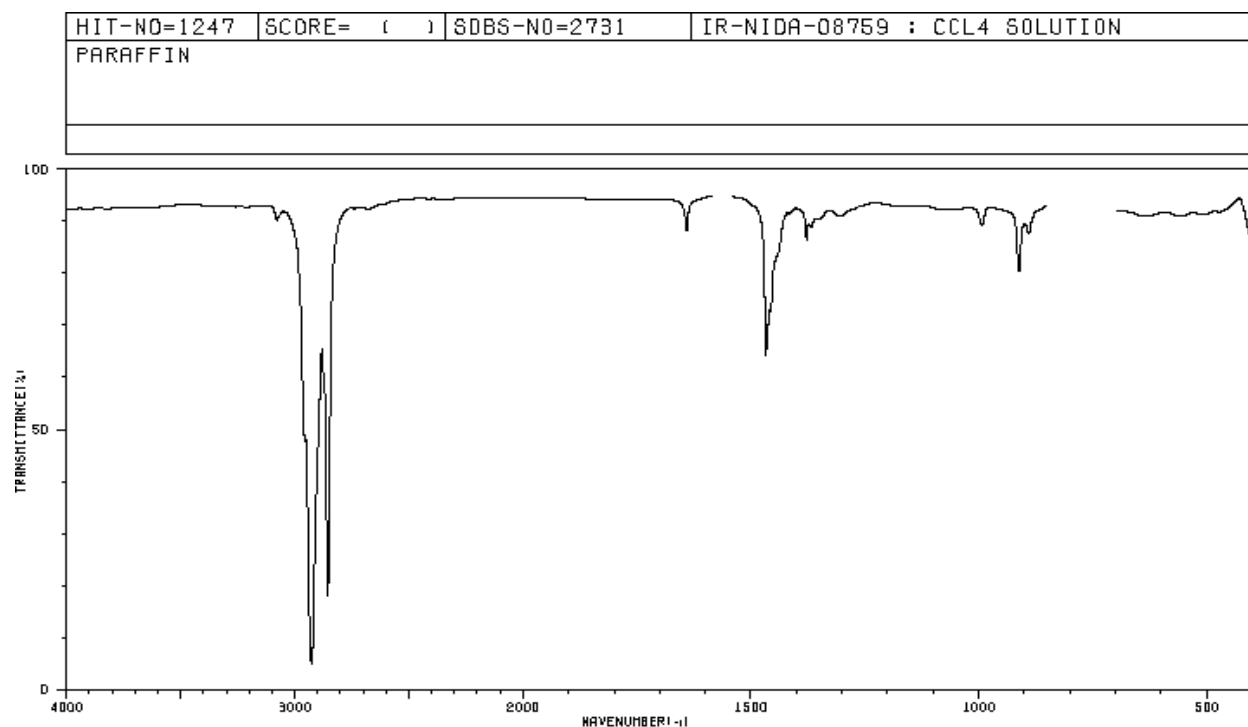


Figure 41 - Reference FTIR spectrum of paraffin wax

Figure 41 shows a reference FTIR spectrum of paraffin wax showing characteristic peaks around 2927 cm^{-1} and 2855 cm^{-1} corresponding to C-H stretching, 1468 cm^{-1} corresponding to CH_2 bending and 1378 cm^{-1} corresponding to CH_3 bending.

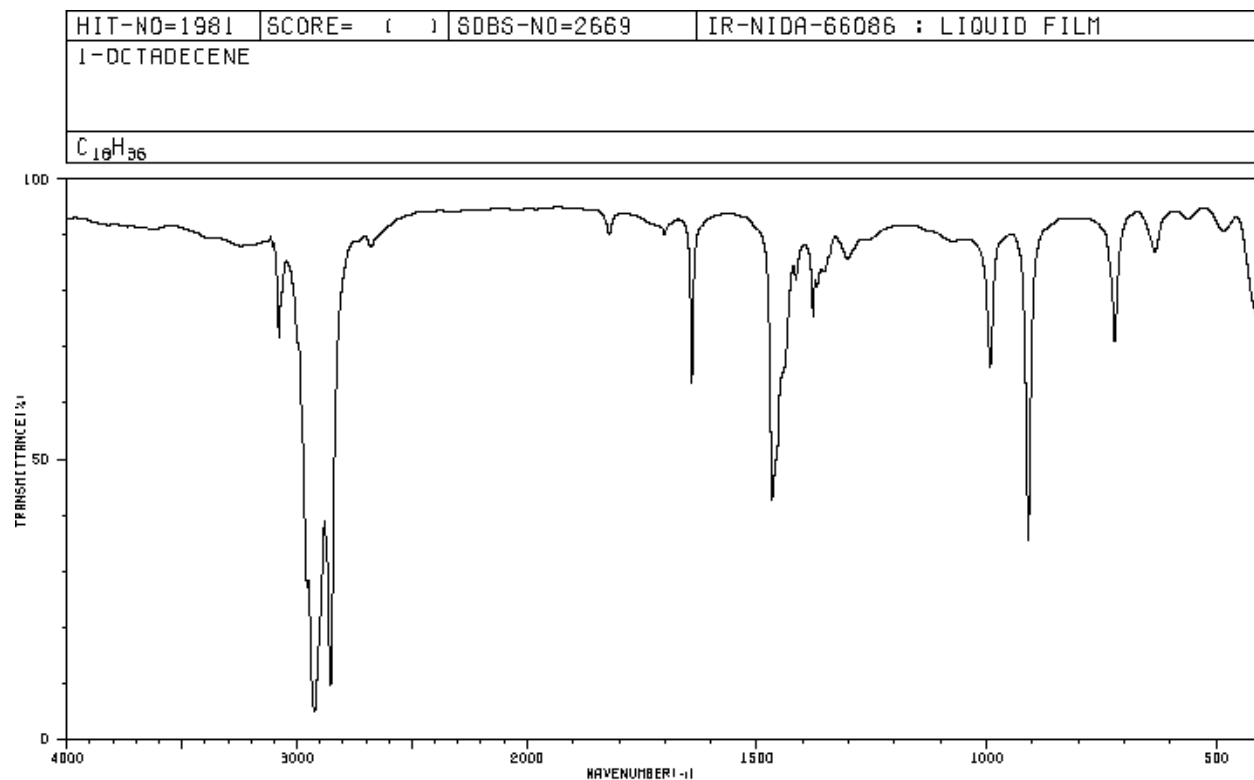


Figure 42 - Reference FTIR spectrum of 1-octadecene

Figure 42 shows a reference FTIR spectrum of 1-octadecene, which can be said to be analogous to higher molecular weight alpha-olefins. The spectrum shows characteristic peaks around 3078 cm^{-1} corresponding to sp^2 C-H stretching (from C=C-H moieties), 2924 cm^{-1} and 2854 cm^{-1} corresponding to sp^3 C-H stretching, 1642 cm^{-1} for C=C stretching and bending moments found at lower wavelengths.

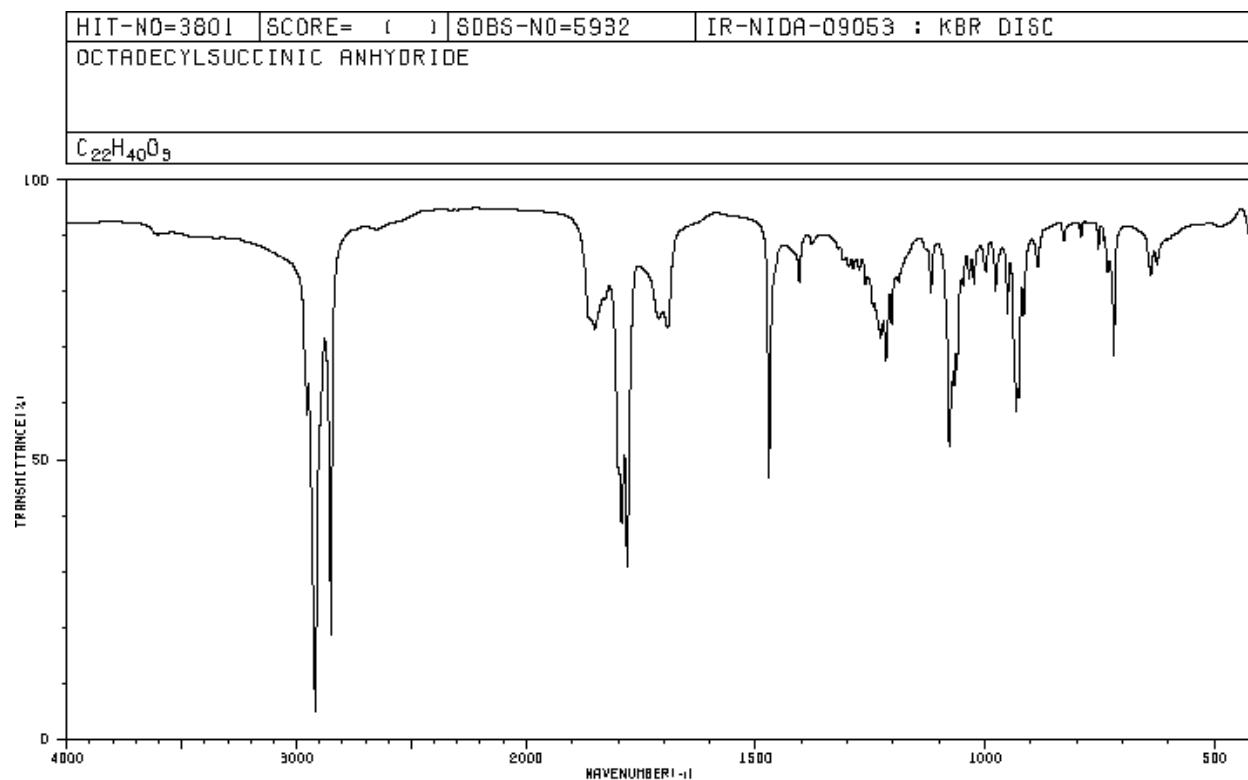


Figure 43 - Reference FTIR spectrum of n-octadecylsuccinic anhydride

Figure 43 shows a reference FTIR spectrum of n-octadecylsuccinic anhydride, used to show the C=O stretches in a single-graft type molecule of maleated paraffin wax. The characteristic C=O stretching frequencies in this spectrum are found around 1867 cm^{-1} and 1792 cm^{-1} .

Appendix C: Cost Estimation

Recent cost estimates for each component used in emulsion fabrication are shown in Table 16 of section 3.5. Using this information we can estimate the possible cost-savings of using experimental emulsifiers over those that are currently being used by Norjohn Ltd. in the production of their emulsions. Yearly production for EWP emulsions is estimated at 9000000 kg of emulsion per year while for gypsum emulsions it is estimated to be 900000 kg of emulsion per year and Table 15 of section 3.5 shows the required amount of each component based off these total emulsion requirements.

The volume and dimensions of the reactor required for emulsifier production on this can be approximated knowing the daily production requirements:

$$Production = 144000 \frac{kg}{year} = \frac{1221 lbs}{day}$$

Assuming that the plant operates 5 days a week for 52 weeks per year, we require 1221 lbs of wax each day, the volume and dimensions of the required reactor can be determined.

Using a 3:1 height:diameter profile and adjusting for 20% head space:

$$V = \frac{Production}{\rho_{wax}}$$

$$V = \frac{1221 lbs}{6.96 \frac{lbs}{gal}} = 175.43 gal = 40524.33 in^3$$

$$V = \pi r^2 h = 3\pi r^3$$

$$r = \sqrt[3]{\frac{V}{3\pi}} = 16.26 in$$

From this radius, the values in Table 17 of section 3.5 follow. To calculate the cost per kilogram of experimental emulsifier we need to know the cost of materials and energy:

$$\text{Cost} = \text{Materials} + \text{Cost of Power}$$

The cost of materials is:

$$\text{Materials} = W_{C30+HA}C_{C30+HA} + W_{MAH}C_{C30+HA}$$

$$\text{Materials} = \left(0.187 \frac{\text{kg MAH}}{\text{kg emulsifier}}\right) \left(1.5 \frac{\$}{\text{kg}}\right) + \left(0.813 \frac{\text{kg C30 + HA}}{\text{kg emulsifier}}\right) \left(1.87 \frac{\$}{\text{kg}}\right)$$

$$\text{Materials} = 1.80 \frac{\$}{\text{kg}}$$

Energy costs include the cost of melting wax, heating it to 200 °C and maintaining that temperature for 8 hours, then maintaining a temperature of 100 °C for storage for 24 hours.

Assuming that heat losses from the reactor are negligible:

$$\text{Power} = \text{reheat} + \text{maintain}_{200} + \text{maintain}_{100}$$

$$\text{reheat} = \left((C_{p,t}W_t) + (C_{p,w}W_w)\right) \left(\frac{\Delta T}{3.42t}\right) + \left(\frac{W_w \Delta H_{fus,w}^\circ}{3.42t}\right)$$

$$\text{maintain} = \frac{K \cdot A \cdot dT \cdot 0.366}{L}$$

$$\text{Power} =$$

$$\left(\left(1315.42 \frac{\text{J}}{\text{lb}\cdot\text{K}} \cdot 1221 \text{ lbs}\right) + \left(227.70 \frac{\text{J}}{\text{lb}\cdot\text{K}} \cdot 592 \text{ lbs}\right)\right) \left(\frac{200^\circ\text{C} - 25^\circ\text{C}}{3.42(2)}\right) +$$

$$\left(\frac{1221 \text{ lbs}}{3.42(2)}\right) + \left(\frac{0.37 \frac{\text{BTU}}{\text{hf}\cdot\text{ft}^2\cdot^\circ\text{F}\cdot\text{in}} \cdot (54.55 \text{ ft}^2) \cdot 0.366}{L}\right) \cdot ((200^\circ\text{C} - 25^\circ\text{C}) + (100^\circ\text{C} - 25^\circ\text{C}))$$

$$\text{Power} = 2.14 \times 10^8 \text{ W} + 9.20 \times 10^2 \text{ W}$$

$$\text{Power} = 2.14 \times 10^8 \text{ W}$$

Since the power required to maintain the reactor at 200 °C and to maintain the product at 100 °C is negligible in comparison to the power required to reheat the C30+HA wax from room temperature to 200 °C, those values are ignored in calculation the total cost of power.

$$\text{Cost of Power} = \frac{\frac{2.14 \times 10^8 \text{ W} \cdot 2 \text{ hours}}{3600 \frac{\text{s}}{\text{hour}} \cdot \frac{1000 \text{ W}}{1 \text{ kW}}} \cdot \left(0.0085 \frac{\$}{\text{kWh}}\right)}{175.43 \text{ kg}}$$

$$\text{Cost of Power} = 1.82 \times 10^{-2} \frac{\$}{\text{kg}}$$

$$\text{Total Cost} = 1.80 \frac{\$}{\text{kg}} + 1.82 \times 10^{-2} \frac{\$}{\text{kg}}$$

$$\text{Total Cost} = 1.82 \frac{\$}{\text{kg}}$$

Knowing the total materials and energy cost of the experimental emulsifier and comparing that to the costs of currently used industrial emulsifiers, a total savings amount can be calculated from the difference

$$\text{Savings} = \text{Gypsum} + \text{EWP}$$

$$\text{Savings} = \$78047.20/\text{y} + \$258249.74/\text{y}$$

$$\text{Savings} = \$336296.94/\text{y}$$